



TECHNISCHE  
UNIVERSITÄT  
WIEN

DISSERTATION

ROTATION INVARIANT DIAGRAMMATIC BASES FOR  
INVARIANT SPACES

Ausgeführt zum Zwecke der Erlangung des akademischen Grades eines  
Doktors der technischen Wissenschaften unter der Leitung von

PRIVATDOZ. DR.RER.NAT. MARTIN RUBEY

E104

Institut für Diskrete Mathematik und Geometrie

eingereicht an der Technischen Universität Wien  
Fakultät für Mathematik und Geoinformation

von

STEPHAN PFANNERER-MITTAS

01026392

Stipendiat der Österreichischen Akademie der Wissenschaften (DOC)

---

Wien, am

---

Unterschrift



---

## KURZFASSUNG

---

In dieser kumulativen Dissertation präsentieren wir kombinatorische Ansätze, um grafische Beschreibungen von Basen der invarianten Unterräume von Tensor Produkten von Darstellungen von Lie Gruppen zu erhalten. Dazu verwenden wir Chord-Diagramme. Das sind Graphen, deren Knoten im Kreis angeordnet werden und die Tensorpositionen der Invarianten kodieren.

Diese Arbeit besteht aus drei Publikationen, welche in internationalen Journalen erschienen sind:

In *Skew characters and cyclic sieving* bestimmen wir, welche Charaktere der symmetrischen Gruppe eine Permutationsdarstellung der zyklischen Gruppe trägt. Diese Resultate können wir auf die Darstellungstheorie von Tensorpotenzen der adjungierten Darstellung der allgemeinen linearen Gruppe anwenden. Dadurch können wir die Existenz einer Bijektion zwischen Permutationen und alternierenden Tableaux (nach Stembridge) beweisen, welche Rotation der Diagramme/Permutationen in Promotion der Tableaux überführt.

Dieses Resultat zeigt nur die Existenz der Bijektion, aber liefert keine explizite Konstruktion. Wir denken, dass es möglich ist, dieses Resultat zu verfeinern und haben als ersten Schritt eine der wichtigsten Identitäten aus dem Beweis verallgemeinert. In *A refinement of the Murnaghan-Nakayama rule by descents for border strip tableaux* erweitern wir diese Identität zu standard Young Tableaux, die eine gegebene Anzahl von Abstiegen haben. Dazu führen wir eine neue Statistik auf Border-Strip Tableaux ein, die die klassische Definition von Abstiegen auf standard Young Tableaux erweitert.

In *Promotion and growth diagrams for fans of Dyck paths and vacillating tableaux* erläutern wir einen neuen Ansatz, um explizite diagrammatische Basen direkt vom Promotion-orbit von Tableaux zu erhalten. Wir verwenden diese Konstruktion, um eine Injektion von  $r$ -Fächern von Dyck Pfaden (resp. Vacillating tableaux) der Länge  $n$  nach Chord-Diagrammen auf  $[n]$  erhalten. Dadurch bekommen wir Diagramme, die eine Basis für die Spindarstellung der Spingruppe, beziehungsweise für die Vektordarstellung der speziellen orthogonalen Gruppe, indizieren.



---

## ABSTRACT

---

In this cumulative dissertation we present combinatorial approaches to obtain pictorial descriptions of bases of invariant spaces of tensor products of representations of Lie groups in terms of certain graphs, which we call chord diagrams. These are graphs whose vertices, arranged in a circle, correspond to the tensor positions of the invariant.

This thesis consists of three publications, which appeared in peer reviewed journals:

In *Skew characters and cyclic sieving* we determine which characters of the symmetric group carry a permutation representation of the cyclic group. We apply our results to the invariant theory of tensor powers of the adjoint representation of the general linear group and prove the existence of a bijection between permutations and J. Stembridge's alternating tableaux, which intertwines rotation and promotion, yielding a diagrammatic basis.

This is only an existential result and no explicit construction. In the hope of finding this bijection we refine one of the key identities in *A refinement of the Murnaghan-Nakayama rule by descents for border strip tableaux*. We extend it to standard Young tableaux and border strip tableaux with a given number of descents. To do so, we introduce a new statistic for border strip tableaux, extending the classical definition of descents in standard Young tableaux.

In *Promotion and growth diagrams for fans of Dyck paths and vacillating tableaux* we discuss a new approach to construct a diagrammatic basis from the promotion orbit of tableaux. In particular we construct an injection from the set of  $r$ -fans of Dyck paths (resp. vacillating tableaux) of length  $n$  into the set of chord diagrams on  $[n]$ . This way we obtain suitable diagrams for the spin representation of the spin group and the vector representation of the special orthogonal group.



---

## ACKNOWLEDGEMENTS

---

Firstly, I want to express my gratitude to my supervisor Martin Rubey. He has always been very supportive and in our joint research project we had lots of fun working together. I especially want to say thank you for opening me the door to one of my ongoing research collaborations, which I believe also helped me getting a post doc position to continue my career in academia.

Additionally, I want to thank all my collaborators for the countless hours we have been working on beautiful problems together.

I am also very thankful for the work of my reviewers of this thesis, Christian Krattenthaler and Brendon Rhoades and all the anonymous reviewers of my research articles that are also part of this document.

A PhD in Mathematics requires not only mathematical work but also personal commitment. Therefore, I want to thank all my friends and family members who have supported me along the way. In particular I want to thank my wife Sofie for her constant support and encouragement. Thank you for making it possible for me to go on international research stays and for our two lovely children Luisa and Valentin. I am grateful for your spirit of adventure going to Canada together.

I am also thankful for the support of my parents. You have supported me not only during my studies, but during my entire life.

Finally, I am much obliged to the Austrian Academy of Sciences (and therefore also to all Austrian taxpayers) for financially supporting my PhD with a DOC fellowship.





---

# CONTENTS

---

## Preamble

1	INTRODUCTION	13
1.1	Problem definition and Background . . . . .	13
1.2	Motivating Example . . . . .	14
1.3	A short introduction to crystal graphs . . . . .	16
2	SUMMARY OF MY RESEARCH	19
2.1	Existence of a diagrammatic basis for the adjoint representation of type $A$	19
2.2	Evaluating $f^\lambda(q, t)$ at roots of unity . . . . .	22
2.3	Explicit construction of chord diagrams . . . . .	22
2.3.1	Vector representation type $C$ . . . . .	24
2.3.2	Vector representation of type $A$ . . . . .	26
2.3.3	Spin representation of type $B$ . . . . .	27
2.3.4	Vector representation of type $B$ . . . . .	27

	Bibliography	29
--	--------------	----

## Publications

I	SKIEW CHARACTERS AND CYCLIC SIEVING	33
II	DESCENTS FOR BORDER STRIP TABLEAUX	69
III	GROWTH DIAGRAMS AND PROMOTION	85



## PREAMBLE



---

## INTRODUCTION

---

### 1.1 PROBLEM DEFINITION AND BACKGROUND

Given a simple Lie Group  $G$  and a representation  $U$ , it is an important problem to study different bases of the invariant space

$$(U^{\otimes n})^G = \{u \in U^{\otimes n} \mid g \cdot u = u \forall g \in G\},$$

where  $G$  acts on  $U^{\otimes n}$  diagonally, that is

$$g \cdot (u_1 \otimes \dots \otimes u_n) = (g \cdot u_1) \otimes \dots \otimes (g \cdot u_n) \quad g \in G.$$

In this thesis we explore methods to obtain purely combinatorial descriptions of a basis in terms of chord diagrams of this space.

**Definition 1.1.** A *chord diagram* of size  $n$  is a (possibly directed multi-) graph with  $n$  vertices arranged on a circle in the corners of a regular  $n$ -gon which are labelled  $1, \dots, n$  in counter-clockwise orientation. We denote the set of chord diagrams with  $n$  vertices with  $\mathcal{G}^n$ .

The *rotation* of a chord diagram is obtained by rotating all edges clockwise by  $\frac{2\pi}{n}$  around the center of the diagram.

There is also a natural action of the symmetric group  $\mathfrak{S}_n$  on  $U^{\otimes n}$ , permuting tensor positions:

$$\sigma \cdot (u_1 \otimes \dots \otimes u_n) = u_{\sigma^{-1}(1)} \otimes \dots \otimes u_{\sigma^{-1}(n)} \quad \sigma \in \mathfrak{S}_n.$$

This action commutes with the diagonal action of  $G$ . The action of the long cycle of the symmetric group can be regarded as an abstraction of rotation of chord diagrams, which motivates the general problem:

**Problem 1.2.** *Define a basis of the invariant space  $(U^{\otimes n})^G$  in terms of chord diagrams, such that the action of the long cycle on invariants and rotation of the diagrams coincide.*

We refer to such a basis as a *rotation invariant diagrammatic basis*. The motivation for studying the problem of finding a rotation invariant diagrammatic basis is Reiner, Stanton and White's cyclic sieving phenomenon, see [20].

The idea of using diagrams to index a basis of the invariant subspace of a tensor power of a representation goes back to Rumer, Teller and Weyl [21]. Specifically Brauer [3] constructed an invariant of the  $2n$ -th tensor power of the vector representation of the symplectic group  $\mathrm{Sp}(2r)$ , given a perfect matching of  $2n$  elements.

Furthermore, he showed that these invariants linearly span the invariant space. Using a result of Sundaram [25] one can show that the invariants obtained from perfect matchings without  $(r + 1)$ -crossings form a basis of this space. It is not hard to see that Brauer's construction translates rotation of the chord diagram to the action of the long cycle of the symmetric group on the corresponding invariant.

Other famous diagrammatic bases are Kuperberg's webs [13] for Lie algebras with rank  $r \leq 2$ .

In this thesis we first use Kashiwara crystal graphs [11] to translate Problem 1.2 into a purely combinatorial problem.

Crystal graphs are certain directed graphs with coloured edges. They are a means to translate from the language of representations to the language of combinatorics. In particular the set of isolated vertices in the crystal graph corresponds to a basis of the invariant space of the representation. The isolated vertices are called the *highest weight words / vertices / elements of weight zero*. For definitions see section 1.3.

Schützenberger's promotion operator on standard Young tableaux can be generalized to a bijection on these isolated vertices. As shown by Westbury [27, Thm. 6.7], promotion coincides, up to sign, with the action of the long cycle on the invariant tensors.

This reduces our problem to:

**Problem 1.3.** *Find a suitable set of chord diagrams and a bijection with highest weight words of weight zero such that rotation and promotion intertwine.*

In our setting all chord diagrams can be either directed or undirected graphs with possibly multiple edges between the same two vertices. We can therefore identify chord diagrams with  $n$  vertices with their *adjacency matrix*. This is a  $n \times n$  matrix  $M = (m_{ij})_{1 \leq i, j \leq n}$  with non-negative integer entries and  $m_{ij}$  denotes the number of edges between vertex  $i$  and vertex  $j$ . In the case of an undirected graph  $M$  is symmetric.

## 1.2 MOTIVATING EXAMPLE

The results of this section are well known and appear also in [13, Section 1]. Let  $V$  be the vector representation of  $SL(2)$ . For odd  $n$  the invariant subspace of  $V^{\otimes n}$  is trivial and for even  $n$  the highest weight words of weight zero in the corresponding crystal graph are words

$$w = w_n \otimes \cdots \otimes w_1$$

satisfying the following conditions:

1.  $w_i \in \{1, 2\}$  for each  $1 \leq i \leq n$ .
2.  $w$  is a *Yamanouchi* word: For each  $i$  the suffix  $w_i \otimes \cdots \otimes w_1$  contains at least as many ones as twos.
3.  $w$  is *balanced*: The number of ones equals the number of twos in the entire word.

They are in direct bijection with rectangular standard Young tableaux of size  $n$  with two rows. These are fillings of a  $2 \times (n/2)$  rectangle with the integers  $\{1, 2, \dots, n\}$  such that the the entries in each row are strictly increasing from left to right and the entries

in each column are strictly increasing from top to bottom. Let  $T$  be a rectangular standard Young tableau with two rows. One obtains a highest weight word of weight zero by setting

$$w_i = \begin{cases} 1 & \text{if } i \text{ is in the first row in } T, \\ 2 & \text{if } i \text{ is in the second row in } T \end{cases}$$

for each  $1 \leq i \leq n$ . It is an easy exercise to check that this is a bijection.

**Example 1.4.**  $2 \otimes 2 \otimes 1 \otimes 2 \otimes 1 \otimes 1 \otimes 2 \otimes 1 \otimes 2 \otimes 2 \otimes 2 \otimes 1 \otimes 2 \otimes 1 \otimes 1 \otimes 1$  is a highest weight word of weight zero. Its corresponding standard Young tableau is

1	2	3	5	9	11	12	14
4	6	7	8	10	13	15	16

*Schützenberger's promotion* bijectively maps the set of standard Young tableaux to itself as follows: Let  $T$  be a standard Young tableau. Its promotion  $\text{pr } T$  is the tableau obtained by the following procedure:

1. Delete the entry 1.
2. For an empty cell slide the unique adjacent entry to the right or below into this cell, such that rows and columns are still strictly increasing.
3. Perform the previous step until the empty cell has no adjacent entry to the right or below and fill the empty cell with  $n + 1$ . (For rectangular standard Young tableaux this is the case when the bottom right cell is empty.)
4. Subtract 1 from each entry.

**Example 1.5.** The promotion of 

1	2	3	5	9	11	12	14
4	6	7	8	10	13	15	16

 is 

1	2	3	4	6	10	13	15
5	7	8	9	11	12	14	16

.

A suitable set of chord diagrams is the set of *non crossing perfect matchings* of size  $n$ . These are undirected graphs such that each vertex has degree one and no two edges cross when drawing the chord diagram in a circle. We want to map non crossing perfect matchings to rectangular standard Young tableaux with two rows. For this we need the following terminology.

**Definition 1.6.** Let  $M$  be a non crossing perfect matching of size  $n$ . We denote its edges as pairs  $(a, b)$  with  $a < b$ . The *set of openers* is the set

$$o(M) = \{a : (a, b) \text{ is an edge of } M\}.$$

Similarly, the set of *set of closers* is the set

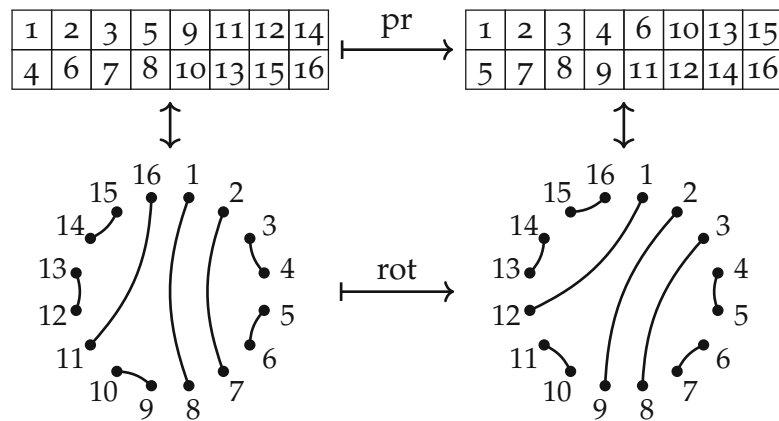
$$c(M) = \{b : (a, b) \text{ is an edge of } M\}.$$

It is easy to verify the following:

**Theorem 1.7.** Let  $M$  be a non crossing perfect matching of size  $n$ . Let  $T(M)$  be the filled  $2 \times (n/2)$  rectangle obtained by writing  $o(M)$  in increasing order from left to right into the first row and writing  $c(M)$  in increasing order from left to right into the second row.

The map  $M \mapsto T(M)$  is a bijection between non crossing perfect matchings of size  $n$  and rectangular standard Young tableaux of size  $n$  with two rows. This map intertwines rotation of the matching with promotion of the tableau.

**Example 1.8.** This commutative diagrams visualises the theorem above.



In the setting of this thesis this means:

**Theorem 1.9.** *The set of non crossing perfect matchings is a rotation invariant diagrammatic basis for  $(V^{\otimes n})^{SL(2)}$ .*

### 1.3 A SHORT INTRODUCTION TO CRYSTAL GRAPHS

In this subsection we provide some background information on crystals and their tensor products and minuscule representations. A detailed introduction can be found in [4] and [8].

Given a root system  $\Phi$  with weight lattice  $\Lambda$  and a dominant weight  $\lambda$ , we associate to the irreducible representation  $V(\lambda)$  its *crystal graph*  $B_\lambda$ . This is a certain connected edge-coloured digraph with  $\dim V(\lambda)$  vertices, each labelled with a weight of the representation. Each edge of the crystal graph is labelled with one of the simple roots of the root system, such that the weight of the target of the edge is obtained from the weight of its source by subtracting the simple root. The edges correspond to the *Kashiwara lowering operators*. There is a unique vertex without in-coming edges, the *highest weight vertex*, and this vertex has weight  $\lambda$ . There is also a unique vertex without out-going edges, the *lowest weight vertex*. The sum of the formal exponentials of the weights of the vertices is the character of the representation. In particular, isomorphism of crystal graphs corresponds to isomorphism of representations. The direct sum of representations is then associated with the disjoint union of the corresponding crystal graphs.

There is a (relatively) simple way to construct the crystal graph of a tensor product of representations given their individual crystal graphs. The vertices of the tensor product  $C_1 \otimes \cdots \otimes C_n$  of crystal graphs, corresponding to an  $n$ -fold tensor product of representations  $U_1, \dots, U_n$  of  $G$ , are the words of length  $n$  whose  $i$ -th letter is a vertex of  $C_i$ . The weight of a vertex in the tensor product is the sum of the weights of its letters. In this context, we refer to the highest weight vertices of the connected components as *highest weight words*. Isolated vertices correspond to copies of the trivial representation and have weight zero. They are referred to as *highest weight words of weight zero*. We denote the set of highest weight words of weight zero with  $(\otimes C_i)_*$ .



**Remark 1.10.** Note that there are two conventions for the order tensor factors. As a set the tensor product is the Cartesian product of the crystals. In Kashiwara's definition the ordered pair  $(x, y)$  is denoted with  $x \otimes y$ . In the alternative definition by Bump and Schilling the pair is written as  $y \otimes x$ .

In this thesis we are using the Bump–Schilling convention and I want to apologize to readers of my other publications. As a rule of thumb: If I have published the paper together with Anne Schilling we are using Bump–Schilling convention. If I have published the paper together with other authors, e.g. Gaetz, Pechenik, Rubey, Striker, Swanson, Westbury, the paper uses Kashiwara's convention.

In general the connected components of  $C_1 \otimes \cdots \otimes C_n$  correspond to the irreducible representations in the decomposition

$$\bigotimes U_i \cong \bigoplus_{\mu \in \Lambda^+} V(\mu)^{\oplus n_\mu},$$

where  $\Lambda^+$  is the set of dominant weights. By definition the invariant space  $(U^{\otimes n})^G$  is isomorphic to the direct sum of one-dimensional irreducible representations in the decomposition. A basis of this space is thus indexed by the connected components with only one vertex, which are given by the highest weight words of weight zero.

We can now define promotion on highest weight words of weight zero and of length  $n$  as follows:

**Definition 1.11** ([27]).  $\text{pr} : (C_1 \otimes \cdots \otimes C_n)_* \rightarrow (C_2 \otimes \cdots \otimes C_n \otimes C_1)_*$  is the map given by the following procedure. Let  $w = w_n \otimes w_{n-1} \otimes \cdots \otimes w_1 \in (C_1 \otimes \cdots \otimes C_n)_*$  be a highest weight vector and assume without loss of generality that  $C_1$  is connected (otherwise we can replace  $C_1$  by the connected component of  $C_1$  containing  $w_1$ ).

- Remove the last letter  $w_1$  of  $w$ , which is the highest weight of  $C_1$ . This leaves a word  $w' = w_n \otimes \cdots \otimes w_2$  which is a lowest weight word.
- Apply the Kashiwara raising operators to obtain a highest weight word  $w''$  in the same component as  $w'$ .
- Prepend the lowest weight of  $C_1$  to the beginning of  $w''$  giving  $\text{pr} w$ .

This map satisfies the identity  $\text{pr}^n = \text{id}$  in all cases relevant to this thesis. It is important to remark that this generalises Schützenberger's promotion map on standard Young tableaux.

Also note that a crystal isomorphism is uniquely determined by the images of highest weight elements and therefore promotion can be extended to a crystal isomorphism

$$\text{pr} : C_1 \otimes \cdots \otimes C_n \rightarrow C_2 \otimes \cdots \otimes C_n \otimes C_1.$$

This isomorphism agrees with the *crystal commutor*  $\sigma_{A,B} : A \otimes B \rightarrow B \otimes A$  defined by Henriques and Kamnitzer [7] with  $A = C_1$  and  $B = C_2 \otimes \cdots \otimes C_n$ .

Due to theorem III.27 by Lennart [14, Thm. 4.4] the crystal commutor can be easily obtained for highest weight words in tensor products of minuscule representations. A representation of a Lie group is *minuscule* if its Weyl group  $W$  acts transitively on the

weights of the representation: the set of weights forms a single orbit under the action of  $W$ .

For a minuscule representation  $V(\lambda)$  of dominant weight  $\lambda$ , the vertices of the associated crystal graph  $B_\lambda$  can be identified with the weights of  $V(\lambda)$ . The edges are given by the Kashiwara lowering operators, as follows. Let  $\{\alpha_i : i \in I\}$  be the set of simple roots and  $s_i \in W$  be the simple reflection corresponding to  $\alpha_i$ . Then there is a coloured edge  $\mu \xrightarrow{i} \mu - \alpha_i$  provided that  $s_i(\mu) = \mu - \alpha_i$ .

---

SUMMARY OF MY RESEARCH

---

In the following we briefly summarize my (partial) solutions to problem 1.2. The corresponding publications are collected in the second part of this thesis.

Recall that dominant weights of  $SL(r)$ ,  $Sp(2r)$  and  $SO(2r + 1)$  are vectors of length  $r$  with weakly decreasing non-negative integer entries. Therefore, dominant weights can be identified with integer partitions into at most  $r$  parts in these cases. A dominant weight of  $Spin(2r + 1)$  is a vector of length  $r$  with weakly decreasing non-negative half-integer entries, such that either all entries are integers or none of them. Finally, a dominant weight of  $GL(r)$  is a vector of length  $r$  with weakly decreasing integer entries, a so-called staircase.

To any highest weight word  $w = w_n \otimes \cdots \otimes w_1$  in a tensor product of crystals  $C_1 \otimes \cdots \otimes C_n$  we bijectively associate a sequence of dominant weights going under names like semistandard, oscillating, alternating, vacillating *tableau*.

Suppose now that in each crystal  $C_i$ ,  $1 \leq i \leq n$ , all vertices have distinct weight. For example, this is the case when all the  $C_i$  correspond to minuscule representations. Then the tableau is given by the sequence  $\emptyset = \mu^0, \mu^1, \dots, \mu^n = \mu$ , where  $\mu^q = \sum_{i=1}^q \text{wt}(w_i)$  is the sum of the weights of the first  $q$  letters from the right. In this case, one can recover the letters of the highest weight word via the successive differences  $\text{wt}(w_i) = \mu^i - \mu^{i-1}$ .

### 2.1 EXISTENCE OF A DIAGRAMMATIC BASIS FOR THE ADJOINT REPRESENTATION OF TYPE $A$

Results from this section are from our paper [2], which is Chapter I in this thesis.

Let  $\mathfrak{gl}_r$  be the adjoint representation of  $GL(r)$ . The highest weight words for  $(\mathfrak{gl}_r^{\otimes n})_*$  are corresponding to Stembridge's alternating tableaux [24]  $\mathcal{A}_n^{(r)}$ . An alternating tableau is a sequence of staircases  $\emptyset = \mu^0, \mu^1, \dots, \mu^{2n} = \mu$ , such that  $\mu^{2q} = \mu^{2q-1} - e_\ell$  for some  $\ell \leq r$ , and  $\mu^{2q+1} = \mu^{2q} + e_k$  for some  $k \leq r$ .

For  $r$  large enough, a suitable set of chord diagrams is the set of permutations of  $\{1, \dots, n\}$  and for  $r = 2$  a suitable set of chord diagrams is the set of noncrossing set partitions without singletons. An explicit bijection between alternating tableaux and these chord diagrams intertwining promotion and rotation is given in [19].

In this thesis we extend this result for arbitrary  $r$ , but instead of an explicit construction, our new result is of implicit nature.

Our results can be phrased in terms of V. Reiner, D. Stanton & D. White's cyclic sieving phenomenon.

**Definition 2.1** ([20]). Let  $X$  be a finite set and let  $\rho$  be a generator of an action of the cyclic group of order  $n$  on  $X$  and let  $f(q) \in \mathbb{N}_0[q]$  be a polynomial with non negative integer coefficients. Further, let  $\xi$  be a primitive  $n$ -th root of unity.

We say that the triple  $(X, \langle \rho \rangle, f(q))$  *exhibits the cyclic sieving phenomenon* if for all  $d \in \mathbb{Z}$

$$\#\{x \in X : \rho^d \cdot x = x\} = f(\xi^d).$$

Let  $\text{SYT}(\lambda)$  denote the set of all *standard Young tableaux* of shape  $\lambda$  and size  $n$ . An entry  $i$  of a standard Young tableau  $T$  is a *descent* of  $T$ , if  $i + 1$  appears in a strictly lower row in  $T$  in English notation. We denote with  $\text{maj}(T)$ , the *major index* of  $T$ , the sum of all descents of  $T$ .

**Theorem 2.2** (See Theorem I.44). *Let  $\lambda$  be a partition of  $n$  and let*

$$f^\lambda(q) := \sum_{T \in \text{SYT}(\lambda)} q^{\text{maj}(T)}$$

*be the generating function of the major index. Then there is a cyclic group action  $\rho$  of order  $n$  such that*

$$\left( \text{SYT}(\lambda) \times \text{SYT}(\lambda), \langle \rho \rangle, f^\lambda(q)^2 \right)$$

*exhibits the cyclic sieving phenomenon.*

We want to point out, that we can only prove the existence of  $\rho$ . For general  $\lambda$  no explicit action is known. In the proof, we use a characterization of P. Alexandersson & N. Amini [1], which says that  $f \in \mathbb{N}_0[q]$  is a cyclic sieving polynomial for a group action of the cyclic group of order  $n$ , if and only if for a primitive  $n$ -th root of unity  $\xi$  and all  $k \mid n$  we have that  $f(\xi^k) \in \mathbb{N}_0$  and

$$\sum_{d|k} \mu(k/d) f(\xi^d) \geq 0,$$

where  $\mu$  is the number-theoretic Möbius function.

Recall that the *Robinson–Schensted correspondence* provides a bijection between permutations of length  $n$  and pairs of standard Young tableaux of size  $n$  with the same shape.

**Definition 2.3.** The *shape*  $\text{sh}(\sigma)$  of a permutation  $\sigma$  is the common shape of the standard Young tableaux corresponding to  $\sigma$  under the Robinson–Schensted correspondence.

As a corollary we obtain:

**Theorem 2.4** (See Corollary I.56). *Let  $P_n$  be the set of partitions of  $n$ . Then there exists a map  $\text{st} : \mathfrak{S}_n \rightarrow P_n$  which is invariant under rotation and equidistributed with the Robinson–Schensted shape. That is,*

$$\text{st} \circ \text{rot} = \text{st} \quad \text{and} \quad \sum_{\sigma \in \mathfrak{S}_n} \mathbf{x}^{\text{st}(\sigma)} = \sum_{\sigma \in \mathfrak{S}_n} \mathbf{x}^{\text{sh}(\sigma)}.$$

Moreover, with  $\mathfrak{S}_n^\lambda := \{\pi \in \mathfrak{S}_n : \text{st}(\pi) = \lambda\}$ , the triple

$$\left( \mathfrak{S}_n^\lambda, \langle \text{rot} \rangle, f^\lambda(q)^2 \right)$$

*exhibits the cyclic sieving phenomenon.*

With this statistic we get a rotation invariant basis:

**Theorem 2.5** (See Theorem I.61). Let  $\mathfrak{S}_n^{(r)} := \{\pi \in \mathfrak{S}_n : \ell(\text{st}(\pi)) \leq r\} = \bigcup_{\substack{\lambda \vdash n \\ \ell(\lambda) \leq r}} \mathfrak{S}_n^\lambda$ .

Then there exists a bijection

$$\mathcal{P}^{(r)} : \mathcal{A}_n^{(r)} \rightarrow \mathfrak{S}_n^{(r)} \quad \text{with} \quad \mathcal{P}^{(r)} \circ \text{pr} = \text{rot} \circ \mathcal{P}^{(r)}.$$

for  $1 \leq r \leq n$ .

Equivalently, the action of promotion on the set of  $\mathfrak{gl}_r$ -alternating tableaux of length  $n$ , and the action of rotation on the set of permutations  $\mathfrak{S}_n^{(r)}$  are isomorphic:

$$(\text{pr}, \mathcal{A}_n^{(r)}) \cong (\text{rot}, \mathfrak{S}_n^{(r)}).$$

Again, we stress that we are unable to present such a statistic, and therefore the basis, explicitly.

**Problem 2.6.** Find an explicit combinatorial statistic (i.e. a map) satisfying Theorem 2.4.

In order to find an explicit statistic to solve Problem 2.6, it can be useful to find additional statistics, which refine Theorem 2.4.

**Definition 2.7.** We define the number of *excedences* of a permutation  $\sigma$  to be

$$\text{ex}(\sigma) = |\{i : \sigma(i) > i\}|$$

and the number of *descents* to be

$$\text{des}(\sigma) = |\{i : \sigma(i) > \sigma(i+1)\}|.$$

We conjecture the following refinement of Theorem 2.4.

**Conjecture 2.8.** Let

$$f^{\lambda,d}(q) := \sum_{T \in \text{SYT}(\lambda), \text{des}(T)=d} q^{\text{maj}(T)}.$$

There exists a map  $\text{st} : \mathfrak{S}_n \rightarrow P_n$  which is invariant under rotation, such that the pairs  $(\text{st}, \text{ex})$  and  $(\text{sh}, \text{des})$  are equidistributed. That is,

$$\text{st} \circ \text{rot} = \text{st} \quad \text{and} \quad \sum_{\sigma \in \mathfrak{S}_n} \mathbf{x}^{\text{st}(\sigma)} y^{\text{ex}(\sigma)} = \sum_{\sigma \in \mathfrak{S}_n} \mathbf{x}^{\text{sh}(\sigma)} y^{\text{des}(\sigma)}.$$

Moreover, with  $\mathfrak{S}_n^{\lambda,d} := \{\pi \in \mathfrak{S}_n : \text{st}(\pi) = \lambda, \text{ex}(\pi) = d\}$ , the triple

$$(\mathfrak{S}_n^{\lambda,d}, \langle \text{rot} \rangle, f^{\lambda,d}(q) \cdot f^\lambda(q))$$

exhibits the cyclic sieving phenomenon.

Instead of working with  $f^{\lambda,d}(q)$ , it is more convenient to work with the bivariate generating function

$$f^\lambda(q, t) := \sum_{T \in \text{SYT}(\lambda)} q^{\text{maj}(T)} t^{\text{des}(T)}.$$

## 2.2 EVALUATING $f^\lambda(q, t)$ AT ROOTS OF UNITY

Results from this section are taken from our paper [18], which is Chapter II of this thesis.

A first step in the direction of Conjecture 2.8 is a combinatorial interpretation of  $f^\lambda(\zeta, t)$ , where  $\zeta$  is a  $k$ -th primitive of unity.

For a filling  $B$  of a Young diagram  $\lambda$  with weakly increasing rows and columns, let  $B^i$  be the collection of cells in  $B$  containing  $i$ . We say that  $B$  is a *border strip tableau with strip size  $k$*  if, for all  $1 \leq i \leq \ell$ , the cells  $B^i$  form a connected skew shape of size  $k$  that does not contain a  $2 \times 2$  rectangle. We denote the set of all border strip tableaux with strip size  $k$  with  $\text{BST}(\lambda, k)$ .

If  $\text{BST}(\lambda, k)$  is not empty, we also say that  $\lambda$  has *empty  $k$ -core*. In this case, it turns out that  $f^\lambda(\zeta, t)$  is, up to sign, a generating function for a very natural statistic on this set.

**Theorem 2.9** (See Theorem II.8). *The statistic  $\text{des}^+$  on border strip tableaux (Definition II.7) has the following property: Let  $\lambda$  be a partition of  $n$  with empty  $k$ -core and let  $\zeta$  be a primitive  $k$ -th root of unity. Then, for some  $\epsilon_{\lambda, k} \in \{\pm 1\}$ ,*

$$f^\lambda(\zeta, t) = \epsilon_{\lambda, k} \cdot \sum_{B \in \text{BST}(\lambda, k)} t^{\text{des}^+(B)}.$$

This refines results of Springer [22, Proposition 4.5] and James & Kerber [10, Theorem 2.7.27], which imply that the evaluation of  $f^\lambda(q)$  at a  $k$ -th primitive root of unity yields the number of border strip tableaux with all strips of size  $k$ , up to sign.

## 2.3 EXPLICIT CONSTRUCTION OF CHORD DIAGRAMS

In the last Chapter III of this thesis, which consists of our publication [15], we present a new method to construct a rotation invariant diagrammatic basis.

For this we first need to embed the representation into a tensor product of minuscule representations. This is always possible, except for the types  $G_2$ ,  $F_4$  and  $E_8$ , where no non trivial minuscule representations exist.

A key ingredient for our approach is a calculation scheme for the crystal commutor and thus for promotion, due to Lenart [14], that makes use of van Leeuwen's local rules [26, Rule 4.1.1], which generalise Fomin's [23, A 1.2.7]. For minuscule representations, van Leeuwen's rules involve obtaining the unique dominant representative of a weight.

**Definition 2.10.** Let  $\lambda$  be a weight of a representation of a Lie group with Weyl group  $W$ . Then  $\text{dom}_W(\lambda)$  is the unique dominant representative of the  $W$ -orbit  $W\lambda$ .

Four weight vectors  $\lambda, \mu, \kappa, \nu \in \Lambda$  depicted in a square diagram  $\begin{array}{cc} \lambda & \nu \\ \square & \\ \kappa & \mu \end{array}$  satisfy the *local rule*, if  $\mu = \text{dom}_W(\kappa + \nu - \lambda)$ .

Let  $U$  be a representation embedded into a tensor product of the  $k$  minuscule representations  $U_1, \dots, U_k$ . Moreover let  $w \in (U^{\otimes n})_*$  be a highest weight word of

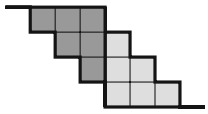
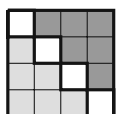
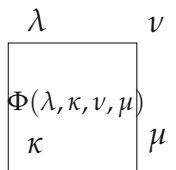
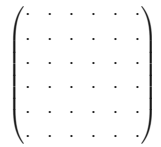
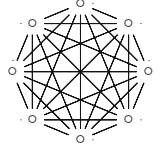
1. Compute promotion repeatedly using a calculation scheme	2. Cut and glue the schema to obtain a square	3. Fill all cells according to a function $\Phi$ with integers	4. Interpret the filled square as adjacency matrix of a graph	5. Read the chord diagram from the adjacency matrix.
				

Figure 1: Overview of the steps in our map

weight zero of length  $n$  and let  $\iota(w) = w_{k \cdot n} \otimes \dots \otimes w_2 \otimes w_1 \in ((U_1 \otimes \dots \otimes U_k)^{\otimes n})_*$  be the highest weight word corresponding to  $w$  of length  $k \cdot n$  using this embedding. Finally let  $T = (\emptyset = \mu^0, \mu^1, \dots, \mu^{k \cdot n} = \emptyset)$  be the corresponding tableau.

The local rules allow us to associate a  $(n \cdot k) \times (n \cdot k)$  square grid with the promotion orbit of  $T$ , where each corner is labelled with a dominant weight, which we call the *promotion matrix* of  $T$ .

Our aim is to construct the adjacency matrix of a chord diagram by filling each cell with a non negative integer. Formally, this is a function  $\Phi$  that depends on the four dominant weights labelling the corners of the cell, and yields a non negative integer.

This filling can then be regarded as an  $(n \cdot k) \times (n \cdot k)$ -adjacency matrix and we obtain a map  $(U^{\otimes n})_* \rightarrow \mathcal{G}^{k \cdot n}$ . This map intertwines promotion and  $k$ -step rotation. Depending on  $U$ , it may also be suitable to combine the vertices in groups of size  $k$  into a single vertex to obtain a function  $M : (U^{\otimes n})_* \rightarrow \mathcal{G}^n$ , that intertwines promotion and rotation.

Our construction is outlined in Figure 1 and can be summarized as follows:

**Construction 2.11.** STEP 1 Iteratively calculate promotion of a highest weight word of weight zero and length  $n$  using local rules and Lenart's scheme a total of  $n$  times.

STEP 2 Group the results into a square grid, called the *promotion matrix*.

STEP 3 Fill the cells of the square grid with certain non-negative integers according to a filling rule  $\Phi$  that only depends on the four corners of the cells in the square grid.

STEP 4 Regard the filling as the adjacency matrix of a graph, which is the chord diagram.

**Definition 2.12.** We denote the set appearing as image  $M((U^{\otimes n})_*)$  with  $\mathcal{G}_U^n$ .

Now we can obtain solutions for the general problem 1.2 by solving the following.

**Problem 2.13.** Fix a representation  $U$  embedded into a the tensor product of  $k$  minuscule representations. For this representation

- define a filling rule  $\Phi$  for promotion matrices,
- prove that  $M$  is injective for this filling rule,
- give a direct description of the image  $\mathcal{G}_U^n$ .

### 2.3.1 Vector representation type C

Let  $V$  be the vector representation of  $\mathrm{Sp}(2r)$ . This representation is minuscule and  $w$  is a highest weight word if and only if  $w_i$  is in  $\{\pm e_j : 1 \leq j \leq r\}$ , and  $\mu^q = \sum_{i=1}^q \mathrm{wt}(w_i)$  is dominant for  $q \leq n$ . The corresponding tableau is called an  $r$ -symplectic oscillating tableau. A suitable set of chord diagrams is the set of  $(r+1)$ -noncrossing perfect matchings of  $\{1, \dots, n\}$ . An explicit bijection between  $r$ -symplectic oscillating tableaux and these  $(r+1)$ -noncrossing perfect matchings intertwining promotion and rotation is given in [19]. We use our Construction 2.11 to obtain another description of the same map.

For the following example fix  $r = 3$ . Consider the oscillating tableau of weight zero

$$O = (000, 100, 200, 210, 211, 210, 110, 100, 000),$$

which corresponds to a highest weight word of weight zero in the crystal of  $V^{\otimes 8}$ . The Weyl group of  $\mathrm{Sp}(2r)$  is the hyperoctahedral group  $\mathfrak{S}_r$  of signed permutations of  $\{\pm 1, \dots, \pm r\}$ . Thus, the dominant representative  $\mathrm{dom}_{\mathfrak{S}_r}(\lambda)$  of a weight  $\lambda$  is obtained by sorting the absolute values of its entries into weakly decreasing order.

Lenart's calculation scheme gives the following

$$\begin{array}{cccccccc} 000 & 100 & 200 & 210 & 211 & 210 & 110 & 100 & 000 \\ & & 000 & 100 & 110 & 111 & 110 & 100 & 110 & 100 & 000 \end{array}$$

where the first row is the tableau  $O$  and the second row is calculated from the first by initializing with  $000$  and then recursively applying the local rules.

From this we can read off the promotion of  $O$ ,

$$\mathrm{pr} O = (000, 100, 110, 111, 110, 100, 110, 100, 000).$$

Now we iteratively apply promotion a total of eight times to obtain the following diagram.

$$\begin{array}{cccccccc} 000 & 100 & 200 & 210 & 211 & 210 & 110 & 100 & 000 \\ & 000 & 100 & 110 & 111 & 110 & 100 & 110 & 100 & 000 \\ & & 000 & 100 & 110 & 111 & 110 & 210 & 200 & 100 & 000 \\ & & & 000 & 100 & 110 & 111 & 211 & 210 & 110 & 100 & 000 \\ & & & & 000 & 100 & 110 & 210 & 211 & 111 & 110 & 100 & 000 \\ & & & & & 000 & 100 & 200 & 210 & 110 & 111 & 110 & 100 & 000 \\ & & & & & & 000 & 100 & 110 & 100 & 110 & 111 & 110 & 100 & 000 \\ & & & & & & & 000 & 100 & 110 & 210 & 211 & 210 & 200 & 100 & 000 \\ & & & & & & & & 000 & 100 & 200 & 210 & 211 & 210 & 110 & 100 & 000 \end{array}$$

Note that the first and last lines are equal and in this example the orbit of promotion has maximal length.



We now transform this diagram by copying everything to the right of the 8-th column into the triangular empty space on the left to obtain the promotion matrix.

	000	100	200	210	211	210	110	100	000
100	000	100	110	111	110	100	110	100	
200	100	000	100	110	111	110	210	200	
210	110	100	000	100	110	111	211	210	
211	111	110	100	000	100	110	210	211	
210	110	111	110	100	000	100	200	210	
110	100	110	111	110	100	000	100	110	
100	110	210	211	210	200	100	000	100	
000	100	200	210	211	210	110	100	000	

Note that the weights on the left and right border are equal by construction.

We now define a filling rule  $\Phi$  for the vector representation of the symplectic group.

**Definition 2.14.** The *filling rule* for oscillating tableaux is

$$\Phi(\lambda, \kappa, \nu, \mu) = \begin{cases} 1 & \text{if } \kappa + \nu - \lambda \text{ contains a negative entry,} \\ 0 & \text{else,} \end{cases} \quad (1)$$

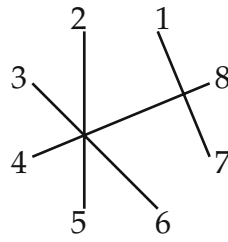
where the cells are labelled as depicted below:

$$\begin{array}{ccc} & \lambda & \nu \\ & \square & \\ \Phi(\lambda, \kappa, \nu, \mu) & & \\ \kappa & & \mu \end{array} \quad (2)$$

To improve readability we will leave cells with filling 0 empty. The filling 1 is rendered as a cross. We obtain:

	1	2	3	4	5	6	7	8	
	000	100	200	210	211	210	110	100	000
1							×		
	100	000	100	110	111	110	100	110	100
2					×				
	200	100	000	100	110	111	110	210	200
3						×			
	210	110	100	000	100	110	111	211	210
4								×	
	211	111	110	100	000	100	110	210	211
5		×							
	210	110	111	110	100	000	100	200	210
6			×						
	110	100	110	111	110	100	000	100	110
7	×								
	100	110	210	211	210	200	100	000	100
8				×					
	000	100	200	210	211	210	110	100	000

The chord diagram corresponding to this filling is a perfect matching with circular layout



One can verify the following:

**Theorem 2.15** (See Theorem III.50). Denote with  $M_O$  the function mapping an oscillating tableau to a chord diagram following above construction. Let  $V$  denote the vector representation of the symplectic group  $\mathrm{Sp}(2r)$ . Then  $M_O : (V^{\otimes 2n})_* \rightarrow \mathcal{G}^{2n}$  is an injection. The chord diagrams  $\mathcal{G}_V^{2n}$  are precisely the  $(r + 1)$ -non-crossing matchings of  $\{1, 2, \dots, 2n\}$  and the map coincides with the one given in [19].

### 2.3.2 Vector representation of type A

Let  $V$  be the vector representation of  $\mathrm{SL}(r)$ . Then the highest weight words can be identified with standard Young tableaux of size  $n$  with at most  $r$  rows: the position of the unique entry equal to 1 in  $w_i$  is the row of the tableau in which the number  $i$  appears. Since the weight lattice of  $\mathrm{SL}(r)$  is the image of  $\mathbb{Z}^r$  in the quotient of  $\mathbb{R}^r$  by the span of  $(1, \dots, 1)$ , a highest weight word has weight zero if and only if all  $r$  rows of the corresponding tableau have the same length.

A diagrammatic basis for the invariant space was constructed by Cautis, Kamnitzer and Morrison [5], generalising Kuperberg's webs for  $\mathrm{SL}(2)$  and  $\mathrm{SL}(3)$ , see [13]. However, only Kuperberg's web bases are preserved by rotation. For these, Petersen, Pylyavskyy and Rhoades [17] demonstrated that the growth algorithm of Khovanov and Kuperberg in [12] intertwines promotion with rotation. Their result was then generalised by Patrias [16] to the invariant space of a tensor product containing not only  $V$  but also its dual  $V^*$  in arbitrary order.

The first generalisation to higher rank was recently achieved by the author of thesis in joint work with Gaetz, Pechenik, Striker and Swanson [6], which is not part of this thesis. An important notion in this work are promotion permutations, which are fillings of the promotion diagram that are essentially given by the following filling rule.

**Definition 2.16.** The *filling rule* for rectangular standard Young tableaux is

$$\Phi(\lambda, \kappa, \nu, \mu) = \begin{cases} 1 & \text{if } \nu - \lambda \neq \mu - \kappa, \\ 0 & \text{else} \end{cases}, \quad (3)$$

where the cells are labelled as in (2).

In Section 1.2 we have seen a bijection between the set of rectangular standard Young tableaux of size  $2n$  and non crossing perfect matchings with  $2n$  vertices. It is straight forward to see, that this bijection can be recovered by our construction using the filling rule (3).

### 2.3.3 Spin representation of type B

Let  $S$  be the spin representation of the spin group  $\text{Spin}(2r + 1)$  and let  $\lambda_i = \frac{1}{2} \sum_{j=1}^r e_j$  be its dominant weight. Then  $w$  is a highest weight word if and only if  $w_i = (\pm \frac{1}{2}, \dots, \pm \frac{1}{2})$  and  $\mu^q$  is dominant for all  $q \leq n$ .

Therefore, a highest weight word  $w$  of weight zero can be identified with a fan of  $r$  Dyck paths of length  $n$ : the first entry of  $w_i$  is  $\frac{1}{2}$  if and only if the top most Dyck path has an up-step at position  $i$ . In general, the  $j$ -th entry of  $w_i$  is  $\frac{1}{2}$  if and only if the  $j$ -th Dyck path has an up-step at position  $i$ .

**Definition 2.17.** The *filling rule* for fans of Dyck paths is

$$\Phi(\lambda, \kappa, \nu, \mu) = \text{number of negative entries in } \kappa + \nu - \lambda, \quad (4)$$

where the cells are labelled as in (2).

**Theorem 2.18** (See Theorem III.51). Denote with  $M_F$  the function mapping a  $r$ -fan of Dyck paths to a chord diagram using the filling rule (4). Then  $M_F : (S^{\otimes n})_* \rightarrow \mathcal{G}^n$  is an injection that intertwines promotion and rotation.

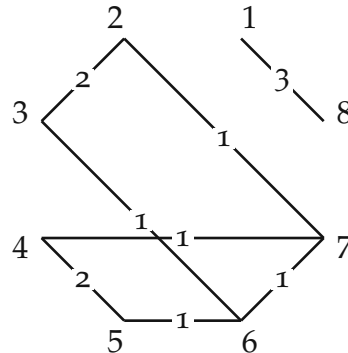
Thus the image of this map gives a rotation invariant diagrammatic basis, but we do not know a nice direct characterisation of the set of chord diagrams obtained by this construction for arbitrary  $r$ .

**Example 2.19.** Consider the 3-fan of Dyck paths of length 8

$$F = (000, 111, 222, 311, 422, 331, 222, 111, 000).$$

We obtain:

$$M_F(F) = \begin{pmatrix} 0 & 0 & 0 & 0 & 0 & 0 & 0 & 0 & 3 \\ 0 & 0 & 2 & 0 & 0 & 0 & 1 & 0 & 0 \\ 0 & 2 & 0 & 0 & 0 & 1 & 0 & 0 & 0 \\ 0 & 0 & 0 & 0 & 2 & 0 & 1 & 0 & 0 \\ 0 & 0 & 0 & 2 & 0 & 1 & 0 & 0 & 0 \\ 0 & 0 & 1 & 0 & 1 & 0 & 1 & 0 & 0 \\ 0 & 1 & 0 & 1 & 0 & 1 & 0 & 0 & 0 \\ 3 & 0 & 0 & 0 & 0 & 0 & 0 & 0 & 0 \end{pmatrix}$$



### 2.3.4 Vector representation of type B

Let  $V$  be the vector representation of  $\text{SO}(2r + 1)$  and let  $\lambda_i = e_1$  be its dominant weight. Then  $w$  is a highest weight word if and only if  $w_i$  is in  $\{\pm e_j : 1 \leq j \leq r\} \cup \{0\}$ ,  $\mu^q$  is dominant for  $q \leq n$  and  $w_i \neq 0$  if  $\mu^{i-1}$  contains an entry equal to 0. The corresponding tableaux are called vacillating tableaux<sup>1</sup> and can be identified with  $r$ -fans of Riordan paths, see [9].

Note that  $V$  is not minuscule. We can use two workarounds:

<sup>1</sup> The name *vacillating tableaux* also appears in the context of partition algebras with a different meaning.

- Embed  $V$  in the tensor product  $S \otimes S$  to obtain a map  $\iota_{V \rightarrow F}$  from vacillating tableaux to  $r$ -fans of Dyck paths.
- Use *virtual crystals* to obtain a map  $\iota_{V \rightarrow O}$  from vacillating tableaux to oscillating tableaux of twice the length.

Combining these maps with the constructions  $M_F$  and  $M_O$ , respectively, we obtain the maps  $M_{V \rightarrow F}$  and  $M_{V \rightarrow O}$ .

Our main result for vacillating tableaux is:

**Theorem 2.20** (See III.57). *The maps  $M_{V \rightarrow F}$  and  $M_{V \rightarrow O}$  are injective and intertwine promotion and rotation. Moreover, for a vacillating tableau  $V$  we have*

$$M_{V \rightarrow O}(V) = M_{V \rightarrow F}(V).$$

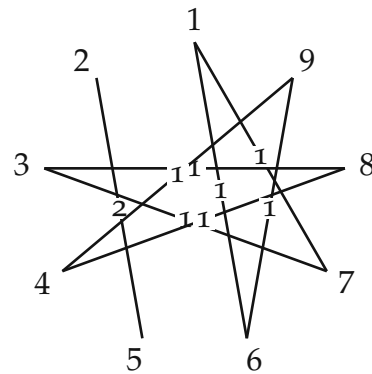
Thus the image of this map gives a rotation invariant diagrammatic basis, but we do not know any direct characterisation of the set of chord diagrams obtained by this construction.

**Example 2.21.** Let  $V = (000, 100, 200, 210, 211, 111, 111, 110, 100, 000)$  a vacillating tableau. We can map this to the oscillating tableau

$$\iota_{V \rightarrow O}(V) = (000, 100, 200, 300, 400, 410, 420, 421, 422, 322, 222, 221, 222, 221, 220, 210, 200, 100, 000).$$

This gives the chord diagram:

$$M_{V \rightarrow O}(V) = \begin{pmatrix} 0 & 0 & 0 & 0 & 0 & 1 & 1 & 0 & 0 \\ 0 & 0 & 0 & 0 & 2 & 0 & 0 & 0 & 0 \\ 0 & 0 & 0 & 0 & 0 & 0 & 1 & 1 & 0 \\ 0 & 0 & 0 & 0 & 0 & 0 & 0 & 1 & 1 \\ 0 & 2 & 0 & 0 & 0 & 0 & 0 & 0 & 0 \\ 1 & 0 & 0 & 0 & 0 & 0 & 0 & 0 & 1 \\ 1 & 0 & 1 & 0 & 0 & 0 & 0 & 0 & 0 \\ 0 & 0 & 1 & 1 & 0 & 0 & 0 & 0 & 0 \\ 0 & 0 & 0 & 1 & 0 & 1 & 0 & 0 & 0 \end{pmatrix}$$



---

## BIBLIOGRAPHY

---

- [1] P. ALEXANDERSSON AND N. AMINI, *The cone of cyclic sieving phenomena*, *Discrete Mathematics*, 342 (2019), pp. 1581–1601.
- [2] P. ALEXANDERSSON, S. PFANNERER, M. RUBEY, AND J. UHLIN, *Skew characters and cyclic sieving*, *Forum of Mathematics, Sigma*, 9 (2021), p. e41.
- [3] R. BRAUER, *On algebras which are connected with the semisimple continuous groups*, *Ann. of Math. (2)*, 38 (1937), pp. 857–872.
- [4] D. BUMP AND A. SCHILLING, *Crystal bases*, World Scientific Publishing Co. Pte. Ltd., Hackensack, NJ, 2017. Representations and combinatorics.
- [5] S. CAUTIS, J. KAMNITZER, AND S. MORRISON, *Webs and quantum skew Howe duality*, *Math. Ann.*, 360 (2014), pp. 351–390.
- [6] C. GAETZ, O. PECHENIK, S. PFANNERER, J. STRIKER, AND J. P. SWANSON, *Rotation-invariant web bases from hourglass plabic graphs*, *ArXiv e-prints*, (2023).
- [7] A. HENRIQUES AND J. KAMNITZER, *Crystals and coboundary categories*, *Duke Math. J.*, 132 (2006), pp. 191–216.
- [8] J. HONG AND S.-J. KANG, *Introduction to quantum groups and crystal bases*, vol. 42 of *Graduate Studies in Mathematics*, American Mathematical Society, Providence, RI, 2002.
- [9] J. JAGENTEUFEL, *A Sundaram type bijection for  $SO(3)$ : vacillating tableaux and pairs of standard Young tableaux and orthogonal Littlewood-Richardson tableaux*, *Electron. J. Combin.*, 25 (2018), pp. Paper 3.50, 44.
- [10] G. JAMES AND A. KERBER, *The Representation Theory of the Symmetric Group*, Cambridge University Press, Dec. 1984.
- [11] M. KASHIWARA, *On crystal bases*, in *Representations of groups (Banff, AB, 1994)*, vol. 16, Amer. Math. Soc., Providence, RI, 1995, pp. 155–197.
- [12] M. KHOVANOV AND G. KUPERBERG, *Web bases for  $sl(3)$  are not dual canonical*, *Pacific J. Math.*, 188 (1999), pp. 129–153.
- [13] G. KUPERBERG, *Spiders for rank 2 Lie algebras*, *Comm. Math. Phys.*, 180 (1996), pp. 109–151.
- [14] C. LENART, *On the combinatorics of crystal graphs. II. The crystal commutor*, *Proc. Amer. Math. Soc.*, 136 (2008), pp. 825–837.

- [15] J. PAPPE, S. PFANNERER, A. SCHILLING, AND M. C. SIMONE, *Promotion and growth diagrams for fans of dyck paths and vacillating tableaux*, *Journal of Algebra*, 655 (2024), pp. 794–842. Special Issue dedicated to the memory of Georgia Benkart.
- [16] R. PATRIAS, *Promotion on generalized oscillating tableaux and web rotation*, *J. Combin. Theory Ser. A*, 161 (2019), pp. 1–28.
- [17] T. K. PETERSEN, P. PYLYAVSKYY, AND B. RHOADES, *Promotion and cyclic sieving via webs*, *J. Algebraic Combin.*, 30 (2009), pp. 19–41.
- [18] S. PFANNERER, *A refinement of the Murnaghan-Nakayama rule by descents for border strip tableaux*, *Combinatorial Theory*, 2 (2022).
- [19] S. PFANNERER, M. RUBEY, AND B. WESTBURY, *Promotion on oscillating and alternating tableaux and rotation of matchings and permutations*, *Algebr. Comb.*, 3 (2020), pp. 107–141.
- [20] V. REINER, D. STANTON, AND D. WHITE, *The cyclic sieving phenomenon*, *J. Combin. Theory Ser. A*, 108 (2004), pp. 17–50.
- [21] G. RUMER, E. TELLER, AND H. WEYL, *Eine für die Valenztheorie geeignete Basis der binären Vektorinvarianten*, *Nachrichten von der Gesellschaft der Wissenschaften zu Göttingen, Mathematisch-Physikalische Klasse*, 1932 (1932), pp. 499–504.
- [22] T. A. SPRINGER, *Regular elements of finite reflection groups*, *Inventiones Mathematicae*, 25 (1974), pp. 159–198.
- [23] R. STANLEY, *Enumerative combinatorics. Vol. 2*, vol. 62 of Cambridge Studies in Advanced Mathematics, 1999.
- [24] J. STEMBRIDGE, *Rational tableaux and the tensor algebra of  $gl_n$* , *J. Combin. Theory Ser. A*, 46 (1987), pp. 79–120.
- [25] S. SUNDARAM, *On the combinatorics of representations of the symplectic group*, 1986. Thesis (Ph.D.)–Massachusetts Institute of Technology.
- [26] M. A. A. VAN LEEUWEN, *An analogue of jeu de taquin for Littelmann’s crystal paths*, *Sém. Lothar. Combin.*, 41 (1998), pp. Art. B41b, 23 pp. (electronic).
- [27] B. WESTBURY, *Invariant tensors and the cyclic sieving phenomenon*, *Electron. J. Combin.*, 23 (2016), pp. Research Paper 25, 40 pp. (electronic).

## PUBLICATIONS





---

 SKEW CHARACTERS AND CYCLIC SIEVING
 

---

## BIBLIOGRAPHIC INFORMATION

Alexandersson P., Pfannerer S., Rubey M. and Uhlin J. Skew characters and cyclic sieving. *Forum of Mathematics, Sigma*. 9:e41, 2021, [doi:10.1017/fms.2021.11](https://doi.org/10.1017/fms.2021.11)

## TABLE OF CONTENTS

Abstract . . . . .	33
1.1 Introduction . . . . .	34
1.1.1 Outline of the paper . . . . .	35
1.2 Cyclic group actions and cyclic sieving . . . . .	36
1.3 Some properties of skew Schur functions . . . . .	38
1.4 Skew characters and their fake degrees . . . . .	39
1.5 Skew border-strip tableaux and the abacus . . . . .	41
1.6 Skew characters and border-strip tableaux . . . . .	48
1.7 Bounds on the number of border-strip tableaux . . . . .	50
1.7.1 Bounds on multinomial coefficients . . . . .	50
1.7.2 The bound for standard Young tableaux of straight shape . . . . .	52
1.7.3 The bound for skew standard Young tableaux . . . . .	56
1.7.4 The general case . . . . .	57
1.8 Cyclic sieving for skew standard tableaux . . . . .	58
1.9 Permutations and invariants of the adjoint representation of $GL_n$ . . . . .	62
Bibliography . . . . .	66

## ABSTRACT

In 2010, B. Rhoades proved that promotion on rectangular standard Young tableaux together with the associated fake-degree polynomial provides an instance of the cyclic sieving phenomenon.

We extend this result to  $m$ -tuples of skew standard Young tableaux of the same shape, for fixed  $m$ , subject to the condition that the  $m^{\text{th}}$  power of the associated fake-degree polynomial evaluates to nonnegative integers at roots of unity. However, we are unable to specify an explicit group action.

Put differently, we determine in which cases the  $m^{\text{th}}$  tensor power of a skew character of the symmetric group carries a permutation representation of the cyclic group.

To do so, we use a method proposed by N. Amini and the first author, which amounts to establishing a bound on the number of border-strip tableaux of skew shape.

Finally, we apply our results to the invariant theory of tensor powers of the adjoint representation of the general linear group. In particular, we prove the existence of a bijection between permutations and J. Stembridge's alternating tableaux, which intertwines rotation and promotion.

## I.1 INTRODUCTION

We determine which tensor powers of a skew character  $\chi^{\lambda/\mu}$  of the symmetric group  $\mathfrak{S}_n$  carry a permutation representation of the cyclic group of order  $n$ .

This problem can be rephrased in terms of V. Reiner, D. Stanton & D. White's *cyclic sieving phenomenon* [19]. Let  $\text{SYT}(\lambda/\mu)$  be the set of standard Young tableaux of skew shape  $\lambda/\mu$ , and let  $f^{\lambda/\mu}(q)$  be G. Lusztig's fake degree polynomial for  $\chi^{\lambda/\mu}$ . Then there exists an action  $\rho$  of the cyclic group of order  $n = |\lambda/\mu|$  such that

$$\left( \underbrace{\text{SYT}(\lambda/\mu) \times \cdots \times \text{SYT}(\lambda/\mu)}_m, \langle \rho \rangle, f^{\lambda/\mu}(q)^m \right)$$

exhibits the cyclic sieving phenomenon, if and only if  $f^{\lambda/\mu}$  evaluates to nonnegative integers at  $n^{\text{th}}$  roots of unity. If  $m$  is even this is always the case. If  $m$  is odd, this is the case if and only if there exists a tiling of  $\lambda/\mu$  with border-strips of size  $k$  of even height for every  $k \mid n$ , see Theorem I.44.

We also show that for any skew shape  $\lambda/\mu$  and any integer  $s > 0$  there is an action  $\tau$  of the cyclic group of order  $s$  on *stretched shapes* such that

$$\left( \text{SYT}(s\lambda/s\mu), \langle \tau \rangle, f^{s\lambda/s\mu}(q) \right)$$

exhibits the cyclic sieving phenomenon, see Theorem I.49.

At this point we are unable to present  $\rho$  and  $\tau$  explicitly for general skew shapes  $\lambda/\mu$ . Instead, we use a characterization of P. Alexandersson & N. Amini [1], which says that  $f \in \mathbb{N}_0[q]$  is a cyclic sieving polynomial for a group action of the cyclic group of order  $n$ , if and only if for a primitive  $n^{\text{th}}$  root of unity  $\zeta$  and all  $k \mid n$  we have that  $f(\zeta^k) \in \mathbb{N}_0$  and

$$\sum_{d|k} \mu(k/d) f(\zeta^d) \geq 0,$$

where  $\mu$  is the number-theoretic Möbius function.

To apply this result, we establish a new bound for the absolute value of the skew character evaluated at a power of the long cycle. More precisely, Theorem I.31 implies that, for any  $k \mid n$ ,

$$|f^{\lambda/\mu}(\zeta^k)| \geq \sum_{d|k, d < k} |f^{\lambda/\mu}(\zeta^d)|$$

provided  $|f^{\lambda/\mu}(\xi^k)| \geq 2$ .

To prove this inequality, we note that  $|f^{\lambda/\mu}(\xi^d)| = |\chi^{\lambda/\mu}((m^d))| = |\text{BST}(\lambda/\mu, m)|$ , the number of border-strip tableaux of shape  $\lambda/\mu$  with strips of size  $m$ , extending the theorems for straight shapes by T. Springer [27] and G. James & A. Kerber [10]. We then approximate the number of border-strip tableaux using a bound by S. Fomin & N. Lulov [8].

Our main motivation is an implication for the invariant theory of the general linear group, as we now explain. Let  $\mathfrak{gl}_r$  be the adjoint representation of  $\text{GL}_r$ , and consider its  $n^{\text{th}}$  tensor power  $\mathfrak{gl}_r^{\otimes n}$ . The symmetric group  $\mathfrak{S}_n$  acts on this space by permuting tensor positions. Thus, using Schur–Weyl duality, we can determine the subspace of  $\text{GL}_n$ -invariants of  $\mathfrak{gl}_r^{\otimes n}$ , regarded as a representation of  $\mathfrak{S}_n$ . This representation turns out to be isomorphic to

$$\bigoplus_{\substack{\lambda \vdash n \\ \ell(\lambda) \leq r}} S_\lambda \otimes S_\lambda,$$

where the direct sum is over all partitions of  $n$  into at most  $r$  parts, and  $S_\lambda$  is the irreducible representation of  $\mathfrak{S}_n$  corresponding to  $\lambda$ . In particular, for  $r \geq n$ , the dimension of the space of invariants equals the size of  $\mathfrak{S}_n$ .

A fundamental question of invariant theory is to find an explicit basis of the space of invariants, which, if possible, enjoys further desirable properties. One such property is invariance under rotation of tensor positions, following G. Kuperberg’s idea of web bases [12].

An elegant and useful solution would be to describe a set of permutations in  $\mathfrak{S}_n$ , and a bijection from these to the basis elements which intertwines rotation of permutations (that is, conjugation with the long cycle) and rotation of tensor positions. It would be even nicer if this set of permutations for the invariants of  $\mathfrak{gl}_r^{\otimes n}$  were a subset of the set of permutations for the invariants of  $\mathfrak{gl}_{r+1}^{\otimes n}$ .

Although it appears to be difficult to exhibit such an intertwining bijection explicitly, our results, combined with previous work of S. Pfannerer, M. Rubey & B. Westbury [17], implies that such a solution must exist, see Theorem I.61.

The existence of such an intertwining bijection is closely related to the existence of a rotation invariant statistic  $\text{st}$  mapping permutations to partitions, such that  $|\{\sigma \in \mathfrak{S}_n : \text{st}(\sigma) = \lambda\}| = |\text{SYT}(\lambda) \times \text{SYT}(\lambda)|$ , see Corollary I.56.

### I.1.1 Outline of the paper

In Section I.2 we recall the definition of the cyclic sieving phenomenon and establish the connection with characters of cyclic group actions. In Sections I.3 to I.6 we generalize T. Springer’s theorem to skew shapes and show, using the Murnaghan–Nakayama rule, the abacus of G. James & A. Kerber and the Littlewood map, that the character evaluation of a skew character is, up to sign, equal to a certain number of border-strip tableaux. We stress that these identities are known for the straight shape case. However, they are somewhat underappreciated gems which deserve more attention.

In Section I.7 we provide the crucial bound on the number of border-strip tableaux of given shape, building on the approximation of S. Fomin & N. Lulov. In Section I.8

we use this bound and the characterization of P. Alexandersson & N. Amini to prove the existence of the group actions announced above for skew standard tableaux.

Finally in Section I.9 we apply our results to permutations and the invariant theory of the adjoint representation of the general linear group.

## I.2 CYCLIC GROUP ACTIONS AND CYCLIC SIEVING

In this section we recall V. Reiner, D. Stanton & D. White's cyclic sieving phenomenon, characters of cyclic group actions and a result of P. Alexandersson & N. Amini characterizing characters arising from cyclic group actions. We also recall R. Brauer's permutation lemma, which guarantees that two actions of the cyclic group which have the same character as linear representations are even isomorphic as group actions.

**Definition I.1** ([19]). Let  $X$  be a finite set and let  $\rho$  be a generator of an action of the cyclic group of order  $n$  on  $X$ .

Given a polynomial  $f(q) \in \mathbb{N}_0[q]$  we say that the triple  $(X, \langle \rho \rangle, f(q))$  *exhibits the cyclic sieving phenomenon* if for all  $d \in \mathbb{Z}$

$$\#\{x \in X : \rho^d \cdot x = x\} = f(\xi^d),$$

where  $\xi$  is a primitive  $n^{\text{th}}$  root of unity. In this case  $f(q)$  is a *cyclic sieving polynomial* for the group action.

In particular, the cardinality of  $X$  is given by  $f(1)$ . More generally, realizing the cyclic group of order  $n$  as the group of  $n^{\text{th}}$  roots of unity and identifying its ring of characters with  $\mathbb{Z}[q]/(q^n - 1)$ , the cyclic sieving polynomial  $f(q)$  modulo  $q^n - 1$  reduces to the character of the group action.

The cyclic sieving phenomenon owes its name to the fact that, mysteriously often, the most natural  $q$ -analogue of the counting formula for the cardinality of  $X$  as a function of  $n$  is a cyclic sieving polynomial. In many cases, the only known way to prove that a given  $q$ -analogue indeed is a cyclic sieving polynomial is to enumerate the number of fixed points of the group action, and verify that the evaluation of the polynomial yields the same number.

**Remark I.2.** If  $(X, \langle \rho \rangle, f(q))$  exhibits the cyclic sieving phenomenon, then so does  $(X, \langle \rho^k \rangle, f(q))$  for any positive integer  $k$ , which restricts the group action to a subgroup. Moreover, for any positive integer  $m$ , the triple  $(X^m, \langle \rho \rangle, f(q)^m)$ , where  $\langle \rho \rangle$  acts on  $X^m$  via  $\rho \cdot (x_1, \dots, x_m) = (\rho \cdot x_1, \dots, \rho \cdot x_m)$ , also exhibits the cyclic sieving phenomenon.

Much attention has been given to prove cyclic sieving phenomena on certain families of tableaux, see Table 1. Most famously, B. Rhoades showed that  $\text{SYT}(a^b)$  exhibits the cyclic sieving phenomenon, where the group action is promotion and the cyclic sieving polynomial is the fake degree polynomial  $f^\lambda(q)$  associated with  $\lambda = (a^b)$ . There are now several alternative proofs of this result, notably [18], [9], [31] and [32]. For an overview of some of these approaches, see [20].

It turns out that it is possible to determine whether a polynomial reduces modulo  $q^n - 1$  to the character of a cyclic group action of order  $n$ .

Set	Group action	Statistic/ $f(q)$	Reference
$\text{SYT}(a^b)$	Promotion	maj	[21]
$\text{SYT}((n-m, 1^m))$	Promotion <sup>†</sup>	$[n-1]_q$	[5]
$\text{SYT}(\lambda)$	Evacuation <sup>‡</sup>	maj	[30]
$\text{SSYT}(a^b, k)$	$k$ -promotion	$q^{-\kappa(\lambda)} s_{a^b}(1, q, \dots, q^{k-1})$	[21]
$\text{COF}(n\lambda/n\mu)$	Cyclic shift	a variant of maj	[3]

Table 1: Summary of known cyclic sieving phenomena on various sets of tableaux. <sup>†</sup>Note that promotion on hook shaped SYT with  $n$  cells has order  $n-1$ . <sup>‡</sup>Evacuation is an involution, so the cyclic group has order two.

**Theorem I.3** ([1, Thm. 2.7]). *Let  $f(q) \in \mathbb{N}_0[q]$  and suppose that  $f(\zeta^d) \in \mathbb{N}_0$  for all  $d \in \{1, \dots, n\}$ , where  $\zeta$  is a primitive  $n^{\text{th}}$  root of unity. Let  $X$  be any set of size  $f(1)$ .*

*Then there exists a cyclic group action  $\rho$  of order  $n$  such that  $(X, \langle \rho \rangle, f(q))$  exhibits the cyclic sieving phenomenon if and only if for every  $k \mid n$ ,*

$$\sum_{d \mid k} \mu(k/d) f(\zeta^d) \geq 0,$$

where  $\mu$  is the number-theoretic Möbius function.

**Remark I.4.** Except for its size, the nature of the set  $X$  is irrelevant in this theorem.

**Remark I.5.** If  $(X, \langle \rho \rangle, f(q))$  exhibits the cyclic sieving phenomenon, the expression

$$\frac{1}{k} \sum_{d \mid k} \mu(k/d) f(\zeta^d)$$

is the number of orbits of size  $k$  of the group action. Therefore, the sum

$$\sum_{d \mid k} \mu(k/d) f(\zeta^d)$$

must be nonnegative and divisible by  $k$ . The condition that the sum is divisible by  $k$  follows from the hypothesis that  $f(q) \in \mathbb{N}_0[q]$  and  $f(\zeta^d) \in \mathbb{N}_0$  for all  $d \in \{1, \dots, n\}$ , see [1, Lem. 2.5].

**Remark I.6.** It may be the case that  $f(q) \in \mathbb{N}_0[q]$  evaluates to nonnegative integers at  $n^{\text{th}}$  roots of unity, but is not a cyclic sieving polynomial. As an example (see [1, Ex. 2.10]), take  $f(q) = q^5 + 3q^3 + q + 10$ . At 6<sup>th</sup> roots of unity,  $f(\zeta^j)$  takes nonnegative integer values. However, for  $k=3$  we have  $\sum_{d \mid k} \mu(k/d) f(\zeta^d) = -3$ .

We conclude this section by recalling a fact that makes cyclic groups special. In general, two non-isomorphic group actions may have the same linear character. This is not the case for group actions of a cyclic group, as R. Brauer's permutation lemma shows:

**Theorem I.7** ([6, 11]). *Two cyclic group actions are isomorphic if and only if they are isomorphic as linear representation, that is, their characters coincide.*

### I.3 SOME PROPERTIES OF SKEW SCHUR FUNCTIONS

In this section we recall some basic properties of skew Schur functions, the Littlewood–Richardson coefficients and fake degree polynomials. We refer to the books by I. G. Macdonald [14] and R. Stanley [28] for definitions. We use English notation for tableaux in all our figures.

Let  $\text{SYT}(\lambda/\mu)$  and  $\text{SSYT}(\lambda/\mu)$  be the set of standard and semi-standard Young tableaux of skew shape  $\lambda/\mu$ , respectively. Given a skew shape  $\lambda/\mu$  with  $n$  cells, the associated *skew Schur function*  $s_{\lambda/\mu}$  is defined as

$$s_{\lambda/\mu}(\mathbf{x}) := \sum_{T \in \text{SSYT}(\lambda/\mu)} \prod_{\square \in \lambda/\mu} x_{T(\square)}.$$

This generalizes the ordinary *Schur function*  $s_\lambda := s_{\lambda/\emptyset}$ . It is well-known that  $\{s_\lambda\}_\lambda$ , where  $\lambda$  runs over all partitions, is a basis for the ring of symmetric functions. Another basis is given by the set of *power sum symmetric functions* indexed by partitions. These are defined as

$$p_\nu(\mathbf{x}) := p_{\nu_1}(\mathbf{x})p_{\nu_2}(\mathbf{x}) \cdots p_{\nu_\ell}(\mathbf{x}), \quad p_j(\mathbf{x}) := x_1^j + x_2^j + \cdots.$$

The *skew characters*  $\chi^{\lambda/\mu}(\nu)$  of the symmetric group  $\mathfrak{S}_n$  are then defined implicitly via

$$s_{\lambda/\mu}(\mathbf{x}) = \sum_{\nu} \chi^{\lambda/\mu}(\nu) \frac{p_\nu(\mathbf{x})}{z_\nu}, \quad (5)$$

where the sum is over all partitions  $\nu$  of the same size as  $\lambda/\mu$ ,  $z_\nu = \prod_j m_j! j^{m_j}$  and  $m_j$  is the number of parts in  $\lambda$  equal to  $j$ .

We define the *Littlewood–Richardson coefficients*  $c_{\mu\nu}^\lambda \in \mathbb{N}_0$  via the expansion of the skew Schur function  $s_{\lambda/\mu}$  in the basis of the ordinary Schur functions,

$$s_{\lambda/\mu}(\mathbf{x}) = \sum_{\nu} c_{\mu\nu}^\lambda s_\nu(\mathbf{x}). \quad (6)$$

Note that  $c_{\mu\nu}^\lambda = 0$  if  $\nu$  and  $\lambda/\mu$  are not of the same size. Combining Equations (5) and (6) we obtain an equivalent expansion for the skew characters,

$$\chi^{\lambda/\mu} = \sum_{\nu} c_{\mu\nu}^\lambda \chi^\nu. \quad (7)$$

Although it is very difficult to determine whether a given Littlewood–Richardson coefficient vanishes, the following particular case is straightforward.

**Lemma I.8.** *Let  $\lambda/\mu$  be a skew shape with  $n$  cells. Then  $c_{\mu,(n)}^\lambda = 0$  if and only if  $\lambda/\mu$  has a column with at least two cells. Similarly,  $c_{\mu,(1^n)}^\lambda = 0$  if and only if  $\lambda/\mu$  has a row with at least two cells.*

*Proof.* We shall first prove the statement

$$c_{\mu,(n)}^\lambda = 0 \iff \lambda/\mu \text{ has a column with at least two cells.}$$

We expand both sides of Equation (6) in the monomial basis. The left hand side contains the monomial  $x_1^n$  if and only if there is no column of  $\lambda/\mu$  with at least two cells. Since the only semi-standard Young tableau of straight shape that contains precisely  $n$  times the letter 1 has shape  $(n)$ , the monomial  $x_1^n$  appears in the right hand side if and only if  $c_{\mu,(n)}^\lambda \neq 0$ .

The statement concerning  $c_{\mu,(1^n)}^\lambda$  follows by applying the involution  $\omega$ , with the property that  $\omega(s_{\lambda/\mu}) = s_{\lambda'/\mu'}$ , on both sides of Equation (6). This yields

$$s_{\lambda'/\mu'}(\mathbf{x}) = \sum_{\nu} c_{\mu,\nu}^\lambda s_{\nu'}(\mathbf{x}).$$

A similar argument as in the previous paragraph now finishes the proof. □

**Definition I.9.** Given a skew standard Young tableau  $T$  with  $n$  cells, a label  $j$  with  $1 \leq j < n$  is a *descent* of  $T$ , if the label  $j + 1$  appears in a row strictly below that of  $j$ . The *major index* of  $T$ , denoted  $\text{maj}(T)$ , is the sum of the descents of  $T$ . The *fake-degree polynomial*  $f^{\lambda/\mu}(q)$  associated with a skew Young diagram  $\lambda/\mu$  is the generating function for the major index:

$$f^{\lambda/\mu}(q) := \sum_{T \in \text{SYT}(\lambda/\mu)} q^{\text{maj}(T)}.$$

The following lemma relates skew Schur functions and fake-degree polynomials.

**Lemma I.10** ([28, Prop. 7.19.11]). *Let  $\lambda/\mu$  be a skew shape with  $n$  cells. Then*

$$s_{\lambda/\mu}(1, q, q^2, \dots) = \frac{f^{\lambda/\mu}(q)}{(1-q)(1-q^2) \cdots (1-q^n)}.$$

#### I.4 SKEW CHARACTERS AND THEIR FAKE DEGREES

A result by T. Springer [27] gives an expression for the evaluation of an irreducible character of the symmetric group at a power of the *long cycle*  $(1, \dots, n) \in \mathfrak{S}_n$ . In this section, we extend this result to skew characters.

**Proposition I.11.** *Let  $\lambda/\mu$  be a skew shape with  $n$  cells and let  $\xi$  be a primitive  $n^{\text{th}}$  root of unity. Then, for  $n = dm$ ,*

$$\chi^{\lambda/\mu}((m^d)) = f^{\lambda/\mu}(\xi^d).$$

We shall deduce this from the following, more general result. This was first proved explicitly by B. Sagan, J. Shareshian and M. Wachs [25, Prop. 3.1], but, as they note, is already implicit in work of J. Désarménien [7]. We include yet another, different, proof.

**Proposition I.12.** *Let  $F(\mathbf{x})$  be a homogeneous symmetric function of degree  $n$ , such that*

$$F(\mathbf{x}) = \sum_{\nu \vdash n} \chi^F(\nu) \frac{p_\nu(\mathbf{x})}{z_\nu}.$$

Furthermore let  $f^F(q)$  be the following variation of the principal specialization of  $F(\mathbf{x})$ :

$$f^F(q) := \left( \prod_{j=1}^n (1 - q^j) \right) F(1, q, q^2, \dots).$$

Then, for a primitive  $n^{\text{th}}$  root of unity  $\zeta$  and  $n = dm$ , we have  $\chi^F((m^d)) = f^F(\zeta^d)$ .

*Proof.* Substituting  $p_k(1, q, q^2, \dots) = (1 - q^k)^{-1}$  in  $F(\mathbf{x})$  we obtain

$$f^F(q) = \left( \prod_{j=1}^n (1 - q^j) \right) \sum_{\nu \vdash n} \frac{\chi^F(\nu)}{z_\nu} \prod_{k=1}^{\ell(\nu)} \frac{1}{1 - q^{\nu_k}}.$$

Each summand on the right hand side approaches 0 as  $q \rightarrow \zeta^d$ , unless  $\nu = (m^d)$ , because the first product has a zero with multiplicity  $d$  at  $q = \zeta^d$ . Taking the limit, removing all summands other than the one corresponding to  $\nu = (m^d)$  and rearranging the expression slightly, we find

$$\lim_{q \rightarrow \zeta^d} f^F(q) = \lim_{q \rightarrow \zeta^d} \left( \prod_{k=1}^d \frac{1}{1 - q^{km}} \prod_{j=1}^n (1 - q^j) \right) \frac{\chi^F((m^d))}{z_{(m^d)}} \prod_{k=1}^d \frac{1 - q^{km}}{1 - q^m}.$$

The last product approaches  $d!$  by l'Hospital's rule, and  $z_{(m^d)} = d!m^d$ . Since  $n = dm$ , we have that the first two products are expressible as

$$\prod_{k=1}^d \frac{1}{1 - q^{km}} \prod_{j=1}^n (1 - q^j) = \prod_{k=0}^{d-1} \prod_{j=1}^{m-1} (1 - q^{j+km}).$$

Now, since  $\zeta^{md} = 1$ , we obtain that

$$f^F(\zeta^d) = \left( \prod_{j=1}^{m-1} (1 - \zeta^{jd}) \right)^d \frac{\chi^F((m^d))}{m^d} = \left( \frac{1}{m} \prod_{j=1}^{m-1} (1 - \zeta^{jd}) \right)^d \chi^F((m^d)). \quad (8)$$

Because  $\zeta^d$  is a primitive  $m^{\text{th}}$  root of unity,  $x^m - 1 = \prod_{j=0}^{m-1} (x - \zeta^{jd})$ . Dividing both sides by  $x - 1$  gives the identity

$$(x^{m-1} + x^{m-2} + \dots + x + 1) = \prod_{j=1}^{m-1} (x - \zeta^{jd}).$$

Setting  $x = 1$  here shows that  $\prod_{j=1}^{m-1} (1 - \zeta^{jd}) = m$ , and this final observation shows that the right hand side of (8) equals  $\chi^F((m^d))$ .  $\square$

*Proof of Proposition I.11.* By Lemma I.10, this is the special case of Proposition I.12 with  $F(\mathbf{x}) = s_{\lambda/\mu}(\mathbf{x})$ .  $\square$



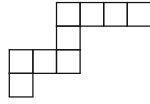


Figure 2: A border-strip of height 3.

## I.5 SKEW BORDER-STRIP TABLEAUX AND THE ABACUS

In this section, we recall the definition of border-strip tableaux, abaci and the Littlewood map. We end with a generalization of a theorem of G. James and A. Kerber.

A *border-strip* (or *ribbon* or *skew hook*) is a connected non-empty skew Young diagram containing no  $2 \times 2$ -square of cells, as in Figure 2. The *height* of a border-strip is one less than the number of rows it spans.

Let  $\lambda/\mu$  be a skew shape. The *size* of  $\lambda/\mu$  is its number of cells, denoted  $|\lambda/\mu|$ . Suppose that  $\nu = (\nu_1, \dots, \nu_\ell)$  is a partition of  $|\lambda/\mu|$ . A *border-strip tableau* of shape  $\lambda/\mu$  and *type*  $\nu$  is a tiling of the Young diagram of  $\lambda/\mu$  with labeled border-strips  $B_1, \dots, B_\ell$  with the following properties:

- the border-strip  $B_j$  has label  $j$  and size  $\nu_j$ ,
- labeling all cells in  $B_j$  with  $j$  results in a labeling of the diagram  $\lambda/\mu$  where labels in every row and every column are weakly increasing.

We let  $\text{BST}(\lambda/\mu, \nu)$  denote the set of all such border-strip tableaux. In particular,  $\text{BST}(\lambda/\mu, 1^n)$  may be identified with the set of standard Young tableaux of shape  $\lambda/\mu$ . In the remainder of the paper, we shall only concern ourselves with border-strip tableaux where all strips have the same size  $d$ , which we denote by  $\text{BST}(\lambda/\mu, d)$ .

The *height* of a border-strip tableau  $T$ , or any tiling of a tableau with border-strips, is the sum of the heights of the border-strips in the partition. The *content* of a cell is given by its column index minus its row index. Observe that within a border-strip, the lowest leftmost cell has the smallest content. By convention, the label of a strip is placed in the unique cell with minimal content in the strip, as done in Figure 3.

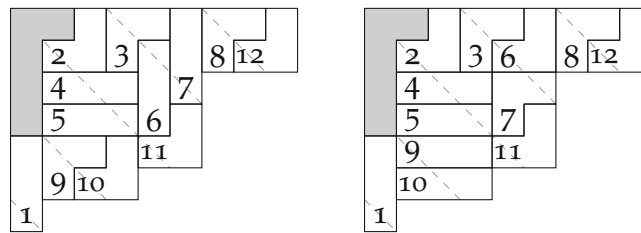


Figure 3: Two border-strip tableaux in  $\text{BST}((9^2, 6^3, 4, 1)/(2, 1^3), 3)$  of height 13 and 9 respectively. In each strip, the label has been placed in the cell with minimal content.

In Equation (5), the skew characters  $\chi^{\lambda/\mu}$  were defined. The skew Murnaghan–Nakayama rule describes a way to compute these skew characters.

**Theorem I.13** (Murnaghan–Nakayama, see [28, Cor. 7.17.5]). *The skew characters are given by the signed sum*

$$\chi^{\lambda/\mu}(\nu) = \sum_{B \in \text{BST}(\lambda/\mu, \nu)} (-1)^{\text{height}(B)}.$$

We will use the abacus model introduced by G. James & A. Kerber [10, Ch. 2.7] to encode partitions and their quotients.

**Definition I.14.** A *bead sequence* is an infinite binary word  $w = (w_i)_{i \in \mathbb{N}_{\geq 1}}$ , such that only a finite number of letters, the *beads*, are equal to 1.

Recording for each 1 in  $w$  the total number of 0's preceding it, yields, apart from some leading zeros, the sequence of parts of an integer partition  $\lambda$ , ordered from the smallest part to the largest. In this case,  $w$  is a *bead sequence for  $\lambda$* .

The  *$d$ -abacus on  $w$*  is the  $d$ -tuple of *runners*  $(w^1, \dots, w^d)$ , with  $w^s = (w_{id+s})_{i \in \mathbb{N}_0}$  for  $1 \leq s \leq d$ .

The partition corresponding to a bead sequence can alternatively be obtained by interpreting each 0 as a horizontal unit step and each 1 as a vertical unit step. This yields, apart from some leading vertical steps, the path tracing the south-east border of the Young diagram in English notation.

Thus, prepending a 1 to a bead sequence we obtain another bead sequence for the same partition. The  $d$ -abacus on the modified bead sequence is obtained from the  $d$ -abacus on the original bead sequence by prepending a bead to the  $d^{\text{th}}$  runner and then cyclically shifting the runners.

We visualize a  $d$ -abacus, as in Figure 4 on the right, by drawing  $d$  runners as vertical lines. Each runner consists of equally spaced spots. Beginning with the top row, processing each row from left to right, a bead is placed if and only if the corresponding letter of the binary word is 1. It will be convenient to color beads before the first empty spot black, and label the remaining positions beginning with 0. The labels of the beads are then the hook lengths of the cells in the first column of the associated partition.

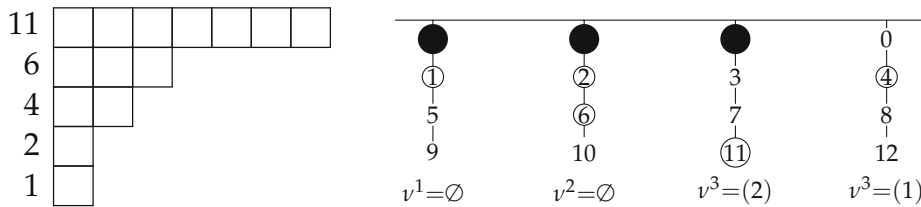


Figure 4: The 4-abacus 1110 1101 0100 0010... for the partition  $(7, 3, 2, 1, 1)$ , together with its 4-quotient.

We can now define the core and the quotient of a partition.

**Definition I.15.** Let  $\lambda$  be a partition and let  $d \geq 1$  be an integer. Then the  *$d$ -core* of  $\lambda$  is the partition associated with the  $d$ -abacus which is obtained from the  $d$ -abacus on any bead sequence for  $\lambda$  by moving up all beads as far as possible.

Given a bead sequence  $w$  for  $\lambda$ , the  *$d$ -quotient of  $\lambda$*  is the  $d$ -tuple of partitions obtained by regarding each runner of the  $d$ -abacus on  $w$  as a bead sequence.

Strictly speaking, the  $d$ -quotient of  $\lambda$  depends on the chosen bead sequence, or more precisely, on its number of beads modulo  $d$ . However, as indicated before, choosing a different bead sequence corresponds to a cyclic permutation of the  $d$ -tuple of partitions

in the  $d$ -quotient. Therefore, if the ordering of the partitions in the quotient is irrelevant, it is not necessary to explicitly fix a bead sequence.

By contrast, the  $d$ -core is independent of the chosen bead sequence. For example, the 4-core of the partition  $(7, 3, 2, 1, 1)$  is  $(2)$ , as can be seen by moving the beads in positions 4 and 11 up in Figure 4, obtaining the bead sequence  $1111\ 1110\ 0100\dots$

The following observation is fundamental to the utility of the abacus.

**Lemma I.16.** *Suppose that the partition  $\lambda$  is obtained from the partition  $\mu$  by adding a border-strip of size  $d$ , whose cell of minimal content has content  $c$  in  $\lambda$ .*

*Then a  $d$ -abacus for  $\mu$  is obtained from a  $d$ -abacus for  $\lambda$  by moving a bead on the  $j^{\text{th}}$  runner up by one position. Provided that  $d$  divides the total number of beads on the abacus, we have  $j \equiv c \pmod{d}$ .*

*Proof.* Let  $(w_i^\lambda)_{i \in \mathbb{N}_{\geq 1}}$  be a bead sequence for  $\lambda$ , and let  $x$  and  $y$  be the column and the row, respectively, of the cell of minimal content of the border-strip which was added to  $\mu$  to obtain  $\lambda$ .

Let  $j$  be the index of the  $x^{\text{th}}$  zero in  $(w_i^\lambda)_{i \in \mathbb{N}_{\geq 1}}$ . Thus,  $w_j^\lambda, w_{j+1}^\lambda, \dots, w_{j+d}^\lambda$  encodes the path tracing the south-east border of the Young diagram of  $\lambda/\mu$ . In particular, since  $\lambda/\mu$  is a border-strip,  $w_{j+d}^\lambda = 1$ . Let

$$w_i^\mu = \begin{cases} 1 & \text{if } i = j \\ 0 & \text{if } i = j + d \\ w_i^\lambda & \text{otherwise.} \end{cases}$$

Equivalently, this is the bead sequence for the  $d$ -abacus obtained by moving a bead up on the  $\bar{j}^{\text{th}}$  runner, with  $\bar{j} \equiv j \pmod{d}$ . Moreover,  $w_j^\mu, w_{j+1}^\mu, \dots, w_{j+d}^\mu$  encodes the path tracing the north-west border of the Young diagram of  $\lambda/\mu$ , so  $(w_i^\mu)_{i \in \mathbb{N}_{\geq 1}}$  is indeed a bead sequence for  $\mu$ .

Let  $\ell$  be the total number of ones in  $(w_i^\lambda)_{i \in \mathbb{N}_{\geq 1}}$ . Then there are  $x - 1$  zeros in  $w_1^\lambda, \dots, w_{j-1}^\lambda$ , and  $\ell - y$  ones. Thus, provided that  $\ell = dk$ , we have  $j = x - 1 + dk - y + 1 \equiv x - y \pmod{d}$ .  $\square$

**Definition I.17.** Let  $\lambda/\mu$  be a skew shape. Then  $\mathbf{w} = (w_i^\lambda, w_i^\mu)_{i \in \mathbb{N}_{\geq 1}}$  is a *(skew) bead sequence for  $\lambda/\mu$*  if  $(w_i^\lambda)_{i \in \mathbb{N}_{\geq 1}}$  and  $(w_i^\mu)_{i \in \mathbb{N}_{\geq 1}}$  are bead sequences for  $\lambda$  and  $\mu$  respectively, and the number of beads in these two bead sequences are the same.

The *(skew)  $d$ -abacus on  $\mathbf{w}$*  is the pair of  $d$ -abaci for  $(w_i^\lambda)_{i \in \mathbb{N}_{\geq 1}}$  and  $(w_i^\mu)_{i \in \mathbb{N}_{\geq 1}}$ .

Suppose that there is a (skew) bead sequence  $\mathbf{w}$  for  $\lambda/\mu$ , such that for all  $1 \leq i \leq d$ , the  $i^{\text{th}}$  pair of runners in the  $d$ -abacus on  $\mathbf{w}$  is a bead sequence for a skew shape  $v^i/\kappa^i$ . Then the corresponding  *$d$ -quotient of  $\lambda/\mu$*  is the  $d$ -tuple  $(v^1/\kappa^1, \dots, v^d/\kappa^d)$ . If there is no such bead sequence, the  $d$ -quotient of  $\lambda/\mu$  does not exist.

We visualize a  $d$ -abacus for  $\lambda/\mu$  by drawing the  $d$ -abacus for  $\mu$  above the  $d$ -abacus for  $\lambda$ , as on the right hand side of Figure 5.

**Lemma I.18.** *Let  $\lambda/\mu$  be a skew shape. Then the  $d$ -quotient of  $\lambda/\mu$  exists if and only if  $\text{BST}(\lambda/\mu, d)$  is non-empty.*

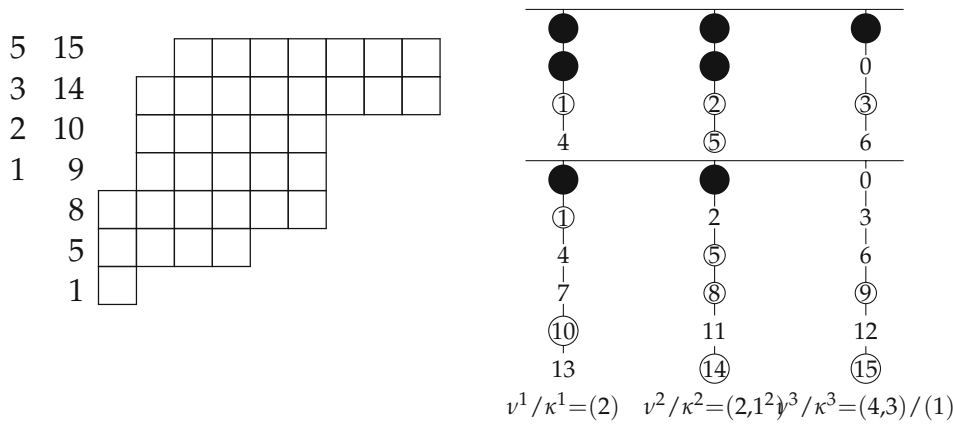


Figure 5: The hook lengths of the first column of the inner and the outer shape of the diagram in Figure 3, and the pair of 3-abaci corresponding to the shape.

*Proof.* It is an immediate consequence of Lemma I.16 that  $\text{BST}(\lambda/\mu, d)$  is non-empty if and only if a  $d$ -abacus for  $\mu$  can be obtained from the  $d$ -abacus for  $\lambda$  by moving up beads along their runners. Put differently, each pair of runners in a  $d$ -abacus for  $\lambda/\mu$  is a bead sequence for some skew shape.  $\square$

**Remark I.19.** Note that in this case the  $d$ -cores of  $\lambda$  and  $\mu$  coincide. In fact, a  $d$ -quotient of a partition  $\lambda$  with core  $\mu$  is precisely a  $d$ -quotient of  $\lambda/\mu$ .

We now recall the Littlewood map as described by, for example, G. James & A. Kerber [10, Ch. 2.7] or I. Pak [16, fig. 2.6], where it is called the rim hook bijection.

Suppose that  $\text{BST}(\lambda/\mu, d)$  is non-empty. Then, given a bead sequence for  $\lambda/\mu$ , let the set of *standard Young tableaux tuples*, denoted by  $\text{SYT-tuples}(\lambda/\mu, d)$ , be the set of  $d$ -tuples  $(T^1, T^2, \dots, T^d)$  of skew tableaux with the following properties:

- the shape of  $T^j$  is  $\lambda^j/\mu^j$ , the  $j^{\text{th}}$  entry of the  $d$ -quotient of  $\lambda/\mu$ ,
- for each tableau  $T^j$ , the cell labels in rows and columns increase,
- each of the numbers  $\{1, 2, \dots, n/d\}$  appears in precisely one tableau.

The *Littlewood map* is a bijection between  $\text{BST}(\lambda/\mu, d)$  and  $\text{SYT-tuples}(\lambda/\mu, d)$ , which we now describe. Fix a bead sequence for  $\lambda/\mu$  and let  $(\lambda^1/\mu^1, \dots, \lambda^d/\mu^d)$  be the corresponding  $d$ -quotient of  $\lambda/\mu$ . Let  $B \in \text{BST}(\lambda/\mu, d)$ .

We define  $(T^1, T^2, \dots, T^d)$  inductively: if  $\lambda/\mu$  is the empty partition, then  $T^i$  is the empty partition for  $1 \leq i \leq d$ . Otherwise let  $\bar{B}$  be the border-strip tableau obtained from  $B$  by deleting the strip with the largest label  $n/d$ , and let  $\bar{\lambda}/\mu$  be its shape. Let  $(\bar{\lambda}^1/\mu^1, \dots, \bar{\lambda}^d/\mu^d)$  be the  $d$ -quotient of  $\bar{\lambda}/\mu$  corresponding to the bead sequence which has as many beads as the chosen bead sequence for  $\lambda/\mu$ . Let  $(\bar{T}^1, \bar{T}^2, \dots, \bar{T}^d)$  be the standard Young tableau tuple corresponding to  $\bar{B}$ .

Then there is a unique index  $1 \leq j \leq d$  with  $\bar{\lambda}^j/\mu^j \neq \lambda^j/\mu^j$ . Moreover,  $\lambda^j/\mu^j$  is obtained from  $\bar{\lambda}^j/\mu^j$  by adding a single cell. The standard Young tableaux tuple  $(T^1, T^2, \dots, T^d)$  is thus obtained from  $(\bar{T}^1, \bar{T}^2, \dots, \bar{T}^d)$  by placing  $n/d$  into this cell of  $T^j$ .

**Remark I.20.** Suppose that the number of beads in the chosen bead sequence for  $\lambda/\mu$  is divisible by  $d$ . Let  $c(x)$  denote the content of the unique cell with minimal content in the  $d$ -strip labeled  $x$  in  $B$ , as shown in Figure 3.

Then it follows immediately from Lemma I.16 that any label  $x$  appearing in  $T^j$  satisfies  $c \equiv j \pmod{d}$ .

Furthermore, two labeled cells in  $T^j$  differ in content by  $k$  if and only if the two cells with these labels in  $B$  differ in content by  $dk$ .

The image of the two border-strip tableaux in Figure 3 are given by the triples in (9) and (10), respectively.

**Example I.21.** The 3-cores of  $\lambda = (9^2, 6^3, 4, 1)$  and  $\mu = (2, 1^3)$  are both given by the partition (2). Provided we choose bead sequences such that the number of beads is divisible by 3, the 3-quotient of  $\lambda$  is  $(2), (2, 1^2), (4, 3)$  and the 3-quotient of  $\mu$  is  $\emptyset, \emptyset, (1)$ . Thus, the 3-quotient of  $\lambda/\mu$  is  $(2), (2, 1^2), (4, 3)/(1)$  and the two tuples

$$\left( \begin{array}{|c|c|} \hline 5 & 6 \\ \hline \end{array}, \begin{array}{|c|c|} \hline 3 & 8 \\ \hline 4 & \\ \hline 9 & \\ \hline \end{array}, \begin{array}{|c|c|c|} \hline 2 & 7 & 12 \\ \hline 1 & 10 & 11 \\ \hline \end{array} \right) \quad (9)$$

$$\left( \begin{array}{|c|c|} \hline 5 & 7 \\ \hline \end{array}, \begin{array}{|c|c|} \hline 3 & 8 \\ \hline 4 & \\ \hline 10 & \\ \hline \end{array}, \begin{array}{|c|c|c|} \hline 2 & 6 & 12 \\ \hline 1 & 9 & 11 \\ \hline \end{array} \right) \quad (10)$$

are elements in  $\text{SYT-tuples}(\lambda/\mu, 3)$ , corresponding to the two tableaux in Figure 3.

**Theorem I.22.** Let  $\lambda/\mu$  be a skew shape of size  $n$  and let  $k$  and  $d$  be positive integers with  $dk \mid n$ . Fix a skew bead sequence for  $\lambda/\mu$ .

Then  $\text{BST}(\lambda/\mu, dk)$  is non-empty if and only if  $\text{BST}(\lambda/\mu, k)$  is non-empty and, for the  $k$ -quotient  $(v^1/\kappa^1, \dots, v^k/\kappa^k)$  of  $\lambda/\mu$ , each set  $\text{BST}(v^i/\kappa^i, d)$  is non-empty for  $1 \leq i \leq k$ .

In this case  $d \mid \gcd(|v^1/\kappa^1|, \dots, |v^k/\kappa^k|)$  and

$$|\text{BST}(\lambda/\mu, dk)| = \binom{\sum_i |v^i/\kappa^i|/d}{|v^1/\kappa^1|/d, \dots, |v^k/\kappa^k|/d} \prod_{i=1}^k |\text{BST}(v^i/\kappa^i, d)|. \quad (11)$$

**Remark I.23.** The case  $d = 1$  for straight shapes is classical and can be found in [10, eq. (2.7.32)] or [8].

*Proof.* Let us first prove the special case  $d = 1$ . Since the Littlewood map is bijective, it suffices to count the number of standard Young tableaux tuples  $(T^1, T^2, \dots, T^d)$  with shapes  $(v^1/\kappa^1, \dots, v^k/\kappa^k)$ . This number is

$$|\text{BST}(\lambda/\mu, k)| = |\text{SYT-tuples}(\lambda/\mu, k)| = \binom{\sum_i |v^i/\kappa^i|}{|v^1/\kappa^1|, \dots, |v^k/\kappa^k|} \prod_{i=1}^k |\text{SYT}(v^i/\kappa^i)|,$$

where the multinomial coefficient counts the number of ways to distribute the labels among the skew shapes.

Now we reduce the general statement to the case  $d = 1$ . First notice, that  $|\text{BST}(\lambda/\mu, dk)| \leq |\text{BST}(\lambda/\mu, k)|$ , because there exists a natural injection which splits each strip of length  $dk$  into  $d$  strips of length  $k$ .

Let  $\mathbf{w} = (w_i^\lambda, w_i^\mu)_{i \in \mathbb{N}_{\geq 1}}$  be a bead sequence for  $\lambda/\mu$ . For simplicity we write  $\mathbf{w}_i := (w_i^\lambda, w_i^\mu)$ . For  $1 \leq s \leq k$  let  $\mathbf{w}^s = (\mathbf{w}_{ik+s})_{i \in \mathbb{N}_0}$  be the  $s^{\text{th}}$  runner in the  $k$ -abacus on  $\mathbf{w}$ .

By Lemma I.18 it suffices to prove that all runners in the  $dk$ -abacus on  $\mathbf{w}$  are bead sequences for skew shapes if and only if all runners in the  $d$ -abacus on  $\mathbf{w}^s$  are bead sequences for skew shapes for all  $1 \leq s \leq k$ . For  $1 \leq t \leq d$ , the  $t^{\text{th}}$  runner in the  $d$ -abacus on  $\mathbf{w}^s$  is

$$\mathbf{w}^{s,t} = (\mathbf{w}_{(j \cdot d + t - 1) \cdot k + s})_{j \in \mathbb{N}_0} = (\mathbf{w}_{(j \cdot (dk) + (t-1)k + s)})_{j \in \mathbb{N}_0}.$$

Because  $1 \leq (t-1)k + s < dk$ , this is precisely the  $((t-1)k + s)^{\text{th}}$  runner in the  $dk$ -abacus on  $\mathbf{w}$ , giving the equivalence.

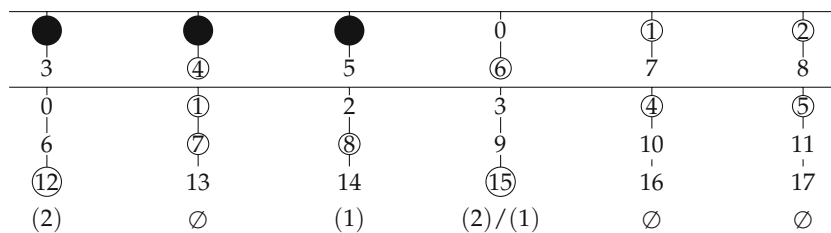
Suppose now that  $|\text{BST}(\lambda/\mu, dk)|$  is non-empty and let  $(v^{s,1}/\kappa^{s,1}, \dots, v^{s,d}/\kappa^{s,d})$  be the  $d$ -quotient of  $v^s/\kappa^s$ . The above equation on runners shows that the collection of skew shapes  $v^{s,t}/\kappa^{s,t}$  for  $1 \leq s \leq k$  and  $1 \leq t \leq d$  coincides with the collection of skew shapes in the  $dk$ -quotient for  $\lambda/\mu$ .

To conclude the argument, we compute

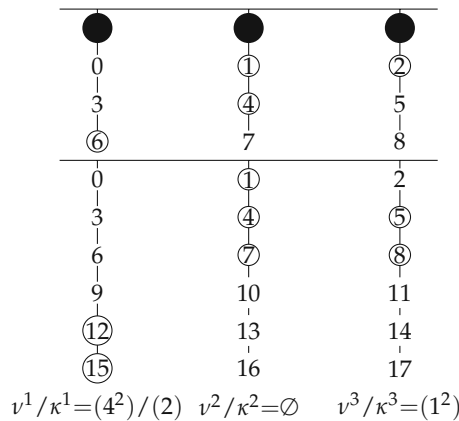
$$\begin{aligned} & \left( \begin{array}{c} |\lambda/\mu|/dk \\ |v^1/\kappa^1|/d, \dots, |v^k/\kappa^k|/d \end{array} \right) \prod_{i=1}^k |\text{BST}(v^i/\kappa^i, d)| \\ &= \left( \begin{array}{c} |\lambda/\mu|/dk \\ |v^1/\kappa^1|/d, \dots, |v^k/\kappa^k|/d \end{array} \right) \prod_{i=1}^k \left( \begin{array}{c} |v^i/\kappa^i|/d \\ |v^{i,1}/\kappa^{i,1}|, \dots, |v^{i,d}/\kappa^{i,d}| \end{array} \right) \prod_{j=1}^d |\text{SYT}(v^{i,j}/\kappa^{i,j})| \\ &= \left( \begin{array}{c} |\lambda/\mu|/dk \\ |v^{1,1}/\kappa^{1,1}|, \dots, |v^{k,d}/\kappa^{k,d}| \end{array} \right) \prod_{i=1}^k \prod_{j=1}^d |\text{SYT}(v^{i,j}/\kappa^{i,j})| \\ &= |\text{BST}(\lambda/\mu, dk)|. \end{aligned}$$

□

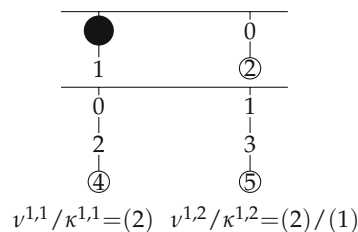
**Example I.24.** Consider the skew shape  $\lambda/\mu = (9,7,4^2,3^2,1)/(3,2,1^2)$  of 24. A corresponding skew 6-abacus is as follows. Note that the lower abacus, corresponding to the outer shape  $\lambda$ , can be obtained from the upper abacus, corresponding to the inner shape  $\mu$ , by moving down beads along a runner. Following Lemma I.16, this corresponds to the fact that  $\text{BST}(\lambda/\mu, 6)$  is non-empty.



On the other hand, the skew 3-abacus with the same number of beads is the following:



Finally, as illustration of the proof, consider the skew 2-abacus for  $v^1/\kappa^1$ , corresponding to the first runner in the skew 3-abacus above, and having the same number of beads as this abacus. Observe that the (skew) bead sequences, and therefore also the corresponding skew shapes, are the same as on the first and the fourth runner of the 6-abacus:



As a corollary we obtain a useful characterization of shapes with precisely one border-strip tableau.

**Corollary I.25.** *Let  $\lambda/\mu$  be a skew shape of size  $n \in \mathbb{N}_{\geq 1}$  and let  $k$  be a positive integer with  $k \mid n$ . Suppose that  $\text{BST}(\lambda/\mu, k)$  is non-empty.*

*Then  $\text{BST}(\lambda/\mu, k)$  contains precisely one element if and only if all skew shapes in the skew  $k$ -quotient of  $\lambda/\mu$  are empty, with exactly one exception, which is either a single row  $(n/k)$  or a single column  $(1^{n/k})$ .*

*In this case  $\lambda/\mu$  is a border-strip and  $\text{BST}(\lambda/\mu, dk)$  contains precisely one element for all  $d \mid \frac{n}{k}$ .*

*Proof.* Let  $(v^1/\kappa^1, \dots, v^k/\kappa^k)$  be the skew  $k$ -quotient of  $\lambda/\mu$ . Applying Theorem I.22 with  $d = 1$  we obtain that  $|\text{BST}(\lambda/\mu, k)| = 1$  if and only if  $|\text{BST}(v^i/\kappa^i, 1)| = 1$  for all  $i$  and the multinomial coefficient in Equation (11) evaluates to 1.

Since  $\text{BST}(v^i/\kappa^i, 1)$  is the set of standard Young tableaux of shape  $v^i/\kappa^i$ , we have that  $|\text{BST}(v^i/\kappa^i, 1)| = 1$  if and only if  $v^i/\kappa^i$  is a single row or a single column. Furthermore, the multinomial coefficient equals 1 if  $|v^i/\kappa^i| = 0$  for all but one  $i$ .

Suppose now that  $|\text{BST}(\lambda/\mu, k)| = 1$ . Let  $v^j/\kappa^j$  be the unique non-empty element in the quotient, which therefore has size  $n/k$ . Because  $v^j/\kappa^j$  is a single row or a single

column,  $|\text{BST}(v^j/\kappa^j, n/k)| = 1$ . For  $i \neq j$  we trivially have  $|\text{BST}(v^i/\kappa^i, n/k)| = 1$ . Thus, by Theorem I.22 with  $d = n/k$ , we have  $|\text{BST}(\lambda/\mu, n)| = |\text{BST}(\lambda/\mu, \frac{n}{k} \cdot k)| = 1$ , which implies that  $\lambda/\mu$  is a border-strip.

Finally, recall that  $|\text{BST}(\lambda/\mu, dk)| \leq |\text{BST}(\lambda/\mu, k)|$ , because there is a natural injection which splits each strip of length  $dk$  into  $d$  strips of length  $k$ . Therefore, provided that  $d \mid \frac{n}{k}$ ,

$$1 = |\text{BST}(\lambda/\mu, n)| \leq |\text{BST}(\lambda/\mu, dk)| \leq |\text{BST}(\lambda/\mu, k)| = 1.$$

□

## I.6 SKEW CHARACTERS AND BORDER-STRIP TABLEAUX

In this section we show that, up to sign, the evaluation of a skew character at a  $d^{\text{th}}$  power of a cycle equals the number of border-strip tableaux with all strips having size  $d$ . The non-skew case follows from a result by D. White [33] and via a different technique by G. James and A. Kerber [10, Eq. 2.7.26]. Our proof is slightly different and uses the techniques by I. Pak [16]. The fact that the Murnaghan–Nakayama rule is cancellation-free in the skew case is also briefly stated in [13, p.1047], and is implicit in [26].

We include a straightforward proof here for convenience, as we have found no single reference which connects all three quantities; evaluations at roots of unity of fake-degree polynomials, skew characters, and the number of skew border-strip tableaux.

**Definition I.26.** Let  $T = (T^1, \dots, T^d) \in \text{SYT-tuples}(\lambda/\mu, d)$ . Suppose that, after swapping labels  $i$  and  $i+1$  in  $T$ , the resulting tuple  $T'$  is still an element of  $\text{SYT-tuples}(\lambda/\mu, d)$ . Then this transposition is a *flip* on  $T$ .

The result of a flip on the border-strip tableau corresponding to  $T$  under the Littlewood map is the image of  $T'$  under the Littlewood map.

**Example I.27.** The two flips  $(6, 7)$  and  $(9, 10)$  send the tableau tuple (9) to the tableau tuple (10). These correspond to the border-strip tableaux in Figure 3.

**Lemma I.28.** *All elements of  $\text{SYT-tuples}(\lambda/\mu, d)$  are connected via a sequence of flips.*

This lemma is essentially [16, Thm. 3.2]. For convenience, we include a proof using our framework.

*Proof.* Fix a bead sequence for  $\lambda/\mu$  and let  $(\lambda^1/\mu^1, \dots, \lambda^d/\mu^d)$  be the corresponding  $d$ -quotient of  $\lambda/\mu$ . Let us first describe the *superstandard filling*  $S := (S^1, \dots, S^d) \in \text{SYT-tuples}(\lambda/\mu, d)$ . We will then show that  $S$  can be obtained from any other tableau by a sequence of flips.

The cells in  $S^1$  are labeled with the numbers  $1, \dots, |\lambda^1/\mu^1|$ , the cells in  $S^2$  are labeled with numbers  $|\lambda^1/\mu^1| + 1, \dots, |\lambda^1/\mu^1| + |\lambda^2/\mu^2|$ , and so forth. The labels in each tableau  $S^i$  are then distributed in the lexicographically smallest fashion, when reading row by row from top to bottom.

It now suffices to prove that for arbitrary  $T \in \text{SYT-tuples}(\lambda/\mu, d)$ , we can obtain  $S$  from  $T$  by a sequence of flips. We describe a sorting algorithm which rearranges the



labels, starting with 1 and then continuing with  $2, 3, \dots$  so that these labels agree with the corresponding labels in  $S$ .

Suppose that, at some point during the procedure, all cells in  $T$  with labels at most  $i - 1$  agree with  $S$ , but the cell labeled  $i$  in  $S$  is labeled  $j > i$  in  $T$ . We then first flip  $j$  and  $j - 1$ , then  $j - 1$  and  $j - 2$ , etc. until  $i + 1$  and  $i$  are flipped, at which point  $i$  is in the correct spot. We show inductively that all these flips are possible to perform: by construction, the cells above and to the left of the cell labeled with  $j$  in  $T$  must have labels smaller than  $i < j - 1$ . Because all tableaux in  $T$  are standard, the cells below and to the right of the cell labeled with  $j - 1$  contain labels strictly larger than  $j$ . Performing this algorithm in order for all  $i = 1, 2, \dots$  ensures that we eventually reach  $S$  from  $T$ .  $\square$

By analyzing the effect of flipping  $i$  and  $i + 1$  on the corresponding border-strip tableau, we now show that the height of the latter remains invariant.

**Lemma I.29** ([16, Lem. 4.1]). *Suppose that  $B$  and  $B'$  in  $\text{BST}(\lambda/\mu, d)$  are related by a flip. Then  $(-1)^{\text{height}(B)} = (-1)^{\text{height}(B')}$ .*

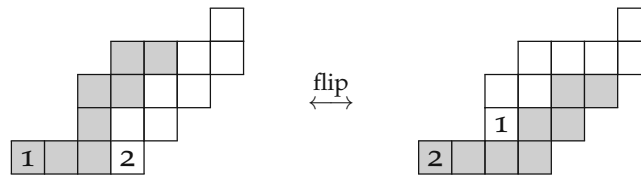
*Proof.* Let  $T$  and  $T'$  be the standard Young tableau tuples corresponding to  $B$  and  $B'$  respectively, and let  $T'$  be obtained from  $T$  by flipping  $i$  and  $i + 1$ .

Since the tuples of shapes of  $T$  and  $T'$  restricted to the labels  $\{1, \dots, j\}$  coincide for  $j \notin \{i, i + 1\}$ , the border-strip tableaux  $B$  and  $B'$  only differ in the two border-strips labeled  $i$  and  $i + 1$ .

If these are disconnected, that is, no cell in the first strip is horizontally or vertically adjacent to a cell in the second, only the labels  $i$  and  $i + 1$  are interchanged in  $B$  and  $B'$ .

Otherwise, the two border-strips must form a skew shape, since labels are increasing in every row and every column of a border-strip tableau. Because this skew shape is a union of two border-strips, it can be partitioned into three parts: a (non-empty) middle part which consists of all pairs of cells  $(b_1, b_2)$  whose contents are equal, a part to the left of this middle part and a part to the right of this middle part.

A flip necessarily fixes the left and right part, while it swaps the cells in the middle part. Hence, the strips either both increase or both decrease in height by 1, as illustrated in the following example:



$\square$

Together with Proposition I.11 we can now conclude the main result of this section.

**Corollary I.30.** *Let  $\lambda/\mu$  be a skew shape of size  $n = dm$ . Then the signed sum*

$$\chi^{\lambda/\mu}((m^d)) = \sum_{B \in \text{BST}(\lambda/\mu, m)} (-1)^{\text{height}(B)}$$

*in the Murnaghan–Nakayama rule, Theorem I.13, is cancellation-free. In particular,*

$$f^{\lambda/\mu}(\xi^d) = \chi^{\lambda/\mu}((m^d)) = \varepsilon |\text{BST}(\lambda/\mu, m)|,$$

*where  $\xi$  is a primitive  $n^{\text{th}}$  root of unity and  $\varepsilon = (-1)^{\text{height}(B)}$  for any  $B \in \text{BST}(\lambda/\mu, m)$ .*

The goal of this section is to prove the following theorem.

**Theorem I.31.** *Let  $\lambda/\mu$  be a skew shape with  $n$  cells and let  $k$  be a positive integer with  $k \mid n$ . Suppose that  $|\text{BST}(\lambda/\mu, k)| \geq 2$ . Then*

$$|\text{BST}(\lambda/\mu, k)| \geq \sum_{d \mid \frac{n}{k}, d > 1} |\text{BST}(\lambda/\mu, dk)|.$$

*Additionally, the inequality holds if  $n/k$  is a prime number.*

**Example I.32.** For  $\lambda = (10, 1^2) \vdash 12$  we have  $|\text{BST}(\lambda, 3)| = 1$  and  $|\text{BST}(\lambda, 6)| + |\text{BST}(\lambda, 12)| = 2$ . By contrast, for  $\lambda = (9, 1^3) \vdash 12$ , we have  $|\text{BST}(\lambda, 1)| = 165$ ,  $|\text{BST}(\lambda, 2)| = 5$ ,  $|\text{BST}(\lambda, 3)| = 3$  and  $|\text{BST}(\lambda, 4)| = |\text{BST}(\lambda, 6)| = |\text{BST}(\lambda, 12)| = 1$ , and therefore

$$|\text{BST}(\lambda, k)| \geq \sum_{d \mid \frac{n}{k}, d > 1} |\text{BST}(\lambda, dk)|$$

for all  $k$ .

**Remark I.33.** For  $k = 1$ , apart from the single row and single column partitions, there are only three shapes  $\lambda/\mu$  where equality is attained:  $(2^2)$ ,  $(3^2)$  and  $(2^3)$ . Other than that, the minimal difference between the two sides of the inequality is attained for hooks of the form  $(n - 1, 1)$ . In this case it equals  $n - \tau(n)$ , where  $\tau(n)$  is the number of divisors of  $n$ .

Our strategy is to reduce the theorem to the case of straight shapes and  $k = 1$ , which we prove in Section I.7.2, employing a bound due to S. Fomin & N. Lulov.

In Section I.7.3 we extend this to the case of skew shapes and  $k = 1$ , essentially using the expansion of a skew character into irreducible characters.

Finally, in Section I.7.4 we deduce the general case from the inequality with  $k = 1$ , using a bound on the quotient of a multinomial coefficient and a multinomial coefficient with stretched entries proved in Section I.7.1 and Theorem I.22 and Corollary I.25.

### 1.7.1 Bounds on multinomial coefficients

We first prove two inequalities related to multinomial coefficients. For this we use the approximation due to H. Robbins.

**Proposition I.34** ([23]). *For any positive integer  $n$ ,*

$$n! = \sqrt{2\pi n} n^{n+1/2} e^{-n+r_n} \quad \text{for some} \quad \frac{1}{12n+1} < r_n < \frac{1}{12n}.$$

**Lemma I.35.** *For any positive integer  $d$  and positive integers  $m_1, \dots, m_k$  summing to  $m$ ,*

$$\frac{\binom{dm}{dm_1, \dots, dm_k}}{\binom{m}{m_1, \dots, m_k}} \geq \frac{1}{d^{(k-1)/2}} \left( \frac{m^m}{\prod_{j=1}^k m_j^{m_j}} \right)^{d-1}. \quad (12)$$

*Proof.* For  $d = 1$  or  $k = 1$  the statement is trivial, so we assume  $d > 1$  and  $k > 1$ .

The left hand side of (12) is equal to

$$\frac{(dm)! \prod_j (m_j)!}{\prod_j (dm_j)! m!},$$

which by Proposition I.34 is larger than or equal to

$$\frac{m^{(d-1)m}}{d^{(k-1)/2} \prod_i m_i^{(d-1)m_i}} \exp\left(\frac{1}{12dm+1} - \frac{1}{12m} + \sum_j \frac{1}{12m_j+1} - \frac{1}{12dm_j}\right).$$

It remains to show that, for  $\varepsilon = 1/12$ ,

$$\frac{1}{dm+\varepsilon} + \sum_j \frac{1}{m_j+\varepsilon} \geq \frac{1}{m} + \sum_j \frac{1}{dm_j},$$

provided  $k > 1$  and  $d > 1$ . Set  $M = m \sum_j \frac{1}{m_j}$  and notice that  $M \geq k \geq 2$ . Furthermore,  $m \sum_j \frac{1}{m_j+\varepsilon} \geq \frac{m}{1+\varepsilon} \sum_j \frac{1}{m_j} = \frac{1}{1+\varepsilon} M$  and  $\frac{dm}{dm+\varepsilon} \geq \frac{1}{1+\varepsilon}$ . Thus, it suffices to prove that, for  $d \geq 2$ ,  $M \geq 2$  and  $\varepsilon = 1/12$ ,

$$\frac{1}{1+\varepsilon}(1+dM) \geq d+M.$$

This can be seen, for example, by replacing  $d$  with  $2+\tilde{d}$  and  $M$  with  $2+\tilde{M}$ .  $\square$

**Corollary I.36.** For any integer  $d > 1$  and  $k > 1$  positive integers  $m_1, \dots, m_k$  summing to  $m$ ,

$$\frac{\binom{dm}{dm_1, \dots, dm_k}}{\binom{m}{m_1, \dots, m_k}} \geq \prod_{j=1}^k (\tau(dm_j) - 1),$$

where  $\tau(n)$  is the number of divisors of  $n$ .

*Proof.* We use the inequality  $n/2 \geq \tau(n) - 1$ , valid for  $n \geq 1$ . By Lemma I.35 it is then sufficient to show that

$$\frac{1}{d^{(k-1)/2}} \left( \frac{m^m}{\prod_{j=1}^k m_j^{m_j}} \right)^{d-1} > \left( \frac{d}{2} \right)^k \prod_{j=1}^k m_j,$$

or, equivalently,

$$\left( \prod_{j=1}^k \frac{1}{m_j} \right) \left( \frac{m^m}{\prod_{j=1}^k m_j^{m_j}} \right)^{d-1} > \frac{1}{\sqrt{d}} \left( \frac{d}{2} \right)^k d^{k/2}.$$

We will show the stronger inequality

$$\left( \frac{m^m}{\prod_{j=1}^k m_j^{m_j+1}} \right)^{\frac{1}{k}} > \left( \frac{d\sqrt{d}}{2} \right)^{\frac{1}{d-1}}. \quad (13)$$

It is not hard to see that the right hand side of this inequality, as a real function of  $d > 1$ , attains its maximum between 3 and 4 and is unimodal. By direct inspection we see that for integral  $d$  the maximum of the right hand side is attained at  $d = 3$ , where it is  $(\frac{27}{4})^{\frac{1}{4}} \approx 1.61$ .

To find the minimum of the left hand side of inequality (13), we consider the function

$$h(z) = \frac{(z + \check{m})^{z+\check{m}}}{z^{z+1}}, \text{ where } z \geq 1.$$

For  $\check{m} = 1$  we have  $h(z) = (1 + 1/z)^{z+1}$ , which is strictly decreasing towards Euler's number  $e$  as  $z$  increases. For  $\check{m} \geq 2$  we show that  $h$  is strictly increasing. Indeed, the derivative of  $\ln h(z)$  equals

$$\ln \left( 1 + \frac{\check{m}}{z} \right) - \frac{1}{z}.$$

This expression is positive for  $\check{m} \geq 2$  and  $z \geq 1$ , since we have

$$\begin{aligned} \exp \left( \frac{1}{z} \right) &= 1 + \frac{1}{z} \left( 1 + \sum_{k \geq 2} \frac{1}{k! z^{k-1}} \right) \\ &\leq 1 + \frac{1}{z} \left( 1 + \sum_{k \geq 2} \frac{1}{k!} \right) = 1 + \frac{e-1}{z} < 1 + \frac{\check{m}}{z}. \end{aligned}$$

For  $k = 2$  and  $m_2 = 1$ , the left hand side of (13) equals  $\sqrt{h(m_1)}$  with  $\check{m} = 1$ . It is thus strictly larger than  $\sqrt{e} \approx 1.64$ , which in turn is larger than  $(27/4)^{1/4}$ , the maximum of the right hand side of (13).

For  $k = 2$  and  $m_2 > 1$  and for  $k \geq 3$  the analysis of  $h$  implies that the left hand side of (13) is strictly increasing in each of the variables  $m_i$ ,  $1 \leq i \leq k$ , because it equals

$$\left( \frac{h(m_i)}{\prod_{j \neq i} m_j^{m_j+1}} \right)^{1/k},$$

with  $\check{m} = \sum_{j \neq i} m_j$ . For  $k = 2$  and  $m_2 > 1$ , this expression is minimized at  $m_1 = 1$ , where it is larger than  $\sqrt{e}$  as shown above. For  $k > 2$  the minimum is attained at  $m_1 = \dots = m_k = 1$ , and is equal to  $k$ .  $\square$

### 1.7.2 The bound for standard Young tableaux of straight shape

The goal of this subsection is to prove the special case of Theorem I.31 where  $\mu = \emptyset$  and  $k = 1$ . Note that we have the equivalence

$$|\text{BST}(\lambda, 1)| \geq \sum_{d|n, d>1} |\text{BST}(\lambda, d)| \iff \frac{\sum_{d|n} |\text{BST}(\lambda, d)|}{|\text{BST}(\lambda, 1)|} \leq 2. \quad (14)$$

For the remainder of this subsection we focus on proving the latter inequality for  $\lambda \notin \{(n), (1^n)\}$ . We shall first make use the following theorem by S. Fomin and N. Lulov.

**Theorem I.37** ([8]). For any partition  $\lambda \vdash n$ , we have

$$|\text{BST}(\lambda, d)| \leq Q(n, d) \cdot |\text{BST}(\lambda, 1)|^{1/d} \quad \text{where} \quad Q(n, d) := \sqrt[d]{\frac{d^n}{\binom{n}{n/d, \dots, n/d}}}. \quad (15)$$

We introduce the auxiliary function  $B_n(x)$  as

$$B_n(x) := \sum_{d|n} Q(n, d) x^{\frac{1}{d}-1}. \quad (16)$$

By plugging  $x = |\text{BST}(\lambda, 1)|$  into (16), and using (15), we have that

$$\begin{aligned} B_n(|\text{BST}(\lambda, 1)|) &= \sum_{d|n} Q(n, d) |\text{BST}(\lambda, 1)|^{\frac{1}{d}-1} \\ &= \frac{\sum_{d|n} Q(n, d) |\text{BST}(\lambda, 1)|^{1/d}}{|\text{BST}(\lambda, 1)|} \\ &\geq \frac{\sum_{d|n} |\text{BST}(\lambda, d)|}{|\text{BST}(\lambda, 1)|}. \end{aligned}$$

Hence, if we can show that  $B_n(x) \leq 2$  for suitable values of  $x$  and  $n$  we obtain the second inequality in (14).

**Lemma I.38.** *The inequality*

$$\frac{\sum_{d|n} |\text{BST}(\lambda, d)|}{|\text{BST}(\lambda, 1)|} \leq 2$$

holds for all partitions  $\lambda \vdash n$  other than  $(n)$  and  $(1^n)$  with  $n$  composite.

*Proof.* When  $n$  is a prime number the statement is trivial. Otherwise, we distinguish between several cases.

**Case**  $\lambda = (n-1, 1)$  or  $\lambda = (2, 1^{n-2})$ . In this case,

$$|\text{BST}(\lambda, d)| = \begin{cases} n-1 & \text{if } d=1 \\ 1 & \text{otherwise,} \end{cases}$$

and we observe that  $n-1 \geq \tau(n)-1$ , where  $\tau(n)$  is the number of divisors of  $n$ .

**Case**  $|\lambda| \leq 8$ . The remaining 14 partitions (and their conjugates) not covered previously can be verified by hand.

**Case**  $|\lambda| \geq 9$ . As we noted before, it suffices to show that  $B_n(|\text{BST}(\lambda, 1)|) \leq 2$ . To do so it suffices to prove the following three properties, whenever  $n \geq 9$ :

- the function  $x \mapsto B_n(x)$  is strictly decreasing for fixed  $n$
- $B_n\left(\frac{n^2}{3}\right) \leq 2$  and
- $|\text{BST}(\lambda, 1)| \geq \frac{n^2}{3}$  for  $\lambda \notin \{(n), (1^n), (n-1, 1), (2, 1^{n-2})\}$ .

The first item is obvious from the definition of  $B_n(x)$ , as all exponents of  $x$  are negative. The second item is proved later in Lemma I.40. We proceed by verifying the third item.

Suppose that  $|\lambda| \geq 9$  and that  $\lambda$  is not one of the excluded shapes. We will prove the statement by induction on the size of  $\lambda$ . To be able to perform the inductive step we first consider the following four *exceptional shapes*. If  $\lambda$  is a hook of the form  $(n-2, 1^2)$  or its conjugate, then  $|\text{BST}(\lambda, 1)| = \binom{n-1}{2}$ . Moreover, if  $\lambda = (n-2, 2)$  or its conjugate, then  $|\text{BST}(\lambda, 1)| = \frac{n(n-3)}{2}$ . In both cases the inequality is true for  $n \geq 9$ .

The base cases of the induction,  $|\lambda| \in \{9, 10\}$ , can be verified using a computer, so we proceed to do the inductive step.

If  $\lambda$  is a rectangle and  $n \geq 11$ , we can either remove two cells from the last row, or the last column, to obtain two new partitions  $\mu$  and  $\nu$  of size  $n-2$ , respectively. A simple bijective argument shows that

$$|\text{BST}(\lambda, 1)| = |\text{BST}(\mu, 1)| + |\text{BST}(\nu, 1)|.$$

By induction,  $|\text{BST}(\lambda, 1)| \geq 2(n-2)^2/3 \geq n^2/3$ , where the last inequality is true for  $n \geq 7$ . Note that  $\mu$  and  $\nu$  are not among the excluded shapes.

If  $\lambda$  is not a rectangle, and  $\lambda$  is not an exceptional shape, we obtain two partitions  $\mu$  and  $\nu$  of size  $n-1$  by removing two distinct corners of  $\lambda$ . This is possible because  $\lambda$  is not a rectangle.

These partitions  $\mu$  and  $\nu$  are not among the excluded shapes, because  $\lambda$  is not one of the exceptional shapes. Therefore we have

$$|\text{BST}(\lambda, 1)| \geq |\text{BST}(\mu, 1)| + |\text{BST}(\nu, 1)|.$$

The inequality follows as above by induction. □

**Lemma I.39.** For positive integers  $d \mid n$ , we have

$$Q(n, d) \leq \sqrt{n}, \tag{17}$$

where  $Q(n, d) = \left( \frac{d^n}{n!/((n/d)!)^d} \right)^{1/d}$  is as in (15).

*Proof.* First we prove (17) for  $n \in \{1, 2\}$  by direct inspection. For  $n \geq 3$  we use again Robbins' approximation, Proposition I.34. We have that

$$\begin{aligned} Q(n, d) &= \left( \frac{d^n}{n!/((n/d)!)^d} \right)^{\frac{1}{d}} = \frac{d^{n/d} (n/d)!}{(n!)^{1/d}} \\ &= (2\pi n)^{-\frac{1}{2d}} \left( 2\pi \frac{n}{d} \right)^{\frac{1}{2}} \exp \left( r_{n/d} - \frac{r_n}{d} \right). \end{aligned}$$

By plugging this into (17) and simplifying the expressions it suffices to show that

$$\exp(2ndr_{n/d} - 2nr_n) \leq (2\pi n M_d)^n, \tag{18}$$

where  $M_d := \left( \frac{d}{2\pi} \right)^d$ . By now using the approximations  $r_{n/d} < \frac{d}{12n}$  and  $r_n > 0$  we have

$$2ndr_{n/d} - 2nr_n \leq 2ndr_{n/d} \leq \frac{2nd^2}{12n} = \frac{d^2}{6}$$

and thus the left hand side of (18) can be bound with  $\exp(\frac{d^2}{6})$ .

**Claim:** For positive integers,  $n \geq 3$ ,  $n \geq d$ , we have

$$\exp\left(\frac{d^2}{6}\right) \leq (2\pi n M_d)^n. \quad (19)$$

**Case  $d \geq 8$ .** In this case we have  $\exp(1/6) < \frac{d}{2\pi}$ , and therefore  $\exp(\frac{d^2}{6}) < M_d^d \leq M_d^n \leq (2\pi n M_d)^d$ . This proves (19).

**Case  $1 \leq d \leq 7$ .** Direct inspection shows that  $2\pi M_d \geq 2\pi M_2 = 2/\pi$ , so for  $n \geq 2$  we have  $2\pi n M_d > 1$  and therefore  $(2\pi n M_d)^n$  is strictly increasing in  $n$ .

Finally, direct inspection now verifies that (19) is already satisfied for  $n = 3$  and each  $d \in \{1, \dots, 7\}$ . This proves the claim and concludes the proof.  $\square$

**Lemma I.40.** For integers  $n \geq 9$  we have  $B_n\left(\frac{n^2}{3}\right) \leq 2$ .

*Proof.* We first verify the inequality for all  $n$  in the range  $9 \leq n \leq 120$ . This can be done using a computer. For  $n \geq 121$ , we shall bound  $B_n(x)$  from above by  $g_n(x)$ , defined as

$$g_n(x) = 1 + \sqrt{nx}^{-\frac{1}{2}} + 2nx^{-\frac{2}{3}}.$$

A simple computation shows that for  $n = 121$ , we have that  $g_n\left(\frac{n^2}{3}\right) \approx 1.999$ . Hence, if we can show that

- $B_n(x) \leq g_n(x)$  for all  $x \geq 1$  and
- $n \mapsto g_n\left(\frac{n^2}{3}\right)$  is strictly decreasing,

then we are done. We proceed with the first point. Recall that the number of divisors of  $n$  is at most  $2\sqrt{n}$  for  $n \geq 1$ . We thus obtain

$$\begin{aligned} B_n(x) &= \sum_{d|n} Q(n, d) x^{\frac{1}{d}-1} \\ &= 1 + \sum_{d|n, d>1} Q(n, d) x^{\frac{1}{d}-1} \\ \{\text{by Lemma I.39}\} &\leq 1 + \sum_{d|n, d>1} \sqrt{nx}^{\frac{1}{d}-1} \\ &\leq 1 + \sqrt{nx}^{-\frac{1}{2}} + \sqrt{n} \sum_{d|n, d>1} x^{\frac{1}{3}-1} \\ &\leq 1 + \sqrt{nx}^{-\frac{1}{2}} + 2nx^{-\frac{2}{3}} \\ &= g_n(x). \end{aligned}$$

For the second point, it is enough to note that

$$g_n(n^2/3) = 1 + \frac{\sqrt{3}}{\sqrt{n}} + \frac{2 \times 9^{1/3}}{\sqrt[3]{n}}$$

which is obviously decreasing in  $n$ .  $\square$

### 1.7.3 The bound for skew standard Young tableaux

We now extend the result of the previous section to skew shapes.

**Lemma I.41.** *Let  $\lambda/\mu$  be a skew shape with  $n$  cells. Then*

$$|\text{BST}(\lambda/\mu, 1)| \geq \sum_{d|n, d>1} |\text{BST}(\lambda/\mu, d)|.$$

*if and only if  $\lambda/\mu$  is neither the partition  $(n)$  nor the partition  $(1^n)$ .*

*Proof.* We distinguish two cases:

**Case 1:**  $\lambda/\mu$  has at least two cells in some row and in some column.

We prove the following sequence of inequalities:

$$\begin{aligned} |\text{BST}(\lambda/\mu, 1)| &= \sum_{\nu \vdash n} c_{\mu, \nu}^{\lambda} |\text{BST}(\nu, 1)| \\ &\geq \sum_{\nu \vdash n} c_{\mu, \nu}^{\lambda} \sum_{d|n, d>1} |\text{BST}(\nu, d)| \end{aligned} \quad (20)$$

$$\geq \sum_{d|n, d>1} |\text{BST}(\lambda/\mu, d)|. \quad (21)$$

We first prove inequality (20), for each summand separately. That is, we show that for all partitions  $\nu \vdash n$ ,

$$c_{\mu, \nu}^{\lambda} |\text{BST}(\nu, 1)| \geq c_{\mu, \nu}^{\lambda} \sum_{d|n, d>1} |\text{BST}(\nu, d)|.$$

Since  $\lambda/\mu$  has at least two cells in the same row and two cells in the same column, we can apply Lemma I.8. It follows that  $c_{\mu, (1^n)}^{\lambda} = c_{\mu, (n)}^{\lambda} = 0$ . Thus, the inequality holds for  $\nu = (1^n)$  and  $(n)$ . For all other partitions  $\nu \vdash n$ , the inequality follows from Lemma I.38.

We now change the order of summation and prove inequality (21), again separately for each summand. That is, for fixed  $d > 1$  with  $dm = n$ , we show

$$\sum_{\nu \vdash n} c_{\mu, \nu}^{\lambda} |\text{BST}(\nu, d)| \geq |\text{BST}(\lambda/\mu, d)|.$$

Indeed, we have

$$\begin{aligned} \sum_{\nu \vdash n} c_{\mu, \nu}^{\lambda} |\text{BST}(\nu, d)| &= \sum_{\nu \vdash n} c_{\mu, \nu}^{\lambda} |\chi^{\nu}((d^m))| \\ &\geq \left| \chi^{\lambda/\mu}((d^m)) \right| \\ &= |\text{BST}(\lambda/\mu, d)|. \end{aligned}$$

The two equalities follow from Corollary I.30, whereas the inequality is obtained by taking absolute values on both sides of the expansion of the skew character into irreducible characters, Equation (7), evaluated at  $(d^m)$  and applying the triangle inequality.

**Case 2:** all columns or all rows of  $\lambda/\mu$  contain at most one cell.



By symmetry we may assume that every connected component of  $\lambda/\mu$  is a single row. Let the lengths of these rows be  $n_1, n_2, \dots, n_r$ . We have  $\text{BST}(\lambda/\mu, d) = \emptyset$  unless all  $n_i$  are multiples of  $d$ . In this case we find by explicit enumeration that

$$|\text{BST}(\lambda/\mu, d)| = \binom{n/d}{n_1/d, n_2/d, \dots, n_r/d}.$$

It then suffices to prove that

$$\binom{n}{n_1, n_2, \dots, n_r} \geq \sum_{d>1, d|\text{gcd}(n_1, n_2, \dots, n_r)} \binom{n/d}{n_1/d, n_2/d, \dots, n_r/d}.$$

This inequality is an easy consequence of Corollary I.36. □

#### 1.7.4 The general case

We are now ready to prove Theorem I.31 itself.

*Proof of Theorem I.31.* Let  $(v^1/\kappa^1, \dots, v^k/\kappa^k)$  be the skew  $k$ -quotient of  $\lambda/\mu$ . We first establish, for  $1 \leq i \leq k$ , the inequality

$$(\tau(|v^i/\kappa^i|) - 1)|\text{BST}(v^i/\kappa^i, 1)| \geq \sum_{\substack{d \mid |v^i/\kappa^i| \\ d>1}} |\text{BST}(v^i/\kappa^i, d)|.$$

If  $v^i/\kappa^i$  is neither the single row nor the single column partition, the bound for skew standard Young tableaux, Lemma I.41, applies. Moreover, in this case  $|v^i/\kappa^i| \geq 3$  and therefore  $\tau(|v^i/\kappa^i|) - 1 \geq 1$ . Otherwise,  $|\text{BST}(v^i/\kappa^i, d)| = 1$  for all  $d \mid |v^i/\kappa^i|$ , and the inequality holds trivially.

Thus, setting  $g = \text{gcd}(|v^1/\kappa^1|, \dots, |v^k/\kappa^k|)$ ,

$$\begin{aligned} \prod_{\substack{i=1 \\ v^i/\kappa^i \neq \emptyset}}^k (\tau(|v^i/\kappa^i|) - 1) |\text{BST}(v^i/\kappa^i, 1)| &\geq \prod_{\substack{i=1 \\ v^i/\kappa^i \neq \emptyset}}^k \sum_{\substack{d \mid |v^i/\kappa^i| \\ d>1}} |\text{BST}(v^i/\kappa^i, d)| \\ &\geq \sum_{\substack{d|g \\ d>1}} \prod_{\substack{i=1 \\ v^i/\kappa^i \neq \emptyset}}^k |\text{BST}(v^i/\kappa^i, d)| \\ &= \sum_{\substack{d|g \\ d>1}} \prod_{i=1}^k |\text{BST}(v^i/\kappa^i, d)| \\ \{\text{By Theorem I.22}\} &= \sum_{\substack{d|g \\ d>1}} \frac{|\text{BST}(\lambda/\mu, dk)|}{\binom{\sum_i |v^i/\kappa^i|/d}{|v^1/\kappa^1|/d, \dots, |v^k/\kappa^k|/d}}. \end{aligned}$$

Note that, for any  $d \geq 1$ , there is exactly one border-strip tableaux having empty shape:  $|\text{BST}(\emptyset, k)| = 1$ . Suppose that  $g = \text{gcd}(|v^1/\kappa^1|, \dots, |v^k/\kappa^k|) > 1$  and there are at least

two non-empty skew shapes among  $\nu^1/\kappa^1, \dots, \nu^k/\kappa^k$ . Then we can apply the above inequality and Corollary I.36 and obtain

$$\begin{aligned}
|\text{BST}(\lambda/\mu, k)| &= \binom{\sum_i |\nu^i/\kappa^i|}{|\nu^1/\kappa^1|, \dots, |\nu^k/\kappa^k|} \prod_{i=1}^k |\text{BST}(\nu^i/\kappa^i, 1)| \\
&\geq \binom{\sum_i |\nu^i/\kappa^i|}{|\nu^1/\kappa^1|, \dots, |\nu^k/\kappa^k|} \prod_{\substack{i=1 \\ \nu^i/\kappa^i \neq \emptyset}}^k \left( \tau(|\nu^i/\kappa^i|) - 1 \right)^{-1} \\
&\quad \sum_{d|g, d>1} |\text{BST}(\lambda/\mu, dk)| \binom{\sum_i |\nu^i/\kappa^i|/d}{|\nu^1/\kappa^1|/d, \dots, |\nu^k/\kappa^k|/d}^{-1} \\
&\geq \sum_{d|g, d>1} |\text{BST}(\lambda/\mu, dk)| \\
&= \sum_{d>1} |\text{BST}(\lambda/\mu, dk)|.
\end{aligned}$$

If  $g = \gcd(|\nu^1/\kappa^1|, \dots, |\nu^k/\kappa^k|) = 1$ , the inequality is trivially true.

If there is precisely one non-empty skew shape  $\nu/\kappa$  among  $\nu^1/\kappa^1, \dots, \nu^k/\kappa^k$ , we have  $|\text{BST}(\lambda/\mu, dk)| = |\text{BST}(\nu/\kappa, d)|$  for all  $d$  by Theorem I.22.

If  $\nu/\kappa$  is neither  $(n/k)$  nor  $(1^{n/k})$ , Lemma I.41 applies and we have

$$|\text{BST}(\lambda/\mu, k)| = |\text{BST}(\nu/\kappa, 1)| \geq \sum_{d|\frac{n}{k}, d>1} |\text{BST}(\nu/\kappa, d)| = \sum_{d|\frac{n}{k}, d>1} |\text{BST}(\lambda/\mu, dk)|.$$

Otherwise, if  $\nu/\kappa$  is either  $(n/k)$  or  $(1^{n/k})$ , Corollary I.25 implies that there is only one element in  $\text{BST}(\lambda/\mu, k)$ .  $\square$

## I.8 CYCLIC SIEVING FOR SKEW STANDARD TABLEAUX

In this section we apply the bounds established in the previous section and Theorem I.3 to prove the existence of several cyclic sieving phenomena for various families of skew standard Young tableaux.

Let us first put the bound from Theorem I.31 into the form required to apply Theorem I.3.

**Proposition I.42.** *Let  $\lambda/\mu$  be a non-empty skew shape with  $n$  cells, let  $m \in \mathbb{N}_0$  and let  $k$  be a positive integer with  $k \mid n$ . Then*

$$\sum_{d|\frac{n}{k}} \mu(d) |\text{BST}(\lambda/\mu, dk)|^m \geq 0,$$

or, equivalently,

$$\sum_{d|k} \mu(k/d) |f^{\lambda/\mu}(\xi^d)|^m \geq 0,$$

for a primitive  $n^{\text{th}}$  root of unity  $\xi$ .

*Proof.* The equivalence follows from Corollary I.30 and replacing  $d$  with  $\frac{n}{dk}$  and  $k$  with  $\frac{n}{k}$ . We prove the first inequality.

If  $|\text{BST}(\lambda/\mu, k)| = 1$ , we also have  $|\text{BST}(\lambda/\mu, dk)| = 1$  for any  $d \mid \frac{n}{k}$  by Corollary I.25. Therefore,

$$\sum_{d \mid \frac{n}{k}} \mu(d) |\text{BST}(\lambda/\mu, dk)|^m = \sum_{d \mid \frac{n}{k}} \mu(d) = \begin{cases} 1 & \text{if } n = k \\ 0 & \text{if } n \neq k \end{cases} \geq 0.$$

This reasoning also covers the case  $m = 0$ .

Otherwise, since  $\mu(1) = 1$  and  $\mu(d) \geq -1$ , we have

$$\sum_{d \mid \frac{n}{k}} \mu(d) |\text{BST}(\lambda/\mu, dk)|^m \geq |\text{BST}(\lambda/\mu, k)|^m - \sum_{d \mid \frac{n}{k}, d > 1} |\text{BST}(\lambda/\mu, dk)|^m \geq 0,$$

where the final inequality follows from Theorem I.31.  $\square$

**Remark I.43.** One might think that  $|f^{\lambda/\mu}(\zeta^d)|$  could be the number of fixed points of a group action, despite the fact that  $|f^{\lambda/\mu}(q)|$  is not a polynomial. However, this is not the case.

For example, consider  $\lambda = (2, 1)$ . Then  $f^\lambda(q) = q + q^2$  and, for a 3<sup>rd</sup> root of unity  $\zeta$ , we have  $|f^\lambda(\zeta^3)| = |\text{BST}(\lambda, 1)| = 2$  and  $|f^\lambda(\zeta)| = |\text{BST}(\lambda, 3)| = 1$ . This is incompatible with the possible orbit sizes of a group action on a set with two elements. Indeed, for  $k = 3$  we obtain

$$\frac{1}{k} \sum_{d \mid k} \mu(k/d) |f^\lambda(\zeta^d)| = \frac{1}{3}(-1 + 2),$$

which, by Remark I.5, would have to be an integer.

Taking into account the previous remark, it makes sense to look for shapes  $\lambda/\mu$  such that the character  $f^{\lambda/\mu}$  evaluated at roots of unity is nonnegative.

**Theorem I.44.** *Let  $\lambda/\mu$  be a skew shape with  $n$  cells and let  $m$  be a positive integer. Then there is a cyclic group action  $\rho$  of order  $n$  such that*

$$\left( \underbrace{\text{SYT}(\lambda/\mu) \times \cdots \times \text{SYT}(\lambda/\mu)}_m, \langle \rho \rangle, f^{\lambda/\mu}(q)^m \right)$$

*exhibits the cyclic sieving phenomenon if and only if  $m$  is even, or  $m$  is odd and for each positive integer  $k$  with  $k \mid n$  there is a tiling of  $\lambda/\mu$  of even height with strips of size  $k$ .*

**Remark I.45.** The case  $m = 2$  of this proposition does not extend to squares of arbitrary representations of the symmetric group. For example, consider the representation with character  $\chi^{(4)} + \chi^{(2,1^2)}$ . Its fake degree polynomial is  $f(q) = 1 + q^3 + q^4 + q^5$ . Then we obtain, for a primitive fourth root of unity  $\zeta$ , that  $f(\zeta)^2 = 4$  and  $f(\zeta^2)^2 = 0$ . This violates the condition in Theorem I.3 for  $k = 2$ , because  $\mu(2)f(\zeta)^2 + \mu(1)f(\zeta^2)^2 = -4$ .

*Proof.* Let  $\zeta$  be an  $n^{\text{th}}$  primitive root of unity. Then Proposition I.42 together with Theorem I.3 ensures the existence of  $\rho$ , provided  $f^{\lambda/\mu}(\zeta^d)^m$  is nonnegative for all  $d \mid n$ . Conversely, nonnegativity is a necessary condition because, given a cyclic group action  $\rho$ , the number of fixed points of  $\rho^d$  equals  $f^{\lambda/\mu}(\zeta^d)^m$ .

It remains to consider the case of odd  $m$ . By Corollary I.30  $f^{\lambda/\mu}(\zeta^d)$ , with  $d = \frac{n}{k}$ , is nonnegative if and only if there is a tiling of  $\lambda/\mu$  of even height with strips of size  $k$ .  $\square$

**Corollary I.46.** Let  $\lambda = (a, 1^{n-a})$  be a hook-shaped partition of  $n$ . Then there is a cyclic group action  $\rho$  such that  $(\text{SYT}(\lambda), \langle \rho \rangle, f^\lambda(q))$  exhibits the cyclic sieving phenomenon if and only if  $n$  and  $a$  are odd and  $a - 1 \pmod m$  is even for  $m \mid n, 1 \leq m < a$ .

*Proof.* Suppose that  $n$ , and  $a$  are odd, and  $m \mid n$ . In particular,  $m$  is odd, too. Note that there is a unique tiling of a hook with border-strips of size  $m$ . We have to show that the height of this tiling is even if and only if  $a - 1 \pmod m$  is even.

Recall that the height of a tile is one less than the number of rows it spans. If, and only if  $a - 1 \pmod m$  is even, the height of the tile covering the top left corner of the shape must be even: this tile must cover an odd number of cells in the first row and, since its size  $m$  is odd, an even number of cells in the first column. Since the height of all other tiles is evidently even, too, so is the total height.

If the parity of  $n$  and  $a$  is different, then the tiling with a single strip of size  $n$  has height  $n - a$ , which is odd. If both  $n$  and  $a$  are even, the tiling with two strips of size  $n/2$  has odd height: if  $a \leq n/2$ , the height is  $n - a - 1$ , otherwise the height is  $n - 1$ .  $\square$

**Remark I.47.** According to the previous theorem, for  $\lambda = (3, 1^{n-3})$  a cyclic group action of order  $n$  with character  $f^\lambda(q) = q^{(n-2)(n-3)/2} \frac{[n-1]_q [n-2]_q}{[2]_q}$  exists for all odd  $n > 3$ . In this case, there should be one singleton orbit and  $(n - 3)/2$  orbits of size  $n$ . Indeed, an appropriate group action can be constructed as follows:

Identify a tableau with the two labels  $x < y$  different from 1 in the first row. Note that  $y - x \in \{1, 2, \dots, n - 2\}$ , and only the pair  $(2, n)$  has difference  $n - 2$ . We let the generator of the group action  $\eta$  act as follows:

$$\eta(x, y) := \begin{cases} (2, n) & \text{if } x = 2, y = n, \\ (x + 2, y + 2) & \text{if } 2 \leq x < y \leq n - 2, \\ (2, x + 1) & \text{if } y = n - 1, \\ (3, x + 1) & \text{if } x > 2, y = n. \end{cases}$$

We then note that if  $(u, v) = \eta(x, y)$ , then  $v - u \in \{y - x, (n - 2) - (y - x)\}$ . This explains why there are  $(n - 3)/2$  orbits of length  $n$ . We leave the remaining details to the reader.

**Remark I.48.** It turns out that one can determine the number of border-strips  $\lambda/\mu$  of size  $n$  which carry a cyclic group action of order  $n$  and character  $f^{\lambda/\mu}(q)$ .

A different way to ensure positivity of the character  $f^{\lambda/\mu}$  is to decrease the order of the cyclic group as in Remark I.2.

**Theorem I.49.** Let  $\lambda/\mu$  be a skew shape such that every row contains a multiple of  $m$  cells. Then there is a cyclic group action  $\rho$  of order  $m$  such that

$$\left( \text{SYT}(\lambda/\mu), \langle \rho \rangle, f^{\lambda/\mu}(q) \right)$$

exhibits the cyclic sieving phenomenon.

*Proof.* By Theorem I.3 it suffices to show that for a primitive  $m^{\text{th}}$  root of unity  $\zeta$  and every  $k \mid m$

$$\sum_{d \mid k} \mu(k/d) f^{\lambda/\mu}(\zeta^d) \geq 0.$$

Let  $|\lambda/\mu| = dm$ . By Proposition I.42, we have

$$\sum_{d \mid k} \mu(k/d) |f^{\lambda/\mu}(\zeta^d)| \geq 0$$

for an  $n^{\text{th}}$  root of unity  $\zeta$  and every  $k \mid dm$ . Let  $\zeta = \zeta^{\frac{n}{m}}$ . Then, by Corollary I.30,

$$f^{\lambda/\mu}(\zeta^d) = f^{\lambda/\mu}(\zeta^{d \frac{n}{m}}) = (-1)^{\text{height}(B)} |\text{BST}\left(\lambda/\mu, \frac{m}{d}\right)|.$$

Since the length of every row of  $\lambda/\mu$  is a multiple of  $m$ , there is a filling with border-strips of size  $\frac{m}{d} \mid m$ , where every strip has height 0.  $\square$

We remark that stretching shapes seems to be a fruitful way to construct cyclic sieving phenomena, as was previously shown with fillings related to Macdonald polynomials by P. Alexandersson & J. Uhlin [3]. We also mention the following conjecture, which has recently been proved in the non-skew case in [15, Cor. 3.3].

**Conjecture I.50** ([1, Conj. 3.4]). *There is an action  $\beta$  on the set of semi-standard Young tableaux  $\text{SSYT}(m\lambda/m\mu, k)$  of order  $m$  such that*

$$\left( \text{SSYT}(m\lambda/m\mu, k), \langle \beta \rangle, s_{m\lambda/m\mu}(1, q, q^2, \dots, q^{k-1}) \right)$$

*exhibits the cyclic sieving phenomenon.*

For some shapes  $\lambda/\mu$ , the tiling may have odd height, but one can multiply  $f^{\lambda/\mu}(q)$  with  $q^{n/2}$ , provided that the size  $n$  of  $\lambda/\mu$  is even, to obtain positivity at roots of unity. An important example is the case of rectangular shapes. In this case, B. Rhoades proved that promotion, together with a natural  $q$ -analogue of the hook length formula exhibits the cyclic sieving phenomenon. The following result is much weaker, because it only establishes the existence of a group action, but it is also much easier to prove, and illustrates the method.

**Theorem I.51** ([21]). *Let  $\lambda = a^b$  be a rectangular diagram with  $n = ab$  cells, and set  $\kappa(\lambda) := \sum_j \binom{\lambda'_j}{2}$ . Then there is a cyclic group action  $\partial$  of order  $n$  such that*

$$\left( \text{SYT}(\lambda), \langle \partial \rangle, q^{-\kappa(\lambda)} f^\lambda(q) \right)$$

*exhibits the cyclic sieving phenomenon.*

*Proof.* It is a well-known result by R. Stanley [28, Cor. 7.21.5], that

$$q^{-\kappa(\lambda)} f^\lambda(q) = \frac{[n]_q!}{\prod_{\square \in \lambda} [h(\square)]_q}$$

where  $h(\square)$  is the hook-value of  $\square$ . In particular,  $q^{-\kappa(\lambda)} f^\lambda(q)$  is a polynomial. We must check that this is nonnegative whenever  $q$  is an  $n^{\text{th}}$  root of unity. Suppose that

$m \mid n$ ,  $n = dm$  and let  $\zeta$  be a primitive  $n^{\text{th}}$  root of unity. Corollary I.30 implies that  $f^\lambda(\zeta^d)$  is non-zero only if and only if  $\text{BST}(a^b, m)$  is non-empty. Using the abacus, one can show that  $m \mid a$  or  $m \mid b$  if and only if the  $m$ -core is empty, which, for straight shapes, is equivalent to  $|\text{BST}(a^b, m)| > 0$ . From here, it is a straightforward exercise to show that  $\kappa(\lambda) = ba(a-1)/2$  and that  $\zeta^{-d \cdot ba(a-1)/2} f^\lambda(\zeta^d)$  is nonnegative for all  $d \mid n$ .

Finally, Proposition I.42 and Theorem I.3 gives the result.  $\square$

## I.9 PERMUTATIONS AND INVARIANTS OF THE ADJOINT REPRESENTATION OF $\text{GL}_n$

In this section we apply our results to study the space of invariants of tensor powers of the adjoint representation  $\mathfrak{gl}_r$  of the general linear group  $\text{GL}_r$ .

**Definition I.52.** The *rotation*  $\text{rot } \sigma$  of a permutation  $\sigma \in \mathfrak{S}_n$  is the permutation obtained by conjugating with the long cycle  $(1, \dots, n)$ .

**Remark I.53.** Equivalently, if  $M_\sigma$  is the permutation matrix corresponding to  $\sigma$ , then  $M_{\text{rot } \sigma}$  is obtained by removing the first column of  $M_\sigma$  and appending it on the right, and then removing the first row and appending it at the bottom.

Yet equivalently, let  $D_\sigma$  be the chord diagram associated with  $\sigma$ , that is, the directed graph with vertices  $\{1, \dots, n\}$  arranged counterclockwise on a circle, and arcs  $(i, \sigma(i))$ . Then  $D_{\text{rot } \sigma}$  is the chord diagram obtained by rotating the graph clockwise. See Figure 6 for an illustration.

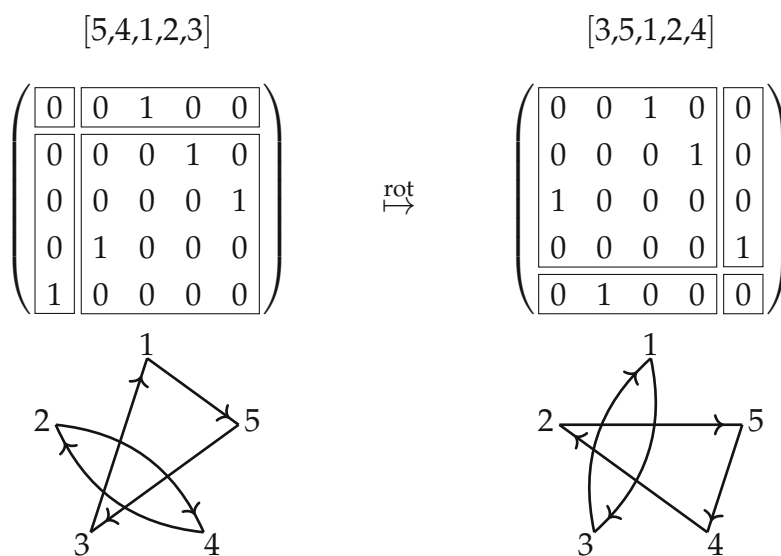


Figure 6: Rotation of  $\pi = [5,4,1,2,3]$  as conjugation by the long cycle  $(1, 2, 3, 4, 5)$ , cyclic shift of the permutation matrix and rotation of the chord diagram. Note that  $\text{sh}([5,4,1,2,3]) = (3, 1^2)$  and  $\text{sh}([3,5,1,2,4]) = (3, 2)$

The following theorem makes the character of rotation explicit.

**Theorem I.54** ([4, 22, 24]).

$$\left( \mathfrak{S}_n, \langle \text{rot} \rangle, \sum_{\lambda \vdash n} f^\lambda(q)^2 \right)$$

exhibits the cyclic sieving phenomenon.

*Proof.* Consider the adjoint representation of  $\mathfrak{S}_n$ , that is,  $\mathfrak{S}_n$  acting on itself by conjugation, or relabelling. It is well-known (see, e.g., [28, Ex. 7.71a]) that the character of this representation equals  $\sum_{\lambda \vdash n} \chi^\lambda \bar{\chi}^\lambda$ . Since the restriction of the adjoint representation to the cyclic group generated by the long cycle  $(1, \dots, n)$  is precisely the action  $\text{rot}$ , the result follows from Proposition I.11.  $\square$

**Definition I.55.** Recall that the *Robinson–Schensted correspondence* provides a bijection

$$\mathfrak{S}_n \leftrightarrow \{(P, Q) \in \text{SYT}(\lambda) \times \text{SYT}(\lambda) : \lambda \vdash n\}.$$

The *shape*  $\text{sh}(\sigma)$  of a permutation  $\sigma$  is the common shape of the standard Young tableaux  $P$  and  $Q$  corresponding to  $\sigma$  under the Robinson–Schensted correspondence. We let  $R_\lambda$  denote the set of permutations of shape  $\lambda$ .

We are now ready to prove the first major result of this section.

**Corollary I.56.** *Let  $P_n$  be the set of partitions of  $n$ . Then there exists a map  $\text{st} : \mathfrak{S}_n \rightarrow P_n$  which is invariant under rotation and equidistributed with the Robinson–Schensted shape. That is,*

$$\text{st} \circ \text{rot} = \text{st} \quad \text{and} \quad \sum_{\sigma \in \mathfrak{S}_n} \mathbf{s}_{\text{st}(\sigma)}(\mathbf{x}) = \sum_{\sigma \in \mathfrak{S}_n} \mathbf{s}_{\text{sh}(\sigma)}(\mathbf{x}).$$

Moreover, with  $\mathfrak{S}_n^\lambda := \{\pi \in \mathfrak{S}_n : \text{st}(\pi) = \lambda\}$ , the triple

$$(\mathfrak{S}_n^\lambda, \langle \text{rot} \rangle, f^\lambda(q)^2)$$

exhibits the cyclic sieving phenomenon.

We stress that we are unable to present such a statistic explicitly.

**Remark I.57.** Let us remark that the distribution of the shape of a permutation is well studied. Writing  $f^\lambda$  for the number of standard Young tableaux of shape  $\lambda$ , we have  $\sum_{\sigma \in \mathfrak{S}_n} \mathbf{s}_{\text{sh}(\sigma)}(\mathbf{x}) = \sum_{\lambda \vdash n} (f^\lambda)^2 \mathbf{s}_\lambda(\mathbf{x})$ . This is closely related to the *Plancherel measure*, which assigns to each partition  $\lambda$  of size  $n$  the probability  $(f^\lambda)^2/n!$  that a permutation of size  $n$ , chosen uniformly at random, has shape  $\lambda$ .

*Proof.* By Theorem I.44 there exists an action of the cyclic group of order  $n$  on  $R_\lambda$  with character  $(f^\lambda(q))^2$ . Let  $\rho$  be the direct sum over all  $\lambda \in P_n$  of these group actions. Thus,  $(\mathfrak{S}_n, \langle \rho \rangle, \sum_{\lambda \vdash n} f^\lambda(q)^2)$  exhibits the cyclic sieving phenomenon. Since  $\rho$  acts on each  $R_\lambda$  separately, we have

$$\text{sh}(\rho \cdot \sigma) = \text{sh}(\sigma). \quad (22)$$

By Theorem I.7 and Theorem I.54 the action of  $\rho$  and rotation are isomorphic. Therefore we have a bijection  $\phi : \mathfrak{S}_n \rightarrow \mathfrak{S}_n$  with

$$\phi(\text{rot} \sigma) = \rho \cdot \phi(\sigma). \quad (23)$$

Defining  $\text{st}(\sigma) := \text{sh}(\phi(\sigma))$ , we obtain

$$\text{st}(\text{rot} \sigma) = \text{sh}(\phi(\text{rot} \sigma)) \stackrel{(23)}{=} \text{sh}(\rho \cdot \phi(\sigma)) \stackrel{(22)}{=} \text{sh}(\phi(\sigma)) = \text{st}(\sigma).$$

Finally we have

$$\mathfrak{S}_n^\lambda = \phi^{-1}(R_\lambda),$$

yielding the last statement.  $\square$

**Remark I.58.** It is natural to ask whether for  $\lambda \vdash n$  we have

$$\#\{\sigma \in R_\lambda : \text{rot}^d(\sigma) = \sigma\} = f^\lambda(\zeta^d)^2,$$

for a positive integer  $d$  and a primitive  $n^{\text{th}}$  root of unity  $\zeta$ . In this case, the *subset cyclic sieving* technique of P. Alexandersson, S. Linusson & S. Potka [2, Prop. 29] would imply the non-skew,  $m = 2$  case of Theorem I.44. However, this fails already for  $\lambda = (2, 1)$ ; we have that  $R_\lambda = \{132, 213, 231, 312\}$  and  $\text{rot}$  fixes 231 and 312, but  $f^\lambda(q)^2 = q^2(1+q)^2$  evaluates to 1 at  $q = \exp(2\pi i/3)$ .

We now turn to the connection with the invariants of tensor powers of the adjoint representation of  $\text{GL}_r$ , which is the original motivation for this article.

Let  $V$  be an  $r$ -dimensional complex vector space and let  $\mathfrak{gl}_r = \text{End}(V)$  be the adjoint representation  $\text{GL}_r \rightarrow \text{End}(\mathfrak{gl}_r)$ ,  $A \mapsto TAT^{-1}$ .

The space of  $\text{GL}_r$ -invariants of the  $n^{\text{th}}$  tensor power of  $\mathfrak{gl}_r$  is

$$(\mathfrak{gl}_r^{\otimes n})^{\text{GL}_r} = \text{Hom}_{\text{GL}_r}(\mathfrak{gl}_r^{\otimes n}, \mathbb{C}).$$

A basis for this space can be indexed by J. Stembridge's alternating tableaux:

**Definition I.59** ([29]). A *staircase* is a dominant weight of  $\text{GL}_r$ , that is, a vector in  $\mathbb{Z}^r$  with weakly decreasing entries. A  *$\mathfrak{gl}_r$ -alternating tableau*  $\mathcal{A}$  of length  $n$  (and weight zero) is a sequence of staircases

$$\mathcal{A} = (\emptyset = \mu^0, \mu^1, \dots, \mu^{2n} = \emptyset)$$

such that

- for even  $i$ ,  $\mu^{i+1}$  is obtained from  $\mu^i$  by adding 1 to an entry, and
- for odd  $i$ ,  $\mu^{i+1}$  is obtained from  $\mu^i$  by subtracting 1 from an entry.

The set of  $\mathfrak{gl}_r$ -alternating tableaux of length  $n$  is denoted by  $\mathcal{A}_n^{(r)}$ .

B. Westbury defined a natural action, *promotion*, of the cyclic group of order  $n$  on the set of so called invariant words of any finite crystal, in particular alternating tableaux of length  $n$ , generalizing Schützenberger's promotion on rectangular standard Young tableaux. We refrain from giving a definition here and refer to S. Pfannerer, M. Rubey & B. Westbury [17] instead.

For our purposes, it is enough to relate promotion to an action on the  $\text{GL}_r$ -invariants of the  $n^{\text{th}}$  tensor power of  $\mathfrak{gl}_r$ . To do so, note that the symmetric group  $\mathfrak{S}_n$  acts on  $\mathfrak{gl}_r^{\otimes n}$  by permuting tensor positions, and therefore also on the space of invariants. It turns out that the action of the long cycle  $(1, \dots, n) \in \mathfrak{S}_n$  plays a special role:

**Theorem I.60** ([31, Sec. 6.3]). *There is a basis of  $(\mathfrak{gl}_r^{\otimes n})^{\text{GL}_r}$  which is preserved by the action of the long cycle. Moreover, this action is isomorphic to the action of promotion on the set of alternating tableaux.*

Note that B. Westbury's theorem only asserts the existence of the basis, no explicit construction is known. The main result of this section is the following refinement of his assertion.



**Theorem I.61.** Let  $\mathfrak{S}_n^{(r)} := \{\pi \in \mathfrak{S}_n : \ell(\text{st}(\pi)) \leq r\} = \bigcup_{\substack{\lambda \vdash n \\ \ell(\lambda) \leq r}} \mathfrak{S}_n^\lambda$ . Then there exists a bijection

$$\mathcal{P}^{(r)} : \mathcal{A}_n^{(r)} \rightarrow \mathfrak{S}_n^{(r)} \quad \text{with} \quad \mathcal{P}^{(r)} \circ \text{pr} = \text{rot} \circ \mathcal{P}^{(r)}.$$

for  $1 \leq r \leq n$ .

Equivalently, the action of promotion on the set of  $\mathfrak{gl}_r$ -alternating tableaux of length  $n$ , and the action of rotation on the set of permutations  $\mathfrak{S}_n^{(r)}$  are isomorphic:

$$(\text{pr}, \mathcal{A}_n^{(r)}) \cong (\text{rot}, \mathfrak{S}_n^{(r)}).$$

**Remark I.62.** Let us remark that for large dimension, that is,  $r \geq n$ , such a bijection was provided by S. Pfannerer, M. Rubey & B. Westbury [17].

Moreover, using the natural injection  $i : \mathfrak{S}_n^{(r)} \rightarrow \mathfrak{S}_n^{(r+1)}$  and the bijections  $\mathcal{P}^{(r)}$  and  $\mathcal{P}^{(r+1)}$  we define  $\iota := \mathcal{P}^{(r+1)^{-1}} \circ i \circ \mathcal{P}^{(r)}$  and obtain the following commutative diagram:

$$\begin{array}{ccc} (\text{pr}, \mathcal{A}_n^{(r)}) & \xrightarrow{\mathcal{P}^{(r)}} & (\text{rot}, \mathfrak{S}_n^{(r)}) \\ \downarrow \iota & & \downarrow i \\ (\text{pr}, \mathcal{A}_n^{(r+1)}) & \xrightarrow{\mathcal{P}^{(r+1)}} & (\text{rot}, \mathfrak{S}_n^{(r+1)}). \end{array}$$

In particular, this is an injection  $\iota : \mathcal{A}_n^{(r)} \rightarrow \mathcal{A}_n^{(r+1)}$  such that  $\text{pr} \iota(\mathcal{A}) = \iota(\text{pr} \mathcal{A})$ , which answers the question in [17, rmk. 3.9].

To prove Theorem I.61, we first compute a decomposition of the space of invariants as a direct sum of tensor squares of Specht modules.

**Lemma I.63** ([24]). Let  $\mathfrak{gl}_r$  be the adjoint representation of  $\text{GL}_r$ , and, given a partition  $\lambda \vdash n$ , let  $S_\lambda$  be the corresponding irreducible representation of the symmetric group. Then there is an isomorphism of  $\mathfrak{S}_n$ -representations

$$(\mathfrak{gl}_r^{\otimes n})^{\text{GL}_r} \cong \bigoplus_{\substack{\lambda \vdash n \\ \ell(\lambda) \leq r}} S_\lambda \otimes S_\lambda.$$

*Proof.* Let  $V$  be the vector representation of  $\text{GL}_r$ . Schur–Weyl duality asserts that there is an isomorphism of  $(\text{GL}_r \times \mathfrak{S}_n)$ -representations

$$V^{\otimes r} \cong \bigoplus_{\substack{\lambda \vdash n \\ \ell(\lambda) \leq r}} V_\lambda \otimes S_\lambda,$$

where  $V_\lambda$  is an irreducible representation of  $\text{GL}_r$ .

Recall that, by Schur's lemma,  $\text{Hom}_{\text{GL}_r}(V_\lambda, V_\mu)$  contains only the zero map if  $\lambda \neq \mu$ , and all scalar multiples of the identity otherwise. Thus,

$$\begin{aligned}
 (\mathfrak{gl}_r^{\otimes n})^{\text{GL}_r} &\cong \text{Hom}_{\text{GL}_r}((V \otimes V^*)^{\otimes n}, \mathbb{C}) \\
 &\cong \text{End}_{\text{GL}_r}(V^{\otimes n}) \\
 &\cong \text{End}_{\text{GL}_r}\left(\bigoplus_{\substack{\lambda \vdash n \\ \ell(\lambda) \leq r}} V_\lambda \otimes S_\lambda\right) \\
 \{\text{by Schur's Lemma}\} &\cong \bigoplus_{\substack{\lambda \vdash n \\ \ell(\lambda) \leq r}} \text{End}(S_\lambda) \\
 &\cong \bigoplus_{\substack{\lambda \vdash n \\ \ell(\lambda) \leq r}} S_\lambda \otimes S_\lambda.
 \end{aligned}$$

□

*Proof of Theorem I.61.* By Proposition I.11 and Corollary I.56 we obtain that the character of  $\mathfrak{S}_n^\lambda$  equals the character of  $\bigoplus_{\substack{\lambda \vdash n \\ \ell(\lambda) \leq r}} S_\lambda \otimes S_\lambda \downarrow_{\langle(1, \dots, n)\rangle}$ . Summing over all partitions  $\lambda$  of length at most  $r$ , we obtain the character of

$$(\mathfrak{gl}_r^{\otimes n})^{\text{GL}_r} \downarrow_{\langle(1, \dots, n)\rangle} \cong \bigoplus_{\substack{\lambda \vdash n \\ \ell(\lambda) \leq r}} S_\lambda \otimes S_\lambda \downarrow_{\langle(1, \dots, n)\rangle},$$

by Lemma I.63. Therefore, by Brauer's permutation lemma (Theorem I.7) and Westbury's Theorem I.60, the cyclic group actions

$$(\text{pr}, \mathcal{A}_n^{(r)}) \cong (\text{rot}, \mathfrak{S}_n^{(r)})$$

are isomorphic. □

## BIBLIOGRAPHY

- [1] P. ALEXANDERSSON AND N. AMINI, *The cone of cyclic sieving phenomena*, *Discrete Mathematics*, 342 (2019), pp. 1581–1601.
- [2] P. ALEXANDERSSON, S. LINUSSON, AND S. POTKA, *The cyclic sieving phenomenon on circular Dyck paths*, *The Electronic Journal of Combinatorics*, 26 (2019), pp. 1–32.
- [3] P. ALEXANDERSSON AND J. UHLIN, *Cyclic sieving, skew macdonald polynomials and Schur positivity*, *Algebraic Combinatorics*, 3 (2020), pp. 913–939.
- [4] H. BARCELO, V. REINER, AND D. STANTON, *Bimahonian distributions*, *Journal of the London Mathematical Society*, 77 (2008), pp. 627–646.
- [5] M. BENNETT, B. MADILL, AND A. STOKKE, *Jeu-de-taquin promotion and a cyclic sieving phenomenon for semistandard hook tableaux*, *Discrete Mathematics*, 319 (2014), pp. 62–67.

- [6] R. BRAUER, *On the connection between the ordinary and the modular characters of groups of finite order*, Ann. of Math. (2), 42 (1941), pp. 926–935.
- [7] J. DÉARMÉNIEN, *Fonctions symétriques associées à des suites classiques de nombres*, Annales scientifiques de l'École Normale Supérieure, 16 (1983), pp. 271–304.
- [8] S. V. FOMIN AND N. LULOV, *On the number of rim hook tableaux*, Journal of Mathematical Sciences (New York), 87 (1997), pp. 4118–4123.
- [9] B. FONTAINE AND J. KAMNITZER, *Cyclic sieving, rotation, and geometric representation theory*, Selecta Mathematica, 20 (2013), pp. 609–625.
- [10] G. JAMES AND A. KERBER, *The Representation Theory of the Symmetric Group*, Cambridge University Press, 1984.
- [11] L. G. KOVÁCS, *The permutation lemma of Richard Brauer*, Bull. London Math. Soc., 14 (1982), pp. 127–128. A letter to C. W. Curtis.
- [12] G. KUPERBERG, *Spiders for rank 2 Lie algebras*, Communications in Mathematical Physics, 180 (1996), pp. 109–151.
- [13] A. LASCoux, B. LECLERC, AND J.-Y. THIBON, *Ribbon tableaux, Hall–Littlewood functions, quantum affine algebras and unipotent varieties*, J. Math. Phys, 38 (1997), pp. 1041–1068.
- [14] I. G. MACDONALD, *Symmetric functions and Hall polynomials*, Oxford Mathematical Monographs, The Clarendon Press, Oxford University Press, New York, second ed., 1995. With contributions by A. Zelevinsky, Oxford Science Publications.
- [15] Y.-T. OH AND E. PARK,  *$q$ -dimensions of highest weight crystals and cyclic sieving phenomenon*, ArXiv e-prints, (2020).
- [16] I. PAK, *Ribbon tile invariants*, Transactions of the American Mathematical Society, 352 (2000), pp. 5525–5562.
- [17] S. PFANNERER, M. RUBEY, AND B. WESTBURY, *Promotion on oscillating and alternating tableaux and rotation of matchings and permutations*, Algebraic Combinatorics, 3 (2020), pp. 107–141.
- [18] K. PURBHOO, *Wronskians, cyclic group actions, and ribbon tableaux*, Transactions of the American Mathematical Society, 365 (2013), pp. 1977–2030.
- [19] V. REINER, D. STANTON, AND D. E. WHITE, *The cyclic sieving phenomenon*, Journal of Combinatorial Theory, Series A, 108 (2004), pp. 17–50.
- [20] D. RHEE, *Cyclic sieving phenomenon of promotion on rectangular tableaux*, m.s thesis, University of Waterloo, Waterloo, Ontario, Canada, 2012.
- [21] B. RHOADES, *Cyclic sieving, promotion, and representation theory*, Journal of Combinatorial Theory, Series A, 117 (2010), pp. 38–76.

- [22] ———, *Hall–Littlewood polynomials and fixed point enumeration*, *Discrete Mathematics*, 310 (2010), pp. 869–876.
- [23] H. ROBBINS, *A remark on Stirling’s formula*, *The American Mathematical Monthly*, 62 (1955), p. 26.
- [24] M. RUBEY AND B. W. WESTBURY, *A combinatorial approach to classical representation theory*, *ArXiv e-prints*, (2014).
- [25] B. E. SAGAN, J. SHARESHIAN, AND M. L. WACHS, *Eulerian quasisymmetric functions and cyclic sieving*, *Advances in Applied Mathematics*, 46 (2011), pp. 536–562.
- [26] A. SCHILLING, M. SHIMOZONO, AND D. WHITE, *Branching formula for  $q$ -Littlewood–Richardson coefficients*, *Advances in Applied Mathematics*, 30 (2003), pp. 258–272.
- [27] T. A. SPRINGER, *Regular elements of finite reflection groups*, *Inventiones Mathematicae*, 25 (1974), pp. 159–198.
- [28] R. P. STANLEY, *Enumerative Combinatorics: Volume 2*, Cambridge University Press, first ed., 2001.
- [29] J. R. STEMBRIDGE, *Rational tableaux and the tensor algebra of  $g_{ln}$* , *Journal of Combinatorial Theory, Series A*, 46 (1987), pp. 79–120.
- [30] ———, *Canonical bases and self-evacuating tableaux*, *Duke Mathematical Journal*, 82 (1996), pp. 585–606.
- [31] B. W. WESTBURY, *Invariant tensors and the cyclic sieving phenomenon*, *The Electronic Journal of Combinatorics*, 23 (2016).
- [32] ———, *Interpolating between promotion and the long cycle*, *ArXiv e-prints*, (2019).
- [33] D. E. WHITE, *A bijection proving orthogonality of the characters of  $S_n$* , *Advances in Mathematics*, 50 (1983), pp. 160–186.

---

A REFINEMENT OF THE MURNAGHAN–NAKAYAMA RULE BY DESCENTS FOR BORDER STRIP TABLEAUX

---

## BIBLIOGRAPHIC INFORMATION

Pfannerer, S. A refinement of the Murnaghan–Nakayama rule by descents for border strip tableaux. *Combinatorial Theory*, 2(2), 2022, doi:10.5070/C62257882

## TABLE OF CONTENTS

Abstract . . . . .	69
II.1 Introduction . . . . .	70
II.2 Definitions and main theorem . . . . .	71
II.3 The Littlewood quotient map . . . . .	75
II.4 Schur functions . . . . .	78
II.5 The final bijection . . . . .	81
Bibliography . . . . .	83

## ABSTRACT

Lusztig’s fake degree is the generating polynomial for the major index of standard Young tableaux of a given shape. Results of Springer (1974) and James & Kerber (1984) imply that, mysteriously, its evaluation at a  $k$ -th primitive root of unity yields the number of border strip tableaux with all strips of size  $k$ , up to sign. This is essentially the special case of the Murnaghan–Nakayama rule for evaluating an irreducible character of the symmetric group at a rectangular partition.

We refine this result to standard Young tableaux and border strip tableaux with a given number of descents. To do so, we introduce a new statistic for border strip tableaux, extending the classical definition of descents in standard Young tableaux. Curiously, it turns out that our new statistic is very closely related to a descent set for tuples of standard Young tableaux appearing in the quasisymmetric expansion of LLT polynomials given by Haglund, Haiman and Loehr (2005).

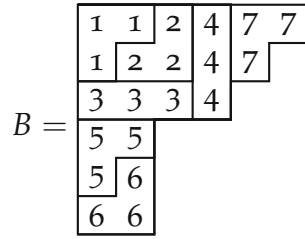


Figure 7: A border strip tableau of height 7.

## II.1 INTRODUCTION

Let  $\text{SYT}(\lambda)$  denote the set of all *standard Young tableaux* of shape  $\lambda$  and size  $n$ . An entry  $i$  of a standard Young tableau  $T$  is a *descent* of  $T$ , if  $i + 1$  appears in a strictly lower row in  $T$  in English notation. Let  $\text{DES}(T)$  denote the set of descents of  $T$  and denote with  $\text{maj}(T)$ , the *major index* of  $T$ , the sum of all descents of  $T$ .

Our main result, Theorem II.8, provides a natural combinatorial interpretation of

$$f^\lambda(q, t) := \sum_{T \in \text{SYT}(\lambda)} q^{\text{maj}(T)} t^{|\text{DES}(T)|}$$

when  $q$  is a root of unity. This refines the classical interpretation of the evaluation of Lusztig's fake degree polynomial  $f^\lambda(q) := f^\lambda(q, 1)$ , as we show below. The bivariate generating function itself was already considered by R. Stanley [12, Proposition 8.13] in the more general setting of  $(P, \omega)$  partitions.

By a result of T. Springer [11, Proposition 4.5],  $f^\lambda(q)$  coincides with the restriction of the irreducible  $\mathfrak{S}_n$ -character  $\chi^\lambda$  to the cyclic subgroup generated by the long cycle, represented as the group of complex roots of unity. More precisely, for  $k \mid n$ , let  $\xi$  be a primitive  $k$ -th root of unity and let  $\rho = (k^{n/k})$  be a rectangular partition, then we have  $f^\lambda(\xi) = \chi^\lambda(\rho)$ . In general, a practical way to compute the character value  $\chi^\lambda(\rho)$  for an arbitrary partition  $\rho$  is the Murnaghan–Nakayama rule [13, Theorem 7.17.3].

Let  $\rho = (\rho_1, \dots, \rho_\ell)$  be a composition of  $n$  and, for a filling  $B$  of a Young diagram  $\lambda$  with weakly increasing rows and columns, let  $B^i$  be the collection of cells in  $B$  containing  $i$ . We say that  $B$  is a *border strip tableau* of type  $\rho$  if, for all  $1 \leq i \leq \ell$ , the cells  $B^i$  form a connected skew shape of size  $\rho_i$  that does not contain a  $2 \times 2$  rectangle. In this case we call  $B^i$  a *border strip* of size  $\rho_i$  and define the *height*  $\text{height}(B^i)$  to be the number of rows it spans minus 1. Furthermore, we define the height of  $B$  to be the sum of the heights of its strips. See Figure 7 for an example of a border strip tableau of height 7.

The Murnaghan–Nakayama rule states that

$$\chi^\lambda(\rho) = \sum_B (-1)^{\text{height}(B)},$$

where the sum is taken over all border strip tableaux of shape  $\lambda$  and type  $\rho$ . In the special case where  $\rho$  is a rectangular partition  $(k^{n/k})$  and all strips in  $B$  have the same size  $k$ , this rule is cancellation free, due to a theorem by G. James and A. Kerber [4,

Theorem 2.7.27]. This means that the parity of  $\text{height}(B)$  only depends on  $\lambda$  and the strip size  $k$ . Thus we obtain

$$f^\lambda(\xi) = \epsilon_{\lambda,k} \cdot |\text{BST}(\lambda, k)|, \quad (24)$$

where  $\text{BST}(\lambda, k)$  is the set of all border strip tableaux of shape  $\lambda$  and type  $(k^{n/k})$ , and  $\epsilon_{\lambda,k} = (-1)^{\text{height}(B)}$  for any border strip tableau  $B \in \text{BST}(\lambda, k)$ .

Our main result, Theorem II.8, refines this special case of the Murnaghan–Nakayama rule as follows. Provided that the set  $\text{BST}(\lambda, k)$  is not empty, it turns out that  $f^\lambda(\xi, t)$  is, up to sign, a generating function for a very natural statistic on this set. That is,

$$f^\lambda(\xi, t) = \epsilon_{\lambda,k} \cdot \sum_{B \in \text{BST}(\lambda, k)} t^{\text{des}^+(B)}.$$

The statistic  $\text{des}^+$  (see Definition II.7) extends the classical definition of descents for standard Young tableaux. The notion of  $\text{DES}(B)$  underlying our new statistic  $\text{des}^+(B)$  coincides with a certain definition of descents under the Littlewood quotient map which arose in the context of LLT polynomials, see Corollary II.20 and Remark II.21.

The motivation to study  $f^\lambda(\xi, t)$  comes from the desire to refine recent results by P. Alexandersson, S. Pfannerer, M. Rubey, and J. Uhlin [1]. They used (24) to show that  $(\chi^\lambda)^2$  carries the action of a permutation representation of the cyclic group of order  $n$ . Equivalently, there exists a cyclic group action  $\tau$  of order  $n$  such that the triple  $(\text{SYT}(\lambda) \times \text{SYT}(\lambda), \tau, (f^\lambda)^2)$  exhibits the cyclic sieving phenomenon introduced by V. Reiner, D. Stanton and D. White [9]. Note that the action  $\tau$  remains unknown. Refining their work may eventually lead to an explicit description of  $\tau$ . See B. Sagan’s survey article [10] for more background on the cyclic sieving phenomenon.

The structure of the paper is as follows: in Section II.2 we introduce relevant definitions, fix notation and state our main theorem. The rest of the sections is dedicated for the proof, which is split up into three important steps. In Section II.3 we introduce the Littlewood quotient map and in Section II.4 we relate our problem to Schur functions. Finally, in Section II.5 we conclude the main result with a bijection.

## II.2 DEFINITIONS AND MAIN THEOREM

We begin by introducing relevant definitions and notation; for more details we refer to the books by I. Macdonald [6] and R. Stanley [13]. A *partition*  $\lambda = (\lambda_1, \dots, \lambda_\ell)$  of  $n$ , written as  $\lambda \vdash n$ , is a weakly decreasing sequence of positive integers that sum up to  $n =: |\lambda|$ . The *Young diagram* of shape  $\lambda$  in English notation is the collection of  $n$  cells, arranged in  $\ell$  left-justified rows of lengths  $\lambda_1, \dots, \lambda_\ell$ . The rows of a Young diagram are indexed from top to bottom starting with one, and the columns are indexed from left to right starting with one. To each cell  $x$  we associate its *content*,  $c(x)$ , which is its column index minus its row index. Finally, we associate to each cell  $x$  its *hook value*,  $h(x)$ , which is the number of cells (strictly) to the right of  $x$  plus the number of cells (strictly) below  $x$  plus one.

Let  $(\lambda, \mu)$  be a pair of partitions such that the Young diagram  $\mu$  is completely contained in the Young diagram  $\lambda$ . The cells that are in  $\lambda$  but not in  $\mu$  form the *skew shape*  $\lambda/\mu$ .

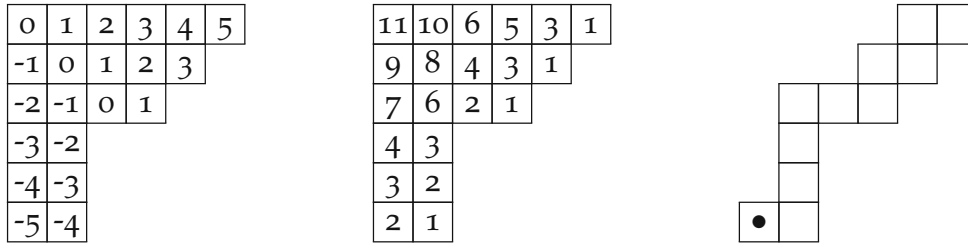


Figure 8: On the left is the Young diagram of the partition 654222, where each cell is filled with its content. In the middle is the same diagram where each cell is filled with its hook value. On the right is a border strip, where its tail is decorated with a bullet.

A *border strip* (or ribbon or rim hook) is a connected skew shape that does not contain a  $2 \times 2$  square. The *tail* of a border strip is its unique cell with smallest content. The *height*  $\text{height}(S)$  of a border strip  $S$  is the number of rows it spans minus one.

**Definition II.1.** A *border strip tableau* of shape  $\lambda \vdash n$  with strip size  $k \mid n$  is a Young diagram filled with the integers  $\{1, \dots, n/k\}$  such that

- the values in each row from left to right and each column from top to bottom are weakly increasing and
- the cells containing the value  $i$  form a border strip of size  $k$  for all  $1 \leq i \leq n/k$ .

The set of all such tableaux is denoted with  $\text{BST}(\lambda, k)$ . The *height*  $\text{height}(B)$  of a border strip tableau  $B$  is the sum of the heights of its border strips.

**Example II.2.** The Young diagram of shape 654222 is given in Figure 8 on the left. In the same Figure on the right we see the skew shape 654222/43111. It is a border strip of size 11 and height 5. The tableau  $B$  in Figure 7 is a border strip tableau in  $\text{BST}(654222, 3)$  of height 7.

**Remark II.3.** A border strip tableau with all strips having size 1 corresponds to a *standard Young tableau*. We also write  $\text{SYT}(\lambda)$  for  $\text{BST}(\lambda, 1)$ .

One may also think of a border strip tableau  $B \in \text{BST}(\lambda, k)$  as a flag of partitions  $\emptyset = v_0 \subset v_1 \subset \dots \subset v_{n/k} = \lambda$  such that  $B^i := v_i/v_{i-1}$  is a border strip of size  $k$  for all  $1 \leq i \leq n/k$ . The cells in  $B^i$  are precisely the cells in  $B$  with label  $i$ .

More generally, we say that a partition  $\nu$  is obtained from  $\lambda$  *by removing* a border strip of size  $k$ , if  $\lambda/\nu$  is a border strip of size  $k$ . Successively removing border strips of size  $k$  from  $\lambda$  as long as possible gives a partition  $\nu_0$  which turns out to be independent from the order in which the strips are removed. Hence,  $\nu_0$  is well defined and called the *k-core* of  $\lambda$ . See also G. James and A. Kerber [4, Chapter 2.7] for further details.

**Proposition II.4.**  $\text{BST}(\lambda, k)$  is not empty, if and only if  $\lambda$  has empty *k-core*.

From now on, we remove all labels in the graphical representation of a border strip tableau that are not in the tail of a strip. We now define the descent set of a border strip tableau, extending the classical definition for standard Young tableaux.



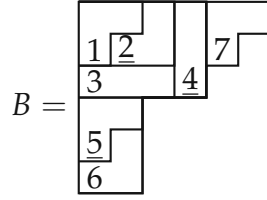


Figure 9: The border strip tableau  $B$  with the labels in the tails of the strips. The descents of  $B$  are underscored. We have  $\text{DES}(B) = \{2, 4, 5\}$ .

**Definition II.5.** Let  $x_i$  be the unique cell with smallest content in a border strip tableau  $B$  that contains  $i$ . We call  $i$  a *descent* of  $B$  if  $x_{i+1}$  appears in a strictly lower row in  $B$  than  $x_i$ .  $\text{DES}(B)$  denotes the set of all descents of  $B$ .

For example, let  $B$  be the border strip tableau in Figure 7. Following our new convention,  $B$  is depicted again in Figure 9. Hence  $\text{DES}(B) = \{2, 4, 5\}$ .

**Definition II.6.** The *major index*  $\text{maj}(T)$  of a standard Young diagram  $T$  is the sum of its descents. We define the generating function

$$f^\lambda(q, t) := \sum_{T \in \text{SYT}(\lambda)} q^{\text{maj}(T)} t^{|\text{DES}(T)|}.$$

Note that  $f^\lambda(q, 1)$  is also known as Lusztig's fake degree polynomial. Also note that  $f^\lambda(1, t)$  is the generating function for the number of descents on  $\text{SYT}(\lambda)$ .

Coming to our main definition, we introduce a new statistic on  $\text{BST}(\lambda, k)$ .

**Definition II.7.** Let  $B \in \text{BST}(\lambda, k)$ , let  $B^1$  be the strip in  $B$  containing 1 and define

$$\text{des}^+(B) := k \cdot |\text{DES}(B)| + \text{height}(B^1).$$

Observe that for  $T \in \text{SYT}(\lambda) = \text{BST}(\lambda, 1)$  this statistic equals the number of descents, that is  $\text{des}^+(T) = |\text{DES}(T)|$ . For example, the tableau  $B$  in Figure 7 has  $\text{des}^+(B) = 10$ .

We can now state our main theorem.

**Theorem II.8.** Let  $\lambda$  be a partition of  $n$  with empty  $k$ -core and let  $\xi$  be a primitive  $k$ -th root of unity. Then, for some  $\epsilon_{\lambda, k} \in \{\pm 1\}$ ,

$$f^\lambda(\xi, t) = \epsilon_{\lambda, k} \cdot \sum_{B \in \text{BST}(\lambda, k)} t^{\text{des}^+(B)}. \quad (25)$$

Furthermore, the sign  $\epsilon_{\lambda, k}$  can be made explicit.

**Proposition II.9.** Under the same assumptions as in Theorem II.8, the map

$$\begin{aligned} \text{sgn} : \text{BST}(\lambda, k) &\rightarrow \{\pm 1\} \\ B &\mapsto (-1)^{\text{height}(B)} \end{aligned}$$

is constant, and  $\epsilon_{\lambda, k} = \text{sgn}(B_0)$ , where  $B_0$  is any border strip tableau in  $\text{BST}(\lambda, k)$ .

**Remark II.10.** Let  $\chi^\lambda$  be the irreducible character of the symmetric group corresponding to  $\lambda$  and let  $\rho = (k^{n/k})$  be the rectangular partition of  $n$  with all parts equal to  $k$ . Then  $\epsilon_{\lambda,k}$  is the sign of the character value  $\chi^\lambda(\rho)$ .

**Example II.11.** To illustrate Theorem II.8 let us consider the partition  $\lambda = 222$ . There are five standard Young tableaux, as depicted below. For each tableau we underscore the descents and calculate its weight in  $f^{222}(q, t)$ .

$$\begin{array}{|c|c|} \hline \underline{1} & 4 \\ \hline \underline{2} & 5 \\ \hline 3 & 6 \\ \hline \end{array} + 
 \begin{array}{|c|c|} \hline \underline{1} & 3 \\ \hline 2 & 5 \\ \hline 4 & 6 \\ \hline \end{array} + 
 \begin{array}{|c|c|} \hline 1 & \underline{2} \\ \hline 3 & 5 \\ \hline 4 & 6 \\ \hline \end{array} + 
 \begin{array}{|c|c|} \hline \underline{1} & 3 \\ \hline 2 & 4 \\ \hline 5 & 6 \\ \hline \end{array} + 
 \begin{array}{|c|c|} \hline 1 & \underline{2} \\ \hline 3 & 4 \\ \hline 5 & 6 \\ \hline \end{array}$$

$$q^{12}t^4 + q^9t^3 + q^{10}t^3 + q^8t^3 + q^6t^2$$

We obtain

$$f^{222}(q, t) = q^{12}t^4 + (q^{10} + q^9 + q^8)t^3 + q^6t^2.$$

Substituting primitive roots of unity for  $q$  we obtain the following polynomials

primitive root	$1^{st} = 1$	$2^{nd} = -1$	$3^{rd}$	$6^{th}$
$f^{222}(\cdot, t)$	$t^4 + 3t^3 + t^2$	$t^4 + t^3 + t^2$	$t^4 + t^2$	$\underbrace{t^4 - 2t^3 + t^2}_{6\text{-core not empty}}$

For  $q = 1$  we get the generating function for the number of descents on  $\text{SYT}(\lambda) = \text{BST}(\lambda, 1)$ . For  $q$  being a second or third root of unity we obtain the generating functions for  $\text{des}^+$  on  $\text{BST}(\lambda, 2)$  and  $\text{BST}(\lambda, 3)$  respectively:

$$\text{BST}(\lambda, 2) : \begin{array}{|c|} \hline \underline{1} \\ \hline \underline{2} \\ \hline 3 \\ \hline \end{array} \quad \begin{array}{|c|c|} \hline \underline{1} & \\ \hline 2 & 3 \\ \hline \end{array} \quad \begin{array}{|c|c|} \hline 1 & \underline{2} \\ \hline 3 & \\ \hline \end{array} \quad \text{BST}(\lambda, 3) : \begin{array}{|c|c|} \hline & \\ \hline 1 & 2 \\ \hline \end{array} \quad \begin{array}{|c|} \hline \underline{1} \\ \hline 2 \\ \hline \end{array}$$

$$t^{2 \cdot 2 + 0} \quad t^{2 \cdot 1 + 0} \quad t^{2 \cdot 1 + 1} \quad t^{3 \cdot 0 + 2} \quad t^{3 \cdot 1 + 1}$$

The signs  $\epsilon_{\lambda,2}$  and  $\epsilon_{\lambda,3}$  are positive, as all border strip tableaux in this example have even height. For a primitive sixth root of unity we obtain a polynomial in which the signs of the nonzero coefficients do not coincide. Since the 6-core of  $\lambda = 222$  is not empty, we do not have a combinatorial interpretation of  $f^\lambda(\zeta, t)$  in this case.

**Remark II.12.** We do not know what is happening in the case where the  $k$ -core is not empty, not even in the case where  $k \mid n$ . For instance let  $\lambda = 82 \vdash 10$  and let  $\zeta = \exp(\frac{2i\pi}{5})$  be a fifth primitive root of unity, then we get

$$f^{82}(\zeta, t) = \frac{1 + \sqrt{5}}{2}t^2 - \frac{1 + \sqrt{5}}{2}t.$$

Thus, even non-integer coefficients may occur.

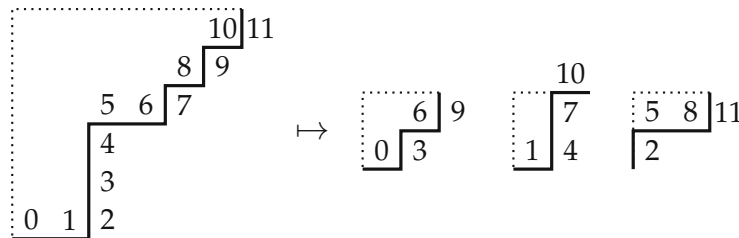
In the following sections we present the proof of Theorem II.8. The crucial steps are as follows: first, we use the Littlewood quotient map to bijectively map border strip tableaux to standard Young tableau tuples, and apply this to the right hand side of Equation (25). Next we express  $f^\lambda(q, t)$  in terms of principal specialisations of the Schur function  $s_\lambda$ . For a primitive root of unity  $\zeta$ , a generalisation of a theorem by V. Reiner, D. Stanton and D. White allows us to regard  $f^\lambda(\zeta, t)$  as generating function over the set of tuples of semistandard Young tableaux. Finally, a bijection links the two resulting expressions.

### II.3 THE LITTLEWOOD QUOTIENT MAP

We start this section by introducing the  $k$ -quotient of a partition  $\lambda$  using a graphical description.

Interpret the lower-right contour of the Young diagram  $\lambda$  as a path with vertical and horizontal steps and append empty rows (vertical steps) to the bottom, such that the total number of rows is divisible by  $k$ . Starting with the leftmost step in the lowest row, we label each step of the path in incremental order, starting with 0. For  $0 \leq s \leq k-1$  let  $\lambda^s$  be the partition one obtains from the steps whose label is congruent to  $s$  modulo  $k$ . The tuple  $(\lambda^0, \lambda^1, \dots, \lambda^{k-1})$  is called the  $k$ -quotient of  $\lambda$ .

**Example II.13.** We construct the 3-quotient of  $\lambda = 654222$ . For a nicer display we put the labels for the horizontal steps on top of each step and the labels for each vertical step to its right. As the number of rows is already divisible by 3, we do not append empty rows.



We obtain the 3-quotient  $(21, 11, 2)$ .

Some fundamental properties of the quotient are the following.

**Proposition II.14** (G. James & A. Kerber [4, Chapter 2.7]). (i) The function that maps a partition  $\lambda \vdash n$  to its  $k$ -quotient is a bijection between the set of partitions with empty  $k$ -core and the set of  $k$ -tuples of partitions  $(\lambda^0, \lambda^1, \dots, \lambda^{k-1})$  with  $|\lambda^0| + |\lambda^1| + \dots + |\lambda^{k-1}| = \frac{n}{k}$ .

(ii) Let  $\lambda$  and  $\mu$  be two partitions with empty  $k$ -core such that  $\lambda/\mu$  is a border strip of size  $k$ . Let  $(\lambda^0, \dots, \lambda^{k-1})$  and  $(\mu^0, \dots, \mu^{k-1})$  be the corresponding  $k$ -quotients for  $\lambda$  and  $\mu$ , respectively. Then there exists an index  $0 \leq s \leq k-1$  such that  $|\lambda^s/\mu^s| = 1$  and  $\lambda^t = \mu^t$  for all  $t \neq s$ .

Alternatively, the  $k$ -quotient of  $\lambda$  can be obtained from the  $k$ -quotient of  $\mu$  by adding a single cell to one of the partitions.

In the following we denote multi-sets with two curly brackets, e.g.  $\{\{a, a, b\}\}$ , and for a multi-set  $X$  and a real number  $k$  we use the notions  $X + k = \{\{x + k : x \in X\}\}$  and  $kX = \{\{k \cdot x : x \in X\}\}$ .

**Proposition II.15** (I. Macdonald [6, Example I.1.8(d)]). Let  $\lambda$  be a partition with empty  $k$ -core and let  $(\lambda^0, \dots, \lambda^{k-1})$  be its  $k$ -quotient. Denote with  $h(\lambda) := \{\{h(x) : x \in \lambda\}\}$  the multi-set of the hook values of all cells of a partition  $\lambda$  and denote with  $h_{0,k}(\lambda) := \{\{h(x) : x \in \lambda, k \mid h(x)\}\}$  the multi-set of hook values, that are divisible by  $k$ , then

$$\frac{1}{k}h_{0,k}(\lambda) = \bigcup_{0 \leq i < k} h(\lambda^i).$$

**Proposition II.16.** Denote with  $c(\lambda) := \{\{c(x) : x \in \lambda\}\}$  the multi-set of the contents of all cells of a partition  $\lambda$ . For  $0 \leq r < k$  denote with  $c_{r,k}(\lambda) := \{\{c(x) : x \in \lambda, k \mid (c(x) + r)\}\}$  the multi-set of contents, that are congruent to  $-r$  modulo  $k$ .

Let  $\lambda$  be a partition with empty  $k$ -core and  $(\lambda^0, \dots, \lambda^{k-1})$  its  $k$ -quotient, then for  $0 \leq r < k$ ,

$$\frac{1}{k}(c_{r,k}(\lambda) + r) = \bigcup_{0 \leq i < k-r} c(\lambda^i) \cup \bigcup_{k-r \leq i < k} (c(\lambda^i) + 1).$$

*Proof.* For  $r = 0$  this result is known, see [6, Example I.1.8(d)]. Let  $\lambda = (\lambda_1, \dots, \lambda_\ell)$  be the partition with as many zero parts appended, such that  $k \mid \ell$  and let  $\ell/k = \hat{\ell}$ .

To deduce the general case we “glue” a rectangular partition with  $r$  columns to the left of  $\lambda$ , which will shift all the contents by  $r$ . More formally, let  $\mu = (r^{\hat{\ell}})$  the partition consisting of  $\hat{\ell}$  parts equal to  $r$  and let  $\lambda + \mu$  be the partition obtained from  $\lambda$  and  $\mu$  by pairwise addition of the parts. Using this notion we have

$$c_{r,k}(\lambda) + r = c_{0,k}(\mu + \lambda) \setminus c_{0,k}(\mu). \quad (26)$$

To apply the results for  $r = 0$ , we also need the  $k$ -quotient of  $\lambda + \mu$ , which we denote with  $(\kappa^0, \dots, \kappa^{k-1})$ . Note that the path for  $\lambda + \mu$  is obtained from the path for  $\lambda$  by prepending  $r$  horizontal steps to it. Thus directly from the construction we obtain

$$\kappa^i = \begin{cases} \lambda^{i-r} & \text{if } i \geq r, \\ \lambda^{k+i-r} + (1^{\hat{\ell}}) & \text{if } i < r. \end{cases} \quad (27)$$

The general case can now be concluded from the case  $r = 0$  using equations (26) and (27).  $\square$

Let  $\Lambda = (\lambda^0, \dots, \lambda^{k-1})$  be a tuple of Young diagrams and let  $|\Lambda|$  be the total number of cells in  $\Lambda$ . A *standard Young tableau tuple* of shapes  $\Lambda$  is a bijective filling of the cells of  $\Lambda$  with the values  $\{1, \dots, |\Lambda|\}$  such that entries in each diagram strictly increase along rows from left to right and along columns from top to bottom. We denote the set of all such fillings with SYT-tuples( $\Lambda$ ).

There exists a bijection between  $\text{BST}(\lambda, k)$  and  $\text{SYT-tuples}(\Lambda)$ , where  $\Lambda$  is the  $k$ -quotient of  $\lambda$ .

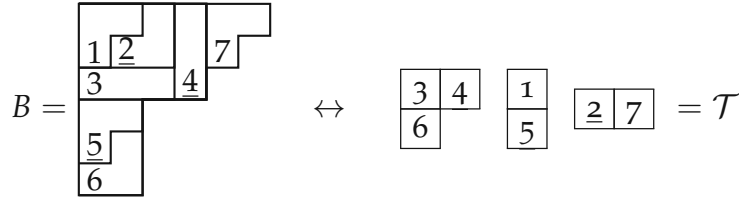
**Definition II.17** (Littlewood quotient map). Fix a border strip tableau  $B$  of shape  $\lambda$ . Regarding  $B$  as a flag of partitions  $\emptyset = v_0 \subset v_1 \subset \dots \subset v_{n/k} = \lambda$ , we denote with  $\Lambda_i$  the  $k$ -quotient of  $v_i$ . By Proposition II.14  $(\emptyset, \dots, \emptyset) = \Lambda_0 \subset \Lambda_1 \subset \dots \subset \Lambda_{n/k} = \Lambda$  is a flag of tuples of Young diagrams, such that two consecutive tuples differ by precisely one cell.

For  $1 \leq i \leq n/k$  denote with  $x_i$  the unique cell in  $\Lambda$  which is contained in  $\Lambda_i$  but not  $\Lambda_{i-1}$ . By filling  $x_i$  with  $i$ , we obtain a standard Young tableau tuple of shapes  $\Lambda$ .

This bijection is called *Littlewood quotient map* by J. Haglund [2] or rim hook bijection by I. Pak [8]. An example is given in Figure 10.

We now describe how descents are transported via this bijection.

**Definition II.18.** Let  $\mathcal{T} = (T^0, \dots, T^{k-1})$  be a standard Young tableau tuple and let  $c(x)$  be the content of an entry  $x$  within its Young diagram. Assume now that  $i \in T^s$  and  $(i+1) \in T^t$ . Then  $i$  is a descent of  $\mathcal{T}$ , if either  $s \leq t$  and  $c(i) > c(i+1)$ , or  $s > t$  and  $c(i) \geq c(i+1)$ .  $\text{DES}(\mathcal{T})$  denotes the set of all descents of  $\mathcal{T}$ .



$B$  as flag:  $\emptyset \subset 21 \subset 33 \subset 333 \subset 444 \subset 44421 \subset 444222 \subset 654222$   
 $\mathcal{T}$  as flag:  $(\emptyset, \emptyset, \emptyset) \subset (\emptyset, 1, \emptyset) \subset (\emptyset, 1, 1) \subset (1, 1, 1) \subset (2, 1, 1) \subset (2, 11, 1) \subset (21, 11, 1) \subset (21, 11, 2)$

Figure 10: The Littlewood quotient map applied to  $B$ . The descents of  $B$  and  $\mathcal{T}$  are highlighted. We have  $\text{DES}(B) = \text{DES}(\mathcal{T}) = \{2, 4, 5\}$ .

**Lemma II.19.** For  $i \in T^s$  let  $c_{\mathcal{T}}(i)$  be the content of  $i$  and let  $c_B(i)$  the content of the tail of the strip containing  $i$  in  $B$ , then  $(c_B(i) - 1) = k \cdot (c_{\mathcal{T}}(i) - 1) + s$ .

*Proof.* Recall that we obtain the  $k$ -quotient of a partition by first adding 0 parts, such that the total number of rows  $\ell$  is divisible by  $k$  and then following the path of the lower-right contour of the Young diagram. We denote such a path with a finite binary sequence  $w = (w_0, w_1, \dots)$  where a 0 is a north step and a 1 is an east step. Then the partitions in the  $k$ -quotient are given by the binary sequences  $w^s := (w_{i \cdot k + s})_{i \geq 0}$  for  $0 \leq s < k$ .

Let  $v_i$  and  $v_{i-1}$  be the partitions with  $\ell$  (possibly zero) parts obtained from  $B$  from all strips with labels at most  $i$  and  $i - 1$  respectively. Denote the path of  $v_i$  with  $(w_0, w_1, \dots)$  and the path of  $v_{i-1}$  with  $(w'_0, w'_1, \dots)$ . As  $v_i/v_{i-1}$  is the border strip containing  $i$ , we have

$$w_i = \begin{cases} 1 - w'_i = 0 & \text{if } i = \ell + c_B(i) - 1, \\ 1 - w'_i = 1 & \text{if } i = \ell + c_B(i) - 1 + k, \\ w'_i & \text{else} \end{cases}$$

Let  $c_B(i) - 1 = k \cdot q + r$  with integers  $q$  and  $0 \leq r < k$  and let  $\ell = k \cdot \hat{\ell}$ . Thus  $w_{\ell + c_B(i) - 1} = w_{k \cdot (\hat{\ell} + q) + r}$  is the  $(\hat{\ell} + q)$ -th step in the path of the  $r$ -th partition in the  $k$ -quotient of  $v_i$ . Similarly  $w_{\ell + c_B(i) - 1 + k}$  is the  $(\hat{\ell} + q + 1)$ -th step in the path of the same partition. The same holds for  $w'_{\ell + c_B(i) - 1}$  and  $w'_{\ell + c_B(i) - 1 + k}$  with respect to the  $r$ -th partition of the  $k$ -quotient of  $v_{i-1}$ . Therefore  $r = s$  and  $q = c_{\mathcal{T}}(i) - 1$ .  $\square$

**Corollary II.20.** Let  $B \in \text{BST}(\lambda, k)$  be a border strip tableau and let  $\mathcal{T} = (T^0, \dots, T^{k-1})$  be the standard Young tableau tuple corresponding to  $B$  via the Littlewood quotient map. Then  $\text{DES}(B) = \text{DES}(\mathcal{T})$ .

Furthermore, let  $s$  be the index of the unique Young diagram in  $\mathcal{T}$  containing 1 and let  $B^1$  be the strip in  $B$  containing 1. Then  $\text{height}(B^1) = k - 1 - s =: \text{idx}_1(\mathcal{T})$ .

*Proof.* Observe that  $i$  is a descent in  $B$ , if and only if  $c_B(i) > c_B(i + 1)$ . Moreover, let  $i \in T^s$  and  $(i + 1) \in T^t$ , then by Lemma II.19  $i$  is a descent in  $\mathcal{T}$  if and only if  $k \cdot c_{\mathcal{T}}(i) + s > k \cdot c_{\mathcal{T}}(i + 1) + t$ . As  $(c_B(i) - 1) = k \cdot (c_{\mathcal{T}}(i) - 1) + s$ , we obtain  $\text{DES}(B) = \text{DES}(\mathcal{T})$ .

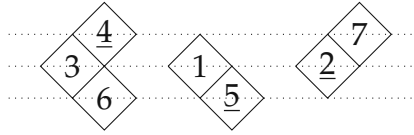


Figure 11: The standard Young tableau tuple in “Austrian notation”. On each dotted horizontal line are cells with the same content.

For the second part of the theorem, note that

$$c_B(1) - 1 = -1 - \text{height}(B^1) \equiv k - 1 - \text{height}(B^1) \pmod{k}.$$

Thus  $\text{height}(B^1) = k - 1 - s$ . □

The following graphical description may be helpful for understanding Definition II.18: Tilt the Young diagrams in  $\mathcal{T}$  by 45 degrees in counter-clockwise direction and align them such that cells with the same content lay on a horizontal line. We call this the “Austrian notation”. Then  $i$  is a descent in  $\mathcal{T}$  if and only if  $(i + 1)$  is

- in a tableau to the left and weakly below  $i$ , or
- in the same tableau or a tableau to the right and strictly below  $i$ .

An example of the graphical description is given in Figure 11.

**Remark II.21.** Definition II.18 agrees with the definition of descents using the content reading order in the Bylund–Haiman model [3, Equations (77) and (80)], which is used in the quasisymmetric expansion of LLT-polynomials. B. Westbury made us aware of this relation when we first presented our results to a broader audience.

We conclude this section by applying the Littlewood quotient map to the right hand side of Equation (25).

**Lemma II.22.** *Let  $\lambda$  be a partition with empty  $k$ -core and let  $\Lambda = (\lambda^0, \dots, \lambda^{k-1})$  be its  $k$ -quotient, then*

$$\sum_{B \in \text{BST}(\lambda, k)} t^{k \cdot |\text{DES}(B)| + \text{height}(B^1)} = \sum_{\mathcal{T} \in \text{SYT-tuples}(\Lambda)} t^{k \cdot |\text{DES}(\mathcal{T})| + \text{id}_{x_1}(\mathcal{T})}. \quad (28)$$

*Proof.* This is a direct consequence of Corollary II.20. □

## II.4 SCHUR FUNCTIONS

In this section we express  $f^\lambda(q, t)$  in terms of Schur functions and evaluate it at roots of unity.

**Definition II.23.** A *semistandard Young tableau* of shape  $\lambda$  is a filling of the Young diagram with positive integers such that the rows are weakly increasing from left to right and the columns are strictly increasing from top to bottom. Let  $\text{SSYT}(\lambda)$  be the set of all semistandard Young tableaux of shape  $\lambda$ .

For a semistandard Young tableau  $T$  we associate the monomial  $\mathbf{x}^T = \prod_{i \geq 1} x_i^{t_i}$  where  $t_i$  is the number of occurrences of the number  $i$  in  $T$ . The *Schur function*  $s_\lambda$  associated with  $\lambda$  is the generating function

$$s_\lambda(x_1, x_2, x_3, \dots) = \sum_{T \in \text{SSYT}(\lambda)} \mathbf{x}^T.$$

When specialising precisely  $m$  variables with 1 and the rest with zero, one obtains the number of semistandard Young tableaux of shape  $\lambda$  with entries bounded from above by  $m$ . We also denote this with

$$s_\lambda(\underbrace{1, \dots, 1}_m, 0, 0, \dots) = s_\lambda(1^m) = \#\text{SSYT of shape } \lambda \text{ with all entries } \leq m.$$

The following identity relates  $f^\lambda(q, t)$  to the principal specialisations of the the Schur function  $s_\lambda$ .

**Theorem II.24** (R. Stanley [12, Proposition 8.3]). *Let  $\lambda \vdash n$  and let  $(t; q)_{n+1} = (1 - t)(1 - tq) \dots (1 - tq^n)$  be the  $q$ -Pochhammer-symbol, then*

$$\frac{f^\lambda(q, t)}{(t; q)_{n+1}} = \sum_{m=0}^{\infty} t^m s_\lambda(1, q, \dots, q^m).$$

This identity is particularly useful for us because the  $q$ -Pochhammer-symbol, as well as the principal specialisations of the Schur functions, can be easily evaluated at roots of unity.

**Proposition II.25.** *Given  $k \mid n$  and a primitive  $k$ -th root of unity  $\zeta$ , we have that*

$$(t; \zeta)_{n+1} = (1 - t)(1 - t^k)^{n/k}.$$

*Proof.* Because  $\zeta$  is a  $k$ -th primitive root of unity we have  $\zeta^{\ell k+r} = \zeta^r$  for integers  $\ell$  and  $r$  and  $x^k - 1 = \prod_{i=0}^{k-1} (x - \zeta^i)$ . We obtain:

$$\begin{aligned} (t; \zeta)_{n+1} &= (1 - t)(1 - t\zeta) \dots (1 - t\zeta^n) = (1 - t) \left( \prod_{i=0}^{k-1} (1 - t\zeta^i) \right)^{n/k} \\ &= (1 - t) \left( t^k \prod_{i=0}^{k-1} (1/t - \zeta^i) \right)^{n/k} = (1 - t) \left( t^k (1/t^k - 1) \right)^{n/k} \\ &= (1 - t)(1 - t^k)^{n/k}. \end{aligned}$$

□

**Theorem II.26.** *Let  $\lambda \vdash n$  be a partition with empty  $k$ -core and with  $k$ -quotient  $(\lambda^0, \dots, \lambda^{k-1})$ , and let  $\zeta$  be a primitive  $k$ -th root of unity. If  $m = \ell \cdot k + r$  for  $0 \leq r < k$ , then*

$$s_\lambda(1, \zeta, \dots, \zeta^{m-1}) = \epsilon_{\lambda, k} \cdot s_{\lambda^0}(1^\ell) \dots s_{\lambda^{k-r-1}}(1^\ell) \cdot s_{\lambda^{k-r}}(1^{\ell+1}) \dots s_{\lambda^{k-1}}(1^{\ell+1}), \quad (29)$$

where  $\epsilon_{\lambda, k}$  is the sign from Proposition II.9.

**Remark II.27.** The case  $r = 0$  in Theorem II.26 is a theorem due to V. Reiner, D. Stanton and D. White [9, Theorem 4.3].

*Proof of Theorem II.26.* Let  $b(\lambda) = \sum (i-1)\lambda_i$  and  $R_{\lambda,k} = \zeta^{b(\lambda)} \frac{\prod_{x \in \lambda, k \nmid m+c(x)} (1-\zeta^{m+c(x)})}{\prod_{x \in \lambda, k \nmid h(x)} (1-\zeta^{h(x)})}$ , then by Proposition II.15, Proposition II.16 and the hook-content formula [13, Theorem 7.21.2] we get:

$$\begin{aligned}
s_\lambda(1, \zeta, \dots, \zeta^{m-1}) &= \zeta^{b(\lambda)} \prod_{x \in \lambda} \frac{1 - \zeta^{m+c(x)}}{1 - \zeta^{h(x)}} = R_{\lambda,k} \cdot \frac{\prod_{x \in \lambda, k \nmid m+c(x)} (1 - \zeta^{m+c(x)})}{\prod_{x \in \lambda, k \nmid h(x)} (1 - \zeta^{h(x)})} \\
&= R_{\lambda,k} \cdot \frac{\prod_{x \in \lambda, k \nmid m+c(x)} (m+c(x))}{\prod_{x \in \lambda, k \nmid h(x)} h(x)} = R_{\lambda,k} \cdot \frac{\prod_{x \in \lambda, k \nmid r+c(x)} (\ell + (r+c(x))/k)}{\prod_{x \in \lambda, k \nmid h(x)} h(x)/k} \\
&= R_{\lambda,k} \cdot \frac{\prod_{u \in \frac{1}{k}(c_r, k(\lambda)+r)} (\ell + u)}{\prod_{u \in \frac{1}{k}h_{0,k}(\lambda)} u} \\
&= R_{\lambda,k} \cdot \frac{\prod_{u \in \cup_{0 \leq i < k-r} c(\lambda^i) \cup \cup_{k-r \leq i < k} (c(\lambda^i)+1)} (\ell + u)}{\prod_{u \in \cup_{0 \leq i < k} h(\lambda^i)} u} \\
&= R_{\lambda,k} \cdot \frac{\prod_{u \in \cup_{0 \leq i < k-r} c(\lambda^i)} (\ell + u) \cdot \prod_{u \in \cup_{k-r \leq i < k} c(\lambda^i)} (\ell + 1 + u)}{\prod_{u \in \cup_{0 \leq i < k-r} h(\lambda^i)} u \cdot \prod_{u \in \cup_{k-r \leq i < k} h(\lambda^i)} u} \\
&= R_{\lambda,k} \prod_{0 \leq i < k-r} s_{\lambda^i}(1^\ell) \cdot \prod_{k-r \leq i < k} s_{\lambda^i}(1^{\ell+1}).
\end{aligned}$$

As  $\lambda$  has empty  $k$ -core each content modulo  $k$  appears  $n/k$  times. Hence,

$$R_{\lambda,k} = \zeta^{b(\lambda)} \frac{\prod_{x \in \lambda, k \nmid m+c(x)} (1 - \zeta^{m+c(x)})}{\prod_{x \in \lambda, k \nmid h(x)} (1 - \zeta^{h(x)})} = \zeta^{b(\lambda)} \frac{\prod_{0 < i \leq k-1} (1 - \zeta^i)^{n/k}}{\prod_{x \in \lambda, k \nmid h(x)} (1 - \zeta^{h(x)})},$$

which does not depend on  $m$ .

As the formula (29) is satisfied for  $r = 0$  due to [9, Theorem 4.3] by V. Reiner, D. Stanton and D. White, we obtain  $R_{\lambda,k} = \epsilon_{\lambda,k}$ .  $\square$

For a partition  $\mu$  we interpret the evaluation of the Schur function  $s_\mu(1^{\ell+1})$  as the number of semistandard Young diagrams with shape  $\mu$  and entries in  $\{1, \dots, \ell+1\}$  and  $s_\mu(1^\ell)$  as the number of semistandard Young diagrams with shape  $\mu$  and entries in  $\{2, \dots, \ell+1\}$ . Then the difference  $s_\mu(1^{\ell+1}) - s_\mu(1^\ell)$  equals the number of semistandard Young diagrams with shape  $\mu$  that contain at least one 1 and maximal entry at most  $\ell+1$ .

Keeping the notation of Theorem II.26, this yields:

**Lemma II.28.** Denote with  $\text{SSYT-tuples}(\Lambda)$  the set of all tuples of semistandard Young tableaux with shapes  $\Lambda = (\lambda^0, \dots, \lambda^{k-1})$  that contain at least one 1. For such a tuple  $\mathfrak{T}$ , let  $\max(\mathfrak{T})$  be the maximal entry. Let  $s$  be the index of the leftmost tableau containing 1 and set  $\text{idx}_1(\mathfrak{T}) := k-1-s$ . Then

$$\begin{aligned}
\frac{1}{(1-t^k)^{n/k-1}} f^\lambda(\zeta, t) &= (1-t)(1-t^k) \sum_{m=0}^{\infty} t^m s_\lambda(1, \zeta, \dots, \zeta^m) = \\
&= \epsilon_{\lambda,k} \cdot \sum_{\mathfrak{T} \in \text{SSYT-tuples}(\Lambda)} t^{k \cdot (\max(\mathfrak{T})-1) + \text{idx}_1(\mathfrak{T})}. \quad (30)
\end{aligned}$$



*Proof.* The first equation is a direct consequence of Theorem II.24 and Proposition II.25.

We abbreviate  $\hat{s}_i^m = |\{\mathfrak{T} \in \text{SSYT-tuples}(\Lambda) : \text{id}_{x_1}(\mathfrak{T}) = i, \max(\mathfrak{T}) \leq m\}|$  and similarly we write  $\mathfrak{s}_i^m = |\{\mathfrak{T} \in \text{SSYT-tuples}(\Lambda) : \text{id}_{x_1}(\mathfrak{T}) = i, \max(\mathfrak{T}) = m\}|$ . With this notion we have

$$\mathfrak{s}_i^m = \begin{cases} \hat{s}_i^m - \hat{s}_i^{m-1} & \text{if } m > 1, \\ \hat{s}_i^1 & \text{if } m = 1. \end{cases}$$

By equation Equation (29) and the combinatorial interpretation of the Schur functions we obtain  $\epsilon_{\lambda,k} s_\lambda(1) = \hat{s}_0^1$  for  $m = 0 = k \cdot 0 + 0$  and for  $m = k \cdot \ell + r > 0$  we have

$$\epsilon_{\lambda,k} (s_\lambda(1, \zeta, \dots, \zeta^m) - s_\lambda(1, \zeta, \dots, \zeta^{m-1})) = \prod_{0 \leq i < k-r-1} s_{\lambda^i}(1^\ell) \cdot (s_{\lambda^{k-r-1}}(1^{\ell+1}) - s_{\lambda^{k-r-1}}(1^\ell)) \cdot \prod_{k-r \leq i < k} s_{\lambda^i}(1^{\ell+1}) = \hat{s}_r^{\ell+1}.$$

Thus

$$\begin{aligned} \epsilon_{\lambda,k} \cdot (1-t)(1-t^k) \sum_{m=0}^{\infty} t^m s_\lambda(1, \zeta, \dots, \zeta^m) &= \\ \epsilon_{\lambda,k} (1-t^k) \left( t^0 s_\lambda(1) + \sum_{m=1}^{\infty} t^m (s_\lambda(1, \zeta, \dots, \zeta^m) - s_\lambda(1, \zeta, \dots, \zeta^{m-1})) \right) &= \\ (1-t^k) \sum_{r=0}^{k-1} \sum_{\ell=0}^{\infty} t^{k \cdot \ell + r} \hat{s}_r^{\ell+1} = \sum_{r=0}^{k-1} \left( t^{k \cdot 0 + r} \hat{s}_r^1 + \sum_{\ell=1}^{\infty} t^{k \cdot \ell + r} (\hat{s}_r^{\ell+1} - \hat{s}_r^\ell) \right) &= \\ \sum_{r=0}^{k-1} \sum_{\ell=0}^{\infty} t^{k \cdot \ell + r} \mathfrak{s}_r^{\ell+1} = \sum_{\mathfrak{T} \in \text{SSYT-tuples}(\Lambda)} t^{k \cdot (\max(\mathfrak{T}) - 1) + \text{id}_{x_1}(\mathfrak{T})}. \end{aligned}$$

□

## II.5 THE FINAL BIJECTION

In this section we discuss the bijection that links together Equation (28) and Equation (30) and proves our main result Theorem II.8.

Denote with  $C_p$  the set of weak compositions with precisely  $p$  parts, that is the set of  $p$ -tuples of non negative integers. Let  $\Lambda = (\lambda^0, \dots, \lambda^{k-1})$  be a  $k$ -tuple of partitions and let  $\ell = |\lambda^0| + \dots + |\lambda^{k-1}|$ . We now present a bijection

$$\phi : C_{\ell-1} \times \text{SYT-tuples}(\Lambda) \rightarrow \text{SSYT-tuples}(\Lambda).$$

**Definition II.29.** Fix  $\alpha = (\alpha_1, \dots, \alpha_{\ell-1}) \in C_{\ell-1}$  and  $\mathcal{T} \in \text{SYT-tuples}(\Lambda)$ . For  $1 \leq s \leq \ell$ , let  $x_s$  be the unique cell in  $\mathcal{T}$  that contains  $s$  and let  $d_s$  be the number of descents in  $\mathcal{T}$  that are strictly smaller than  $s$ . Let  $\mathfrak{T}$  be the tuple of semistandard Young tableaux obtained by filling the cell  $x_s$  with  $1 + d_s + \sum_{i=1}^{s-1} \alpha_i$  and set  $\phi(\alpha, \mathcal{T}) = \mathfrak{T}$ .

An example of the map  $\phi$  is given in Figure 12.

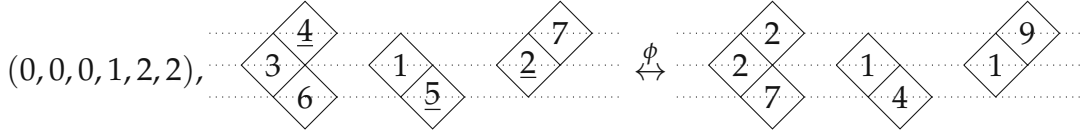


Figure 12: Bijectively mapping a composition and a standard Young tableau tuple to a tuple of semistandard Young tableaux.

**Remark II.30.** It has been brought to our attention by Christian Krattenthaler that this map has the flavor of the MacMahon Verfahren (see [7] and [5, Chapter 10]) and fits into the context of  $P$ -partitions developed by R. Stanley [12].

**Proposition II.31.** *The function  $\phi : C_{\ell-1} \times \text{SYT-tuples}(\Lambda) \rightarrow \text{SSYT-tuples}(\Lambda)$  is a bijection and for  $\phi(\alpha, \mathcal{T}) = \mathfrak{T}$ , we have*

$$|\alpha| + |\text{DES}(\mathcal{T})| + 1 = \max(\mathfrak{T}) \quad \text{and} \quad \text{id}_{x_1}(\mathcal{T}) = \text{id}_{x_1}(\mathfrak{T}),$$

where  $|\alpha| = \alpha_1 + \dots + \alpha_{\ell-1}$  is the sum of its parts.

*Proof.* We first show that  $\phi$  is well defined. Clearly, the tableaux in  $\mathfrak{T}$  are weakly increasing in the rows and the columns and it suffices to show that the columns are strictly increasing. Consider two cells  $x_s$  and  $x_t$  of  $\mathcal{T}$  that contain  $s$  and  $t$ , respectively, such that the cells are in the same tableau and  $x_t$  is in a row strictly below  $x_s$  and in a column weakly left of  $x_s$ . It suffices to show that  $d_s < d_t$ .

As  $\mathcal{T}$  consists of partial standard Young tableaux we have  $s < t$ . For a cell containing  $u$  in the  $j$ -th tableau of  $\mathcal{T}$  let  $\beta(u) = \frac{j}{k} + c(u)$ . Note that  $i$  is a descent in  $\mathcal{T}$ , if and only if  $\beta(i+1) < \beta(i)$ . By definition we have  $\beta(s) > \beta(t)$ . Thus there exists an entry  $i$  with  $s \leq i < t$  and  $\beta(i) > \beta(i+1)$ . Thus  $d_s \leq d_i < d_{i+1} \leq d_t$ . Therefore  $\phi$  is well defined.

By construction the leftmost one in  $\mathfrak{T}$  coincides with the one in  $\mathcal{T}$ , so  $\text{id}_{x_1}(\mathcal{T}) = \text{id}_{x_1}(\mathfrak{T})$ . The maximal entry of  $\mathfrak{T}$  is the filling of  $x_\ell$ , which is  $1 + d_\ell + \sum_{i=1}^{\ell-1} \alpha_i = |\alpha| + |\text{DES}(\mathcal{T})| + 1$ .

It remains to show, that this map is a bijection, by giving the inverse map. To obtain  $\mathcal{T}$  follow the entries from  $\mathfrak{T}$  in increasing order and fill the corresponding cells of  $\mathcal{T}$  with the smallest positive integer, which is not already used. If some values in  $\mathfrak{T}$  coincide fill the corresponding cells of  $\mathcal{T}$  in the unique order, that does not create any descents. Having now  $\mathfrak{T}$  and  $\mathcal{T}$  we can again calculate the values  $d_s$  and obtain the composition  $\alpha$  from the fact that the cell  $x_s$  is filled with  $1 + d_s + \sum_{i=1}^{s-1} \alpha_i$  in  $\mathfrak{T}$ .  $\square$

From this proposition we get:

**Lemma II.32.** *Let  $\lambda \vdash n$  be a partition with empty  $k$ -core and let  $\Lambda = (\lambda^0, \dots, \lambda^{k-1})$  its  $k$ -quotient. Then*

$$\frac{1}{(1-t^k)^{n/k-1}} \sum_{\mathcal{T} \in \text{SYT-tuples}(\Lambda)} t^{k \cdot |\text{DES}(\mathcal{T})| + \text{id}_{x_1}(\mathcal{T})} = \sum_{\mathfrak{T} \in \text{SSYT-tuples}(\Lambda)} t^{k \cdot (\max(\mathfrak{T}) - 1) + \text{id}_{x_1}(\mathfrak{T})}.$$

*Proof.* By our bijection  $\phi$  we have in terms of generating functions

$$\frac{1}{(1-x)^{n/k-1}} \sum_{\mathcal{T} \in \text{SYT-tuples}(\Lambda)} x^{|\text{DES}(\mathcal{T})|} y^{\text{id}_{x_1}(\mathcal{T})} = \sum_{\mathfrak{T} \in \text{SSYT-tuples}(\Lambda)} x^{\max(\mathfrak{T}) - 1} y^{\text{id}_{x_1}(\mathfrak{T})}.$$

The theorem follows by substituting  $x = t^k$  and  $y = t$ . □

Now we can conclude our main theorem.

*Proof of Theorem II.8.* Combining Lemma II.22, Lemma II.28 and Lemma II.32 yields the desired identity. □

#### ACKNOWLEDGEMENTS

The author would like to thank Martin Rubey, Esther Banaian, Bruce Westbury and Christian Krattenthaler for helpful insights and discussions related to this work, as well as the anonymous referees who provided useful and detailed comments on an earlier version of the manuscript. Moreover the author would like to thank the former organisers of the Graduate Online Combinatorics Colloquium (GOCC) Galen Dorpalen-Barry, Alex McDonough and Andrés R. Vindas Meléndez for the opportunity to present this results and gain feedback at an early stage.

#### BIBLIOGRAPHY

- [1] P. ALEXANDERSSON, S. PFANNERER, M. RUBEY, AND J. UHLIN, *Skew characters and cyclic sieving*, Forum of Mathematics, Sigma, 9 (2021), p. e41.
- [2] J. HAGLUND, *The  $q, t$ -Catalan Numbers and the Space of Diagonal Harmonics*, American Mathematical Society, Dec. 2007.
- [3] J. HAGLUND, M. HAIMAN, AND N. LOEHR, *A combinatorial formula for macdonald polynomials*, Journal of the American Mathematical Society, 18 (2005), pp. 735–761.
- [4] G. JAMES AND A. KERBER, *The Representation Theory of the Symmetric Group*, Cambridge University Press, Dec. 1984.
- [5] M. LOTHAIRE, *Algebraic Combinatorics on Words*, Cambridge University Press, Apr. 2002.
- [6] I. MACDONALD, *Symmetric functions and Hall polynomials*, Clarendon Press, Oxford University Press Oxford, 1995.
- [7] P. MACMAHON, *The indices of permutations and the derivation therefrom of functions of a single variable associated with the permutations of any assemblage of objects*, American Journal of Mathematics, 35 (1913), p. 281.
- [8] I. PAK, *Ribbon tile invariants*, Transactions of the American Mathematical Society, 352 (2000), pp. 5525–5561.
- [9] V. REINER, D. STANTON, AND D. WHITE, *The cyclic sieving phenomenon*, Journal of Combinatorial Theory, Series A, 108 (2004), pp. 17–50.
- [10] B. SAGAN, *The cyclic sieving phenomenon: a survey*, Cambridge University Press, 2011, pp. 183–234.

- [11] T. SPRINGER, *Regular elements of finite reflection groups*, *Inventiones Mathematicae*, 25 (1974), pp. 159–198.
- [12] R. STANLEY, *Ordered Structures and Partitions*, PhD thesis, Harvard University, 1971.
- [13] ———, *Enumerative Combinatorics*, vol. 2 of *Cambridge Studies in Advanced Mathematics*, Cambridge University Press, 1999.

---

## PROMOTION AND GROWTH DIAGRAMS FOR FANS OF DYCK PATHS AND VACILLATING TABLEAUX

---

### BIBLIOGRAPHIC INFORMATION

Pappe, J., Pfannerer, S., Schilling, A., and Simone, M. Promotion and growth diagrams for fans of Dyck paths and vacillating tableaux. *Journal of Algebra*, Volume 655, 2024, [doi:10.1016/j.jalgebra.2023.07.038](https://doi.org/10.1016/j.jalgebra.2023.07.038)

### TABLE OF CONTENTS

Abstract . . . . .	85
III.1 Introduction . . . . .	86
III.2 Crystal bases . . . . .	88
III.2.1 Background on crystals . . . . .	88
III.2.2 Virtual crystals . . . . .	90
III.2.3 Highest weights of weight zero . . . . .	95
III.2.4 Promotion via crystal commutor . . . . .	98
III.2.5 Promotion via local rules . . . . .	99
III.3 Chord diagrams . . . . .	100
III.3.1 Promotion matrices . . . . .	100
III.3.2 Fomin growth diagrams . . . . .	107
III.3.3 Fomin growth diagrams: Rule Burge . . . . .	109
III.3.4 Fomin growth diagrams: Rule RSK . . . . .	111
III.4 Main results . . . . .	113
III.4.1 Results for oscillating tableaux . . . . .	114
III.4.2 Results for $r$ -fans of Dyck paths . . . . .	114
III.4.3 Results for vacillating tableaux . . . . .	118
III.4.4 Cyclic sieving . . . . .	122
Bibliography . . . . .	127

### ABSTRACT

We construct an injection from the set of  $r$ -fans of Dyck paths (resp. vacillating tableaux) of length  $n$  into the set of chord diagrams on  $[n]$  that intertwines promotion and rotation. This is done in two different ways, namely as fillings of promotion

matrices and in terms of Fomin growth diagrams. Our analysis uses the fact that  $r$ -fans of Dyck paths and vacillating tableaux can be viewed as highest weight elements of weight zero in crystals of type  $B_r$  and  $C_r$ , respectively, which in turn can be analyzed using virtual crystals. On the level of Fomin growth diagrams, the virtualization process corresponds to the Roby–Krattenthaler blow up construction. One of the motivations for finding rotation invariant diagrammatic bases such as chord diagrams is the cyclic sieving phenomenon. Indeed, we give a cyclic sieving phenomenon on  $r$ -fans of Dyck paths and vacillating tableaux using the promotion action.

### III.1 INTRODUCTION

Interest in invariant subspaces goes back to Rumer, Teller and Weyl [34], who studied the quantum mechanical description of molecules. In particular, they devised diagrammatic bases for the invariant spaces. For  $SL(n)$ , a set of diagrams spanning the invariant space was constructed by Cautis, Kamnitzer and Morrison [5], generalizing Kuperberg’s webs [22] for  $SL(2)$  and  $SL(3)$ .

The dimension of the invariant subspace of a tensor product  $V^{\otimes N}$  of an irreducible representation  $V$  of a Lie algebra  $\mathfrak{g}$  is equal to the number of highest weight elements of weight zero in  $\mathcal{B}^{\otimes N}$ , where  $\mathcal{B}$  is the crystal basis associated to  $V$  [43, 30]. The symmetric group acts on  $V^{\otimes N}$  by permuting tensor positions. By Schur–Weyl duality, this action commutes with the action of the Lie group. In particular, the symmetric group acts on the invariant space of  $V^{\otimes N}$ . It was shown by Westbury [43] that the action of the long cycle corresponds to the action of promotion on highest weight elements of weight zero in  $\mathcal{B}^{\otimes N}$ . In this setting promotion is defined using Henriques’ and Kamnitzer’s commutor [12], see [8, 43, 44]. Note that the full action of the symmetric group on invariant tensors is not yet known in general.

In general, it is desirable to have a correspondence between highest weight elements of weight zero in  $\mathcal{B}^{\otimes N}$  and diagram bases, such as chord diagrams, which intertwine promotion and rotation. For Kuperberg’s webs [22], this was achieved by Petersen, Pylyavskyy and Rhoades [29], Russell [35] and Patrias [28] by showing that the growth algorithm of Khovanov and Kuperberg [19] intertwines promotion with rotation. For the vector representation of the symplectic group and the adjoint representation of the general linear group, such a correspondence between highest weight elements of weight zero and chord diagrams which intertwines promotion and rotation was given in [30].

In this paper, we construct an injection from the set of  $r$ -fans of Dyck paths (resp. vacillating tableaux) of length  $n$  into the set of chord diagrams on  $[n]$  that intertwines promotion and rotation. There is a natural correspondence between  $r$ -fans of Dyck paths (resp. vacillating tableaux) and highest weight elements in the tensor product of the spin crystal (resp. vector representation) of type  $B_r$ . We present this injection in two different ways:

1. as fillings of promotion matrices [23] (see Section III.3.1);
2. in terms of Fomin growth diagrams [7, 33, 21] (see Sections III.3.2–III.3.4).

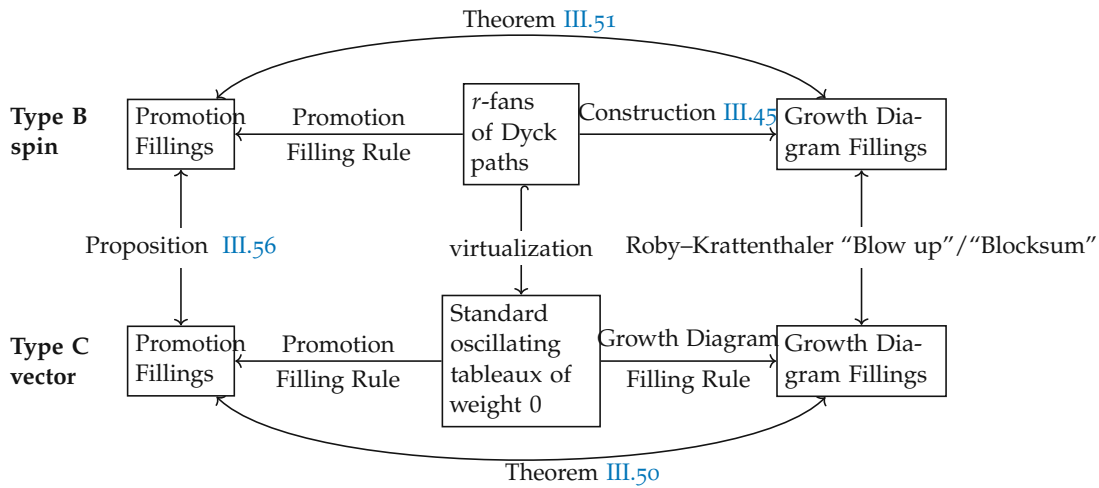


Figure 13: Overview of strategy and results for  $r$ -fans of Dyck paths

While the first description shows that the map intertwines promotion and rotation, the second description shows injectivity. Our proof strategy uses virtualization of crystals (see for example [4]) and results of [30] for oscillating tableaux of weight zero (or equivalently highest weight words of weight zero for the vector representation type  $C_r$ ):

1. Find a virtual crystal morphism for the spin crystals (resp. crystals for the vector representation) of type  $B_r$  into the  $r$ -th (resp. second) tensor power of the crystal of the vector representation of type  $C_r$  (see Section III.2.2).
2. Use this virtualization to map an  $r$ -fan of Dyck paths (resp. vacillating tableau) to an oscillating tableau (see Section III.2.3).
3. Show that this virtualization commutes with promotion and the filling rules.
4. Show that blowing up the filling of the growth diagram corresponds to the filling of the oscillating tableau. In this sense, the blow up on growth diagrams is the analogue of the virtualization on crystals.

An overview of our strategy is shown in Figures 13 and 14.

Having the injective map to chord diagrams gives a first step towards a diagrammatic basis for the invariant subspaces. In addition, Fontaine and Kamnitzer [8] as well as Westbury [43] tied the promotion action on highest weight elements of weight zero to the cyclic sieving phenomenon introduced by Reiner, Stanton and White [31]. In Section III.4.4, we make this cyclic sieving phenomenon more concrete by providing the polynomial in terms of the energy function. For  $r$ -fans of Dyck paths, we conjecture another polynomial, which is the  $q$ -deformation of the number of  $r$ -fans of Dyck paths, to give a cyclic sieving phenomenon. For vacillating tableaux, we give a polynomial inspired by work of Jagenteufel [16] for a cyclic sieving phenomenon.

The paper is organized as follows. In Section III.2, we give a brief review of crystal bases and virtual crystals and provide the virtual crystals for spin and vector representation of type  $B_r$  into type  $C_r$ . We also define promotion on crystals via the crystal commutor. In Section III.3, we give the various filling rules to construct the

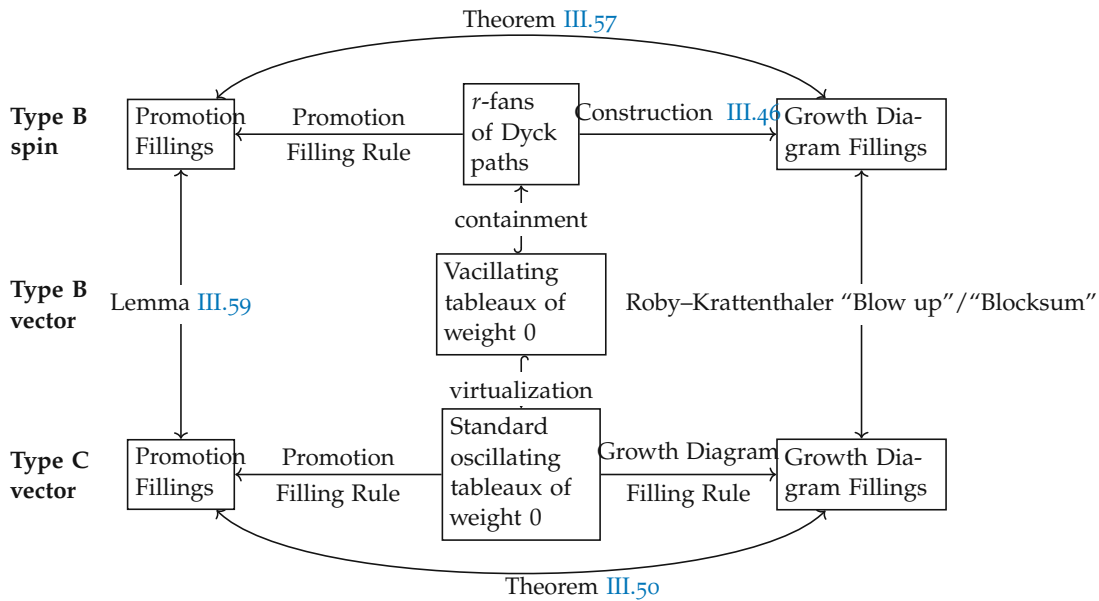


Figure 14: Overview of strategy and results for vacillating tableaux

map to chord diagrams. Section III.4 is reserved for the statements and proofs of our main results.

## III.2 CRYSTAL BASES

### III.2.1 Background on crystals

Crystal bases form a combinatorial skeleton of representations of quantum groups associated to Lie algebras. They were first introduced by Kashiwara [17] and Lusztig [24].

Axiomatically, for a given root system  $\Phi$  with index set  $I$  and weight lattice  $\Lambda$ , a *crystal* is a nonempty set  $\mathcal{B}$  together with maps

$$\begin{aligned} e_i, f_i: \mathcal{B} &\rightarrow \mathcal{B} \sqcup \{\emptyset\} \\ \varepsilon_i, \varphi_i: \mathcal{B} &\rightarrow \mathbb{Z} \\ \text{wt}: \mathcal{B} &\rightarrow \Lambda \end{aligned} \tag{31}$$

for  $i \in I$ , satisfying certain conditions (see for example [4, Definition 2.13]). The operators  $e_i$  and  $f_i$  are called *raising* and *lowering operators*. The map  $\text{wt}$  is the *weight map*. The map  $\varepsilon_i$  (resp.  $\varphi_i$ ) measures how often  $e_i$  (resp.  $f_i$ ) can be applied to the given crystal element. For all crystals considered in this paper, we have for  $b \in \mathcal{B}$

$$\varepsilon_i(b) = \max\{k \geq 0 \mid e_i^k(b) \neq \emptyset\} \quad \text{and} \quad \varphi_i(b) = \max\{k \geq 0 \mid f_i^k(b) \neq \emptyset\}. \tag{32}$$

An element  $b \in \mathcal{B}$  is called *highest weight* if  $e_i(b) = \emptyset$  for all  $i \in I$ .

Here we define certain crystals for the root systems  $B_r$  and  $C_r$  explicitly. Let  $\mathbf{e}_i \in \mathbb{Z}^r$  be the  $i$ -th unit vector with 1 in position  $i$  and 0 everywhere else.



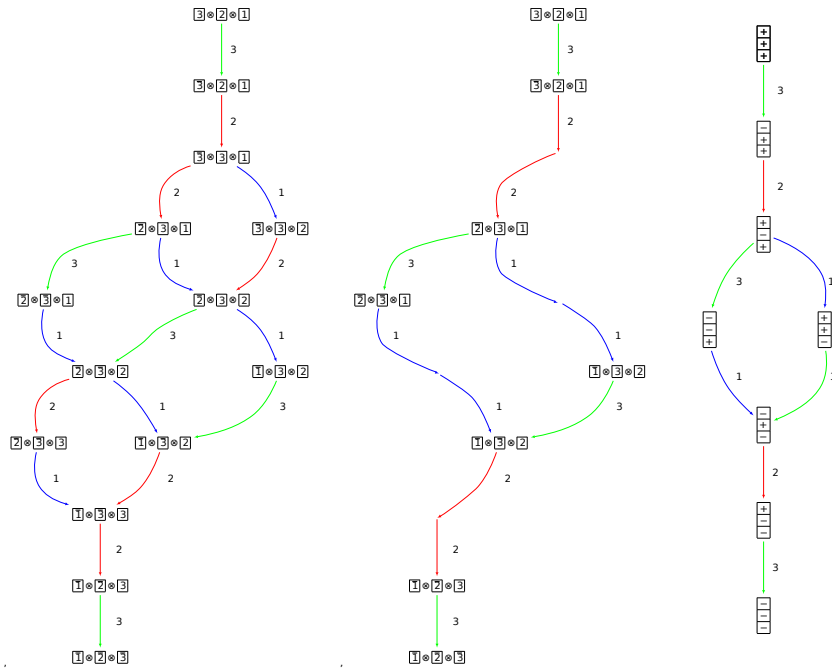


Figure 15: Left: One component of the crystal  $\widehat{\mathcal{V}} = \mathcal{C}_{\square}^{\otimes 3}$  of type  $C_3$ . Middle: The virtual crystal  $\mathcal{V}$  inside  $\widehat{\mathcal{V}}$  of type  $B_3$ . Right: The spin crystal  $\mathcal{B}_{\text{spin}}$  of type  $B_3$ .

**Definition III.1.** The *spin crystal* of type  $B_r$ , denoted by  $\mathcal{B}_{\text{spin}}$ , consists of all  $r$ -tuples  $\epsilon = (\epsilon_1, \epsilon_2, \dots, \epsilon_r)$ , where  $\epsilon_i \in \{\pm\}$ . The weight of  $\epsilon$  is

$$\text{wt}(\epsilon) = \frac{1}{2} \sum_{i=1}^r \epsilon_i \mathbf{e}_i.$$

The crystal operator  $f_r$  annihilates  $\epsilon$  unless  $\epsilon_r = +$ . If  $\epsilon_r = +$ ,  $f_r$  acts on  $\epsilon$  by changing  $\epsilon_r$  from  $+$  to  $-$  and leaving all other entries unchanged. The crystal operator  $f_i$  for  $1 \leq i < r$  annihilates  $\epsilon$  unless  $\epsilon_i = +$  and  $\epsilon_{i+1} = -$ . In the latter case,  $f_i$  acts on  $\epsilon$  by changing  $\epsilon_i$  to  $-$  and  $\epsilon_{i+1}$  to  $+$ . Similarly, the crystal operator  $e_r$  annihilates  $\epsilon$  unless  $\epsilon_r = -$ . If  $\epsilon_r = -$ ,  $e_r$  acts on  $\epsilon$  by changing  $\epsilon_r$  from  $-$  to  $+$ . The crystal operator  $e_i$  for  $1 \leq i < r$  annihilates  $\epsilon$  unless  $\epsilon_i = -$  and  $\epsilon_{i+1} = +$ . In the latter case,  $e_i$  acts on  $\epsilon$  by changing  $\epsilon_i$  to  $+$  and  $\epsilon_{i+1}$  to  $-$ .

The crystal  $\mathcal{B}_{\text{spin}}$  of type  $B_3$  is depicted in Figure 15.

**Definition III.2.** Here we define the *crystals for the vector representation* of type  $B_r$  and  $C_r$ .

1. The crystal  $\mathcal{C}_{\square}$  of type  $C_r$  consists of the elements  $\{1, 2, \dots, r, \bar{r}, \dots, \bar{2}, \bar{1}\}$ . The crystal operator  $f_i$  for  $1 \leq i < r$  maps  $i$  to  $i + 1$ , maps  $\bar{i + 1}$  to  $\bar{i}$  and annihilates all other elements. The crystal operator  $f_r$  maps  $r$  to  $\bar{r}$  and annihilates all other elements. Similarly, the crystal operator  $e_i$  for  $1 \leq i < r$  maps  $i + 1$  to  $i$ , maps  $\bar{i}$  to  $\bar{i + 1}$  and annihilates all other elements. The crystal operator  $e_r$  maps  $\bar{r}$  to  $r$  and annihilates all other elements. Furthermore,  $\text{wt}(i) = \mathbf{e}_i$  and  $\text{wt}(\bar{i}) = -\mathbf{e}_i$ .
2. The crystal  $\mathcal{B}_{\square}$  of type  $B_r$  consists of the elements  $\{1, 2, \dots, r, 0, \bar{r}, \dots, \bar{2}, \bar{1}\}$ . The crystal operator  $f_i$  for  $1 \leq i < r$  maps  $i$  to  $i + 1$ , maps  $\bar{i + 1}$  to  $\bar{i}$  and annihilates

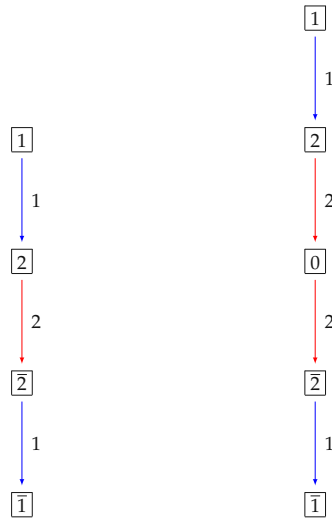


Figure 16: Left: The crystal  $\mathcal{C}_{\square}$  of type  $C_2$ . Right: The crystal  $\mathcal{B}_{\square}$  of type  $B_2$ .

all other elements. The crystal operator  $f_r$  maps  $r$  to  $0$ ,  $0$  to  $\bar{r}$  and annihilates all other elements. Similarly, the crystal operator  $e_i$  for  $1 \leq i < r$  maps  $i + 1$  to  $i$ , maps  $\bar{i}$  to  $\overline{i + 1}$  and annihilates all other elements. The crystal operator  $e_r$  maps  $\bar{r}$  to  $0$ ,  $0$  to  $r$  and annihilates all other elements. Furthermore,  $\text{wt}(i) = \mathbf{e}_i$  and  $\text{wt}(\bar{i}) = -\mathbf{e}_i$  for  $i \neq 0$  and  $\text{wt}(0) = 0$ .

The crystals  $\mathcal{C}_{\square}$  for type  $C_2$  and  $\mathcal{B}_{\square}$  for type  $B_2$  are depicted in Figure 16.

A remarkable property of crystals is that they respect *tensor products*. Given two crystals  $\mathcal{B}$  and  $\mathcal{C}$  associated to the same root system  $\Phi$ , the tensor product  $\mathcal{B} \otimes \mathcal{C}$  as a set is the Cartesian product  $\mathcal{B} \times \mathcal{C}$ . The weight of  $b \otimes c \in \mathcal{B} \otimes \mathcal{C}$  is the sum of the weights  $\text{wt}(b \otimes c) = \text{wt}(b) + \text{wt}(c)$ . Furthermore

$$f_i(b \otimes c) = \begin{cases} f_i(b) \otimes c & \text{if } \varphi_i(c) \leq \varepsilon_i(b), \\ b \otimes f_i(c) & \text{if } \varphi_i(c) > \varepsilon_i(b), \end{cases}$$

and

$$e_i(b \otimes c) = \begin{cases} e_i(b) \otimes c & \text{if } \varphi_i(c) < \varepsilon_i(b), \\ b \otimes e_i(c) & \text{if } \varphi_i(c) \geq \varepsilon_i(b). \end{cases}$$

### III.2.2 Virtual crystals

Stembridge [39] characterized crystals which are associated with quantum group representations for simply-laced root systems in terms of local rules on the crystal graph. Crystals for non-simply-laced root systems can be constructed using virtual crystals, see [4, Chapter 5].

In this paper, we utilize virtual crystals to construct Fomin growth diagrams and the promotion operators for type  $B_r$  using results for type  $C_r$ . Hence let us briefly

review the set-up for virtual crystals. Let  $X \hookrightarrow Y$  be an embedding of Lie algebras such that the fundamental weights  $\omega_i$  and simple roots  $\alpha_i$  map as follows

$$\begin{aligned}\omega_i^X &\mapsto \gamma_i \sum_{j \in \sigma(i)} \omega_j^Y, \\ \alpha_i^X &\mapsto \gamma_i \sum_{j \in \sigma(i)} \alpha_j^Y.\end{aligned}$$

Here  $\gamma_i$  is a multiplication factor,  $\sigma: I^X \rightarrow I^Y / \text{aut}$  is a bijection and  $\text{aut}$  is an automorphism on the Dynkin diagram for  $Y$ .

Let  $\widehat{\mathcal{V}}$  be an ambient crystal associated to the Lie algebra  $Y$ . In [4, Chapter 5] it is assumed that  $\widehat{\mathcal{V}}$  is a crystal for a simply-laced root system. However, in general it may be assumed that  $\widehat{\mathcal{V}}$  is a crystal corresponding to a quantum group representation (which is the case in our setting).

**Definition III.3.** If there is an embedding of Lie algebras  $X \hookrightarrow Y$ , then  $\mathcal{V} \subseteq \widehat{\mathcal{V}}$  is a *virtual crystal* for the root system  $\Phi^X$  if

- V1.** The ambient crystal  $\widehat{\mathcal{V}}$  is a Stembridge crystal or a crystal associated to a representation for the root system  $\Phi^Y$  with crystal operators  $\widehat{e}_i, \widehat{f}_i, \widehat{\varepsilon}_i, \widehat{\varphi}_i$  for  $i \in I^Y$  and weight function  $\widehat{\text{wt}}$ .
- V2.** If  $b \in \mathcal{V}$  and  $i \in I^X$ , then  $\widehat{\varepsilon}_j(b)$  has the same value for all  $j \in \sigma(i)$  and that value is a multiple of  $\gamma_i$ . The same is true for  $\widehat{\varphi}_j(b)$ .
- V3.** The subset  $\mathcal{V} \sqcup \{\emptyset\} \subseteq \widehat{\mathcal{V}} \sqcup \{\emptyset\}$  is closed under the virtual crystal operators

$$e_i := \prod_{j \in \sigma(i)} \widehat{e}_j^{\gamma_i} \quad \text{and} \quad f_i := \prod_{j \in \sigma(i)} \widehat{f}_j^{\gamma_i}.$$

Furthermore, for all  $b \in \mathcal{V}$

$$\varepsilon_i(b) = \max\{k \geq 0 \mid e_i^k(b) \neq \emptyset\} \quad \text{and} \quad \varphi_i(b) = \max\{k \geq 0 \mid f_i^k(b) \neq \emptyset\}.$$

The tensor product of two virtual crystals for the same embedding  $X \hookrightarrow Y$  is again a virtual crystal (see for example [4, Theorem 5.8]).

*Virtual crystal  $B_r \hookrightarrow C_r$  spin to vector*

We will now apply the theory of virtual crystals to the embedding  $B_r \hookrightarrow C_r$ . In this setting  $I^{C_r} = I^{B_r} = \{1, 2, \dots, r\}$ ,  $\sigma(i) = \{i\}$ ,  $\gamma_i = 2$  for  $1 \leq i < r$  and  $\gamma_r = 1$ . We consider as the ambient crystal

$$\widehat{\mathcal{V}} = \mathcal{C}_{\square}^{\otimes r}.$$

Define an ordering  $<$  on the set  $[r] \cup [\bar{r}]$  as follows:

$$1 < 2 < \dots < r < \bar{r} < \dots < \bar{1}.$$

Denote by  $|\cdot|$  the map from  $[r] \cup [\bar{r}]$  to  $[r]$  that sends letters to their corresponding unbarred values.

**Definition III.4.** Let  $\mathcal{V} \subseteq \widehat{\mathcal{V}}$  be given by

$$\mathcal{V} := \{v_r \otimes v_{r-1} \otimes \cdots \otimes v_1 \in \widehat{\mathcal{V}} \mid v_i > v_j \text{ and } |v_i| \neq |v_j| \text{ for all } i > j\}.$$

Let  $f_i = \widehat{f}_i^2$ ,  $e_i = \widehat{e}_i^2$  for  $1 \leq i < r$  and  $f_r = \widehat{f}_r$ ,  $e_r = \widehat{e}_r$ .

**Lemma III.5.**  $\mathcal{V} \sqcup \{\emptyset\}$  is closed under the operators  $f_i$  and  $e_i$  for  $1 \leq i \leq r$ .

*Proof.* Let  $v = v_r \otimes v_{r-1} \otimes \cdots \otimes v_1 \in \mathcal{V}$ . We break into cases depending on the value of  $i$ .

Assume that  $i = r$ . By the definition of  $\mathcal{V}$ ,  $v$  must either contain an  $r$  or  $\bar{r}$ , but not both. If  $v$  contains an  $r$ , then this  $r$  must be to the left of all other unbarred letters and to the right of all barred letters. As  $f_r$  changes the  $r$  to a  $\bar{r}$ ,  $f_r(v)$  is still in  $\mathcal{V}$ . If  $v$  contains an  $\bar{r}$ , then  $f_r(v) = \emptyset \in \mathcal{V} \sqcup \{\emptyset\}$ .

Assume that  $i \neq r$ . Note that the conditions imposed on  $v$  imply that there exists exactly two indices  $j$  and  $k$  such that  $|v_j| = i$  and  $|v_k| = i + 1$ . By the ordering imposed on  $v$ ,  $v$  can only be in the following forms:

- $\cdots \otimes i + 1 \otimes i \otimes \cdots$
- $\cdots \otimes \bar{i} \otimes \overline{i + 1} \otimes \cdots$
- $\cdots \otimes \bar{i} \otimes \cdots \otimes i + 1 \otimes \cdots$
- $\cdots \otimes \overline{i + 1} \otimes \cdots \otimes i \otimes \cdots$

For the first three cases,  $f_i(v) = \emptyset$ . When  $v$  is of the form  $\cdots \otimes \overline{i + 1} \otimes \cdots \otimes i \otimes \cdots$ ,  $f_i$  replaces the  $\overline{i + 1}$  with  $\bar{i}$  and the  $i$  with  $i + 1$ . Since  $v$  does not contain an  $\bar{i}$  nor an  $i + 1$ ,  $f_i(v)$  is an element of  $\mathcal{V}$ .

The fact that  $e_i(v) \in \mathcal{V}$  for all  $i \in 1 \leq i \leq r$  follows similarly. Thus,  $\mathcal{V}$  is closed under the operators  $f_i$  and  $e_i$ .  $\square$

**Lemma III.6.** All elements of  $\mathcal{V}$  are in the connected component of  $\widehat{\mathcal{V}}$  with highest weight element  $r \otimes r - 1 \otimes \cdots \otimes 1$ .

*Proof.* Clearly  $r \otimes r - 1 \otimes \cdots \otimes 1$  is a highest weight element of  $\widehat{\mathcal{V}}$  and the only element in  $\mathcal{V}$  without any barred letters.

Consider  $v = v_r \otimes \cdots \otimes v_1 \in \mathcal{V}$  containing a barred letter. Observe that the number of barred letters in  $e_i(v)$  is at most the number of barred letters in  $v$  whenever  $e_i(v) \neq \emptyset$ . Since  $\widehat{\mathcal{V}}$  is finite and  $\mathcal{V}$  is closed under  $e_i$ , it suffices to show that  $e_i(v) \neq \emptyset$  for some  $i$ . Let  $v_j$  denote the rightmost tensor factor in  $v$  that is a barred letter, and let  $i = |v_j|$ . We break into cases depending on the value of  $i$ .

If  $i = r$ , then  $v_j = \bar{r}$  and  $v$  cannot contain an  $r$ . This implies that  $e_r(v) \neq \emptyset$  as it acts on  $v$  by replacing  $v_j$  by  $r$ . The number of barred letters has decreased by one.

If  $i \neq r$ , then  $v_j = \bar{i}$ . As  $v_j$  is the rightmost barred letter in  $v$ ,  $v$  must be of the form  $\cdots \otimes \bar{i} \otimes \cdots \otimes i + 1 \otimes \cdots$ . Thus,  $e_i$  acts by changing  $\bar{i}$  to  $\overline{i + 1}$  and  $i + 1$  to  $i$ . Note that the rightmost barred letter is closer to  $\bar{r}$ .  $\square$

**Definition III.7.** Let  $\Psi: \mathcal{B}_{\text{spin}} \rightarrow \mathcal{V}$  be the map

$$\Psi(\epsilon_1 \epsilon_2 \cdots \epsilon_r) = v_r \otimes v_{r-1} \otimes \cdots \otimes v_1,$$

where  $v_r > v_{r-1} > \cdots > v_1$  such that if  $\epsilon_i = +$  then  $v$  contains an  $i$  and if  $\epsilon_i = -$  then  $v$  contains an  $\bar{i}$  for all  $1 \leq i \leq r$ .

**Lemma III.8.** *The map  $\Psi$  is a bijective map that intertwines the crystal operators on  $\mathcal{B}_{\text{spin}}$  and  $\mathcal{V}$ .*

*Proof.* From the definition of  $\Psi$ , it is clearly bijective. Let  $\epsilon = \epsilon_1 \epsilon_2 \cdots \epsilon_r \in \mathcal{B}_{\text{spin}}$ . Since the raising and lowering operators of a crystal are partial inverses, it suffices to prove that  $f_i(\epsilon) \neq \emptyset$  if and only if  $f_i(\Psi(\epsilon)) \neq \emptyset$  and  $\Psi(f_i(\epsilon)) = f_i(\Psi(\epsilon))$  whenever  $f_i(\epsilon) \neq \emptyset$ .

Assume that  $f_i(\Psi(\epsilon)) \neq \emptyset$ . If  $i = r$ , then  $\Psi(\epsilon)$  contains an  $r$  implying  $\epsilon_r = +$ . Therefore  $f_r(\epsilon) \neq \emptyset$ . If  $i \neq r$ , then  $\epsilon$  contains both an  $i$  and an  $\bar{i+1}$ . Thus,  $\epsilon_i = +$  and  $\epsilon_{i+1} = -$  implying  $f_i(\epsilon) \neq \emptyset$ .

Assume that  $f_i(\epsilon) \neq \emptyset$ . If  $i = r$ , then  $\epsilon_r = +$  and  $f_r$  acts on  $\epsilon$  by replacing  $\epsilon_r$  with a  $-$ . This implies that  $\Psi(f_r(\epsilon))$  can be obtained from  $\Psi(\epsilon)$  by changing the  $r$  to  $\bar{r}$ , which agrees with the action of  $f_r$ . Therefore  $\Psi(f_r(\epsilon)) = f_r(\Psi(\epsilon))$ . If  $i \neq r$ , then  $\epsilon_i$  must be a  $+$  and  $\epsilon_{i+1}$  must be a  $-$ . Thus,  $f_i$  swaps the signs of  $\epsilon_i$  and  $\epsilon_{i+1}$ . Since  $\epsilon_i = +$  and  $\epsilon_{i+1} = -$ ,  $\Psi(\epsilon)$  must contain both an  $\bar{i+1}$  and an  $i$ . This implies  $\Psi(f_i(\epsilon))$  can be obtained from  $\Psi(\epsilon)$  by replacing the  $\bar{i+1}$  with  $\bar{i}$  and the  $i$  with  $i+1$ . Observe that  $f_i$  acts on  $\Psi(\epsilon)$  in exactly the same manner. Hence,  $\Psi(f_i(\epsilon)) = f_i(\Psi(\epsilon))$ .  $\square$

**Proposition III.9.**  $\mathcal{V}$  is a virtual crystal for the embedding of Lie algebras  $B_r \hookrightarrow C_r$ .

*Proof.* The ambient crystal  $\widehat{\mathcal{V}}$  is a crystal coming from a representation (see for example [4]), ensuring **V1**. Using Lemmas III.5 and III.8, we have  $\Psi(\mathcal{B}_{\text{spin}}) = \mathcal{V}$  is closed under the crystal operators  $f_i$  and  $e_i$ . Since the elements in both  $\mathcal{B}_{\text{spin}}$  and  $\widehat{\mathcal{V}}$  satisfy (32), the string lengths of  $\mathcal{B}_{\text{spin}}$  are the same as the string lengths in  $\mathcal{V}$ , showing **V3**. It is also not hard to see from Definition III.4, that  $\widehat{\varphi}_i(v), \widehat{e}_i(v) \in 2\mathbb{Z}$  for  $v \in \mathcal{V}$  and  $1 \leq i < r$ , proving **V2**.  $\square$

An example of the virtual crystal construction for  $\mathcal{B}_{\text{spin}}$  is given in Figure 15. The virtual crystal of this section also follows from [18]. An affine version of this virtual crystal construction (which implies the one in this section) has appeared in [10, Lemma 4.2].

*Virtual crystal  $B_r \hookrightarrow C_r$  vector to vector*

The crystal  $\mathcal{B}_{\square}$  of Definition III.2 can be realized as a virtual crystal inside the ambient crystal  $\widehat{\mathcal{V}} = \mathcal{C}_{\square}^{\otimes 2}$ .

**Definition III.10.** Define  $\mathcal{V} \subseteq \widehat{\mathcal{V}} = \mathcal{C}_{\square}^{\otimes 2}$  of type  $C_r$  as

$$\mathcal{V} = \{a \otimes a \mid 1 \leq a \leq r\} \cup \{\bar{a} \otimes \bar{a} \mid 1 \leq a \leq r\} \cup \{r \otimes \bar{r}\}$$

with  $f_i = \widehat{f}_i^2, e_i = \widehat{e}_i^2$  for  $1 \leq i < r$  and  $f_r = \widehat{f}_r, e_r = \widehat{e}_r$ .

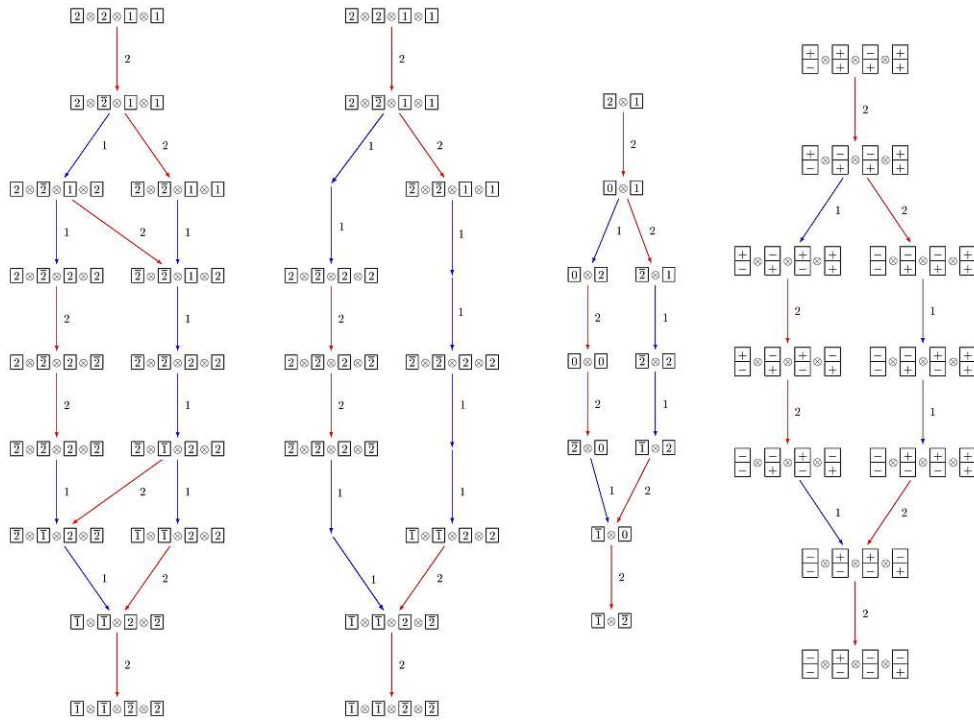


Figure 17: Far Left: One connected component  $\widehat{\mathcal{S}}$  of the crystal  $\widehat{\mathcal{V}}^{\otimes 2} = (\mathcal{C}_{\square}^{\otimes 2})^{\otimes 2}$  of type  $C_2$ . Middle Left: The connected component  $\mathcal{S}$  of the virtual crystal  $\mathcal{V}^{\otimes 2}$  inside  $\widehat{\mathcal{S}}$  induced by Definition III.10. Middle Right: The corresponding connected component  $\mathcal{T}$  of the crystal  $\mathcal{B}_{\square}^{\otimes 2}$  of type  $B_2$  that corresponds to  $\mathcal{S}$  under the embedding given in Definition III.12. Far Right: The connected component  $\mathcal{U}$  of  $(\mathcal{B}_{\text{spin}} \otimes \mathcal{B}_{\text{spin}})^{\otimes 2}$  of type  $B_2$  corresponding to  $\mathcal{T}$  under the isomorphism given in Figure 18.

**Lemma III.11.**  $\mathcal{V} \sqcup \{\emptyset\}$  of Definition III.10 is closed under the operators  $f_i$  and  $e_i$  for  $1 \leq i \leq r$  and all elements in  $\mathcal{V}$  are in the connected component of  $\widehat{\mathcal{V}}$  with highest weight  $1 \otimes 1$ .

*Proof.* We leave this to the reader to check. □

**Definition III.12.** Let  $\Psi: \mathcal{B}_{\square} \rightarrow \mathcal{V}$  be the map  $\Psi(a) = a \otimes a$  and  $\Psi(\bar{a}) = \bar{a} \otimes \bar{a}$  for  $1 \leq a \leq r$  and  $\Psi(0) = r \otimes \bar{r}$ .

**Lemma III.13.** The map  $\Psi$  of Definition III.12 is a bijective map that intertwines the crystal operators on  $\mathcal{B}_{\square}$  and  $\mathcal{V}$ .

*Proof.* We leave this to the reader to check. □

**Proposition III.14.**  $\mathcal{V}$  of Definition III.10 is a virtual crystal for the embedding of Lie algebras  $B_r \hookrightarrow C_r$ .

*Proof.* We leave this to the reader to check. □

An example of the virtual crystal construction for  $\mathcal{B}_{\square}$  is given in Figure 17. The virtual crystal of this section also follows from [18]. An affine version of this virtual crystal construction (which implies the one in this section) has appeared in [10, Theorem 4.8].

### III.2.3 Highest weights of weight zero

A weight  $\lambda \in \Lambda$  is called *minuscule* if  $\langle \lambda, \alpha^\vee \rangle \in \{0, \pm 1\}$  for all coroots  $\alpha^\vee$ . A crystal  $\mathcal{B}$  is called *minuscule* if  $\text{wt}(b)$  is minuscule for all  $b \in \mathcal{B}$ . Note that  $\mathcal{B}_{\text{spin}}$  is a minuscule crystal (see for example [4, Chapter 5.4]).

A weight  $\lambda$  is called *dominant* if  $\langle \lambda, \alpha_i^\vee \rangle \geq 0$  for all  $i \in I$ . Let  $\Lambda^+ \subseteq \Lambda$  denote the set of all dominant weights. Except for spin weights, dominant weights can be identified with partitions, where the fundamental weight  $\omega_h$  corresponds to a column of height  $h$  in the partition. A *partition*  $\lambda$  is a sequence  $\lambda = (\lambda_1, \lambda_2, \dots, \lambda_\ell)$  such that  $\lambda_1 \geq \lambda_2 \geq \dots \geq \lambda_\ell \geq 0$ . We identify partitions that differ by trailing zeroes. That is,  $(3, 2, 0, 0)$  is identified with the partition  $(3, 2)$ .

Let  $\mathcal{B}_1, \mathcal{B}_2, \dots, \mathcal{B}_n$  be minuscule crystals. For any highest weight element

$$u = u_n \otimes \dots \otimes u_1 \in \mathcal{B}_n \otimes \dots \otimes \mathcal{B}_1$$

we may bijectively associate a sequence of dominant weights  $\emptyset = \mu^0, \mu^1, \dots, \mu^n$ , where  $\mu^q := \sum_{i=1}^q \text{wt}(u_i)$ . The final weight  $\mu := \mu^n$  of such a sequence is also the weight of the crystal element  $u$ . If  $\mu$  is zero,  $u$  is a *highest weight element of weight zero*.

Note that the number of highest weight elements of weight zero in a tensor product of crystals is equal to the dimension of the invariant subspace, see for example [43, 30].

#### Oscillating tableaux

Oscillating tableaux were introduced by Sundaram [40].

**Definition III.15** (Sundaram [40]). An  *$r$ -symplectic oscillating tableau*  $\mathcal{O}$  of length  $n$  and shape  $\mu$  is a sequence of partitions

$$\mathcal{O} = (\emptyset = \mu^0, \mu^1, \dots, \mu^n = \mu)$$

such that the Ferrers diagrams of two consecutive partitions differ by exactly one cell, and each partition  $\mu^i$  has at most  $r$  nonzero parts.

The  $r$ -symplectic oscillating tableaux of length  $n$  and shape  $\mu$  are in bijection with highest weight elements in  $\mathcal{C}_{\square}^{\otimes n}$  of type  $C_r$  and weight  $\mu$ . This can be seen by induction on  $n$ . For  $n = 1$ , the only highest weight element is 1 and the only oscillating tableau is  $(\emptyset, \square)$ . Suppose the claim is true for  $n - 1$ . If  $u = b \otimes u_0 \in \mathcal{C}_{\square}^{\otimes n}$  is highest weight, then  $u_0 \in \mathcal{C}_{\square}^{\otimes(n-1)}$  must be highest weight and hence by induction corresponds to an oscillating tableau  $(\emptyset = \mu^0, \mu^1, \dots, \mu^{n-1})$ . The element  $b$  is either an unbarred or barred letter. If  $b$  is the unbarred letter  $a$ ,  $\mu^n$  differs from  $\mu^{n-1}$  by a box in row  $a$ . If  $b$  is the barred letter  $\bar{a}$ ,  $\mu^n$  has one less box in row  $a$  than  $\mu^{n-1}$ . More precisely, for a highest weight element  $b_n \otimes \dots \otimes b_1 \in \mathcal{C}_{\square}^{\otimes n}$ , the corresponding oscillating tableau satisfies  $\mu^q = \sum_{i=1}^q \text{wt}(b_i)$ . This map can be reversed and it is not hard to see that the result is a highest weight element using the tensor product rule.

#### $r$ -fans of Dyck paths

Next we relate highest weight elements of weight zero in  $\mathcal{B}_{\text{spin}}^{\otimes n}$  of type  $B_r$  and  $r$ -fans of Dyck paths. A *Dyck path* of length  $n$  is a path from  $(0, 0)$  to  $(n, 0)$  consisting of up-steps  $(1, 1)$  and down-steps  $(1, -1)$  which never crosses the line  $y = 0$ .

**Definition III.16.** An *r-fan of Dyck paths*  $F$  of length  $n$  is a sequence

$$F = (\emptyset = \mu^0, \mu^1, \dots, \mu^n = \emptyset)$$

of partitions  $\mu^i$  with at most  $r$  parts such that the Ferrers diagram of two consecutive partitions differs by exactly one cell in each part. In other words,  $\mu^i$  differs from  $\mu^{i+1}$  by  $(\pm 1, \pm 1, \dots, \pm 1)$  for  $0 \leq i < n$ .

**Example III.17.** For  $r = 3$  and  $n = 4$ , the following is a 3-fan of Dyck paths

$$F = ((000), (111), (220), (111), (000)).$$

Since  $\mathcal{B}_{\text{spin}}$  of type  $B_r$  is minuscule, by the above discussion  $\epsilon = \epsilon_n \otimes \dots \otimes \epsilon_1 \in \mathcal{B}_{\text{spin}}^{\otimes n}$  is highest weight if and only if  $\sum_{i=1}^q \text{wt}(\epsilon_i)$  is dominant for all  $1 \leq q \leq n$ . Hence highest weight elements of weight zero can be identified with an  $r$ -fan of Dyck paths of length  $n$ : the  $j$ -th entry of  $\epsilon_i$  is  $+$  if and only if the  $j$ -th Dyck path has an up-step at position  $i$ . In particular, for a highest weight element  $\epsilon$  of weight zero, the sequence of dominant weights  $\mu^q := \sum_{i=1}^q 2\text{wt}(\epsilon_i)$  for  $0 \leq q \leq n$  defines an  $r$ -fan of Dyck paths consistent with Definition III.16.

A similar bijection was given in [25].

**Example III.18.** The 3-fan of Dyck paths of Example III.17 corresponds to the element

$$\epsilon = (-, -, -) \otimes (-, -, +) \otimes (+, +, -) \otimes (+, +, +) \in \mathcal{B}_{\text{spin}}^{\otimes 4}.$$

Following Definition III.7, we obtain an embedding from the set of  $r$ -fans of Dyck paths into the set of oscillating tableaux.

**Definition III.19.** For an  $r$ -fan of Dyck paths  $F = (\emptyset = \lambda^0, \lambda^1, \dots, \lambda^n = \emptyset)$  we define the oscillating tableau  $\iota_{F \rightarrow \mathcal{O}}(F) = (\emptyset = \mu^0, \dots, \mu^n = \emptyset)$  as follows. Let  $v^t = \Psi(\lambda^t - \lambda^{t-1})$  for  $1 \leq t \leq n$  with  $\Psi$  as in Definition III.7. Then

$$\mu^{tr+s} = \lambda^t + \sum_{i=1}^s \text{wt}(v_i^{t+1}) \quad \text{for } 0 \leq t < n, 0 \leq s < r.$$

*Vacillating tableaux*

Next we define *vacillating tableaux* which correspond to highest weight elements in  $\mathcal{B}_{\square}^{\otimes n}$  of type  $B_r$ .

**Definition III.20.** A  $(2r + 1)$ -orthogonal *vacillating tableau* of length  $n$  is a sequence of partitions  $V = (\emptyset = \lambda^0, \dots, \lambda^n)$  such that:

- (i)  $\lambda^i$  has at most  $r$  parts.
- (ii) Two consecutive partitions either differ by a box or are equal.
- (iii) If two consecutive partitions are equal, then all their  $r$  parts are greater than 0.

We call  $\lambda^n$  the *weight* of  $V$ .



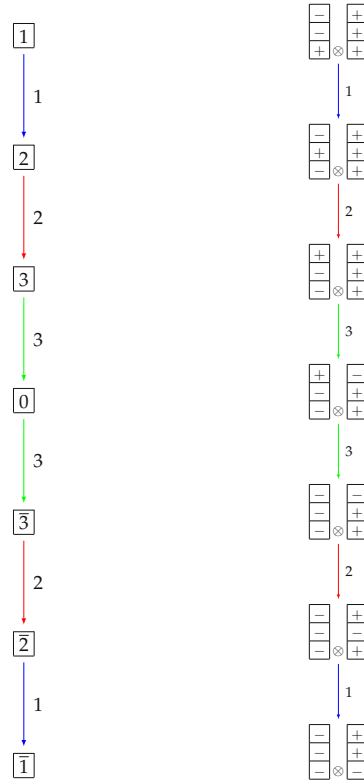


Figure 18: Left:  $\mathcal{B}_\square$  of type  $B_3$ , Right: The component in  $\mathcal{B}_{\text{spin}} \otimes \mathcal{B}_{\text{spin}}$  of type  $B_3$  isomorphic to  $\mathcal{B}_\square$ .

A highest weight element  $u = u_n \otimes \cdots \otimes u_1 \in \mathcal{B}_\square^{\otimes n}$  of type  $B_r$  corresponds to the  $(2r + 1)$ -vacillating tableau  $(\emptyset = \lambda^0, \lambda^1, \dots, \lambda^n)$ , where  $\lambda^q = \sum_{i=1}^q \text{wt}(u_i)$ .

Note that  $\mathcal{B}_\square$  is not minuscule. The crystal  $\mathcal{B}_\square$  is isomorphic to the component with highest weight element  $(+, -, \dots, -) \otimes (+, \dots, +)$  in  $\mathcal{B}_{\text{spin}} \otimes \mathcal{B}_{\text{spin}}$ , see Figure 18. From this we obtain a map from the set of vacillating tableaux of weight zero and length  $n$  into the set of fans of Dyck paths of length  $2n$  that we now explain. Denote by  $\mathbf{1}$  the vector  $\mathbf{e}_1 + \mathbf{e}_2 + \cdots + \mathbf{e}_r$  and write  $\rho < \nu$  if  $\nu = \rho + \mathbf{e}_i$  for some  $i$ .

**Definition III.21.** For a vacillating tableau of weight zero  $V = (\emptyset = \lambda^0, \dots, \lambda^n = \emptyset)$  we define the fan of Dyck paths  $\iota_{V \rightarrow F}(V) = (\emptyset = \mu^0, \dots, \mu^{2n} = \emptyset)$  as follows:

$$\mu^{2i} = 2 \cdot \lambda^i$$

$$\mu^{2i-1} = \begin{cases} 2 \cdot \lambda^{i-1} + \mathbf{1} & \text{if } \lambda^{i-1} < \lambda^i, \\ 2 \cdot \lambda^i + \mathbf{1} & \text{if } \lambda^{i-1} > \lambda^i, \\ 2 \cdot \lambda^{i-1} + \mathbf{1} - 2\mathbf{e}_r & \text{if } \lambda^{i-1} = \lambda^i. \end{cases}$$

Similarly, following Definition III.12, we obtain an embedding from the set of vacillating tableaux of weight zero into the set of oscillating tableaux.

**Definition III.22.** For a vacillating tableau of weight zero  $V = (\emptyset = \lambda^0, \dots, \lambda^n = \emptyset)$  we define the oscillating tableau  $\iota_{V \rightarrow O}(V) = (\emptyset = \mu^0, \dots, \mu^{2n} = \emptyset)$  as follows:

$$\begin{aligned} \mu^{2i} &= 2 \cdot \lambda^i \\ \mu^{2i-1} &= \lambda^{i-1} + \lambda^i + \begin{cases} 0 & \text{if } \lambda^{i-1} \neq \lambda^i, \\ -\mathbf{e}_r & \text{if } \lambda^{i-1} = \lambda^i. \end{cases} \end{aligned}$$

### III.2.4 Promotion via crystal commutator

For finite crystals  $B_\lambda$  of classical type of highest weight  $\lambda$ , Henriques and Kamnitzer [12] introduced the crystal commutator as follows. Let  $\eta_{B_\lambda}: B_\lambda \rightarrow B_\lambda$  be the Lusztig involution, which maps the highest weight vector to the lowest weight vector and interchanges the crystal operators  $f_i$  with  $e_{i'}$ , where  $w_0(\alpha_i) = -\alpha_{i'}$  under the longest element  $w_0$ . This can be extended to tensor products of such crystals by mapping each connected component to itself using the above. Then the *crystal commutator* is defined as

$$\begin{aligned} \sigma: B_\lambda \otimes B_\mu &\rightarrow B_\mu \otimes B_\lambda \\ b \otimes c &\mapsto \eta_{B_\mu \otimes B_\lambda}(\eta_{B_\mu}(c) \otimes \eta_{B_\lambda}(b)). \end{aligned}$$

If we want to emphasize the crystals involved, we write  $\sigma_{A,B}: A \otimes B \rightarrow B \otimes A$ .

Following [8, 43, 44], we define the promotion operator using the crystal commutator.

**Definition III.23.** Let  $C$  be a crystal and  $u \in C^{\otimes n}$  a highest weight element. Then *promotion*  $\text{pr}$  on  $u$  is defined as  $\sigma_{C^{\otimes n-1}, C}(u)$ .

**Remark III.24.** Note that inverse promotion is given by  $\sigma_{C, C^{\otimes n-1}}(u)$ . The conventions in the literature about what is called promotion and what is called inverse promotion are not always consistent. Our convention here agrees with the definition of promotion on posets that removes the letters  $\mathbf{1}$  and slides letters (see for example [38, 2]). The convention here is the opposite of the convention on tableaux which removes the largest letter and uses jeu de taquin slides (see for example [32, 3]).

**Example III.25.** Consider the crystal  $C = B_\square$  of type  $A_2$  (see [4]). Then

$$u = 1 \otimes 3 \otimes 2 \otimes 2 \otimes 1 \otimes 1 \in C^{\otimes 6}$$

is highest weight and

$$\sigma_{C^{\otimes 5}, C}(u) = 2 \otimes 1 \otimes 3 \otimes 1 \otimes 2 \otimes 1.$$

The recording tableaux for the RSK insertion of the words 132211 and 213121 (from right to left) are

$$\begin{array}{|c|c|c|} \hline 1 & 2 & 6 \\ \hline 3 & 4 & \\ \hline 5 & & \\ \hline \end{array} \quad \text{and} \quad \begin{array}{|c|c|c|} \hline 1 & 3 & 5 \\ \hline 2 & 6 & \\ \hline 4 & & \\ \hline \end{array}$$

which are related by the usual (inverse) promotion operator (removing the letter  $\mathbf{1}$ , doing jeu-de-taquin slides, filling the empty cell with the largest letter plus one and subtracting  $\mathbf{1}$  from all entries) on standard tableaux.

**Example III.26.** Promotion on the element  $\epsilon$  in Example III.18 is

$$\sigma_{\mathcal{B}_{\text{spin}}^{\otimes 3}, \mathcal{B}_{\text{spin}}}(\epsilon) = (-, -, -) \otimes (-, +, +) \otimes (+, -, -) \otimes (+, +, +).$$

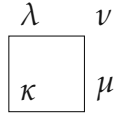
Note that if  $\Psi: C \rightarrow \mathcal{V} \subseteq \widehat{\mathcal{V}}$  is a virtual embedding, then virtualization intertwines with promotion

$$\Psi \circ \sigma_{C^{\otimes n-1}, C} = \sigma_{\widehat{\mathcal{V}}^{\otimes n-1}, \widehat{\mathcal{V}}} \circ \Psi \quad (33)$$

by Axioms V2 and V3 in Definition III.3 as long as the folding  $\sigma$  and the multiplication factors  $\gamma_i$  respect the map  $w_0(\alpha_i) = -\alpha_i$ . This is the case for the virtualizations in this paper.

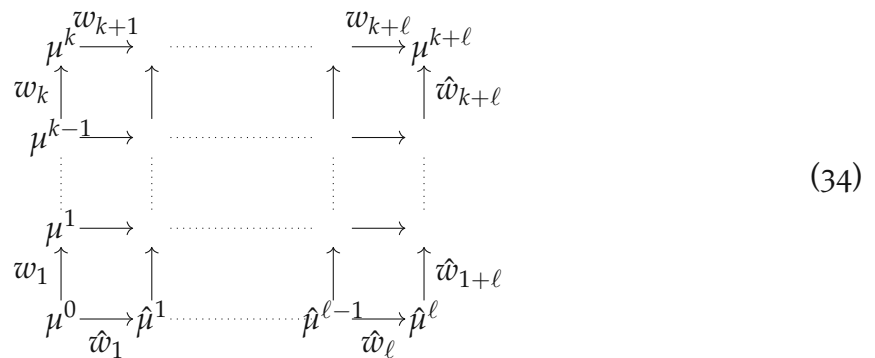
### III.2.5 Promotion via local rules

Adapting local rules of van Leeuwen [41], Lenart [23] gave a combinatorial realization of the crystal commutator  $\sigma_{A,B}$  by constructing an equivalent bijection between the highest weight elements of  $A \otimes B$  and  $B \otimes A$  respectively. The *local rules* of Lenart [23] can be stated as follows: four weight vectors  $\lambda, \mu, \kappa, \nu \in \Lambda$  depicted in a square diagram



satisfy the local rule, if  $\mu = \text{dom}_W(\kappa + \nu - \lambda)$ , where  $W$  is the Weyl group of the root system  $\Phi$  underlying  $A$  and  $B$ . Furthermore,  $\text{dom}_W(\rho)$  is the dominant weight in the Weyl orbit of  $\rho$ .

**Theorem III.27** ([23, Theorem 4.4]). *Let  $A$  and  $B$  be crystals embedded into tensor products  $A_\ell \otimes \dots \otimes A_1$  and  $B_k \otimes \dots \otimes B_1$  of crystals of minuscule representations, respectively. Let  $w = w_{k+\ell} \otimes \dots \otimes w_1$  be a highest weight element in  $A \otimes B$  with corresponding tableau ( $\mathcal{O} = \mu^0, \mu^1, \dots, \mu^{k+\ell} = \mu$ ) Then  $\sigma_{A,B}(w)$  can be computed as follows. Create a  $k \times \ell$  grid of squares as in (34), labelling the edges along the left border with  $w_1, \dots, w_k$  and the edges along the top border with  $w_{k+1}, \dots, w_{k+\ell}$ :*



For each square use the local rule to compute the weight vectors on the square's corners. Given a horizontal edge from  $\kappa$  to  $\mu$  in the  $j$ th column, label the edge by the element in  $A_j$  with weight  $\mu - \kappa$ . Similarly, given a vertical edge from  $\mu$  to  $\nu$  in the  $i$ th row, label the edge by the element in  $B_i$  with weight  $\nu - \mu$ . The labels  $\hat{w}_{k+\ell} \dots \hat{w}_1$  of the edges along the right and the bottom border of the grid then form  $\sigma_{A,B}(w)$  with corresponding tableau ( $\mathcal{O} = \mu^0, \hat{\mu}^1, \dots, \hat{\mu}^{k+\ell-1}, \mu^{k+\ell} = \mu$ ).

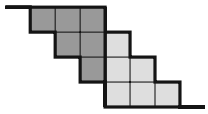
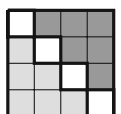
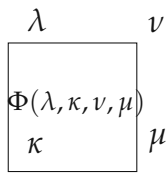
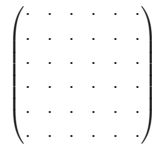
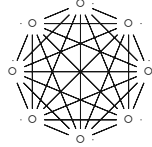
<p>1. Calculate promotion over and over again using a calculation schema</p>	<p>2. Cut and glue the schema to obtain a square</p>	<p>3. Fill all cells according to a function <math>\Phi</math> with integers</p>	<p>4. Interpret the filled square as adjacency matrix of a graph</p>	<p>5. Read the chord diagram from the adjacency matrix.</p>
				

Figure 19: Overview of the steps in our map

**Example III.28.** Performing Lenart’s local rules on the elements in Example III.25 gives

$$\begin{array}{ccccccccc}
 (1, 0, 0) & \xrightarrow{1} & (2, 0, 0) & \xrightarrow{2} & (2, 1, 0) & \xrightarrow{2} & (2, 2, 0) & \xrightarrow{3} & (2, 2, 1) & \xrightarrow{1} & (3, 2, 1) \\
 \uparrow 1 & & \uparrow 1 & & \uparrow 1 & & \uparrow 2 & & \uparrow 2 & & \uparrow 2 \\
 (0, 0, 0) & \xrightarrow{1} & (1, 0, 0) & \xrightarrow{2} & (1, 1, 0) & \xrightarrow{1} & (2, 1, 0) & \xrightarrow{3} & (2, 1, 1) & \xrightarrow{1} & (3, 1, 1)
 \end{array}$$

which recovers  $\sigma_{C^{\otimes 5}, C}(1 \otimes 3 \otimes 2 \otimes 2 \otimes 1 \otimes 1) = 2 \otimes 1 \otimes 3 \otimes 1 \otimes 2 \otimes 1$ .

### III.3 CHORD DIAGRAMS

#### III.3.1 Promotion matrices

In this section we describe a map from highest weight words of weight zero to chord diagrams that intertwines promotion and rotation.

We start with the definition of chord diagrams and their rotation.

**Definition III.29.** A *chord diagram* of size  $n$  is a graph with  $n$  vertices depicted on a circle which are labelled  $1, \dots, n$  in counter-clockwise orientation.

The *rotation* of a chord diagram is obtained by rotating all edges clockwise by  $\frac{2\pi}{n}$  around the center of the diagram.

In our setting all chord diagrams are undirected graphs with possibly multiple edges between the same two vertices. We can therefore identify chord diagrams with their *adjacency matrix*. The adjacency matrix is a symmetric  $n \times n$  matrix  $M = (m_{ij})_{1 \leq i, j \leq n}$  with non-negative integer entries and  $m_{ij}$  denotes the number of edges between vertex  $i$  and vertex  $j$ .

**Proposition III.30.** Let  $M$  be the adjacency matrix of a chord diagram  $G$ . Denote by  $\text{rot } M$  the toroidal shift of  $M$ , that is, the matrix obtained from  $M$  by first cutting the top row and pasting it to the bottom and then cutting the leftmost column and pasting it to the right.

Then  $\text{rot } M$  is the adjacency matrix corresponding to the rotation of  $G$ .

The proof of this proposition is easy and left to the reader as an exercise.

Let us now outline the idea to construct such a rotation and promotion intertwining map and then provide the details on the individual steps on the examples of oscillating tableaux,  $r$ -fans of Dyck paths and vacillating tableaux. A visual guideline can be seen in Figure 19.

**Construction III.31.** The construction is given as follows:

**STEP 1** Iteratively calculate promotion of a highest weight word of weight zero and length  $n$  using Lenart's schema (34) a total of  $n$  times.

**STEP 2** Group the results into a square grid, called the *promotion matrix*.

**STEP 3** Fill the cells of the square grid with certain non-negative integers according to a filling rule  $\Phi$  that only depends on the four corners of the cells in the schema (34).

**STEP 4** Regard the filling as the adjacency matrix of a graph, which is the chord diagram.

We now discuss the filling rules in the various cases. Note that the filling rules are new even in the case of oscillating tableaux as the proofs in [30] did not follow this construction.

### Chord diagrams for oscillating tableaux

Recall that the Weyl group of type  $C_r$  is the hyperoctahedral group  $\mathfrak{S}_r$  of signed permutations of  $\{\pm 1, \pm 2, \dots, \pm r\}$ . Weights are elements in  $\mathbb{Z}^r$  and dominant weights are weakly decreasing integer vectors with non-negative entries (or equivalently partitions). Thus, the dominant representative  $\text{dom}_{\mathfrak{S}_r}(\lambda)$  of a weight  $\lambda$  is obtained by sorting the absolute values of its entries into weakly decreasing order.

We slightly modify Lenart's schema for the crystal commutor (34) by omitting edge labels as only the weights on the corners are needed. Additionally, given an oscillating tableau  $O = (\emptyset = \mu^0, \mu^1, \dots, \mu^n = \mu)$ , we start each row with the zero weight  $\emptyset$  and end each row with the weight  $\mu$ , which makes it easier to iteratively use this schema to calculate promotion. This way the promotion of the oscillating tableau  $O = (\emptyset = \mu^0, \mu^1, \dots, \mu^n = \mu)$  is the unique sequence  $(\emptyset = \hat{\mu}^0, \hat{\mu}^1, \dots, \hat{\mu}^n = \mu)$ , such that all squares in the diagram



satisfy the local rule of Section III.2.5.

Using this schema we iteratively calculate promotion a total of  $n$  times and depict the results in a diagram as seen in Figure 20 on the left. This diagram consists of  $n$  promotion schemas glued together. As  $\text{pr}^n = \text{id}$ , the labels on the top and the bottom row must be equal to  $\mu^0, \dots, \mu^n$ .

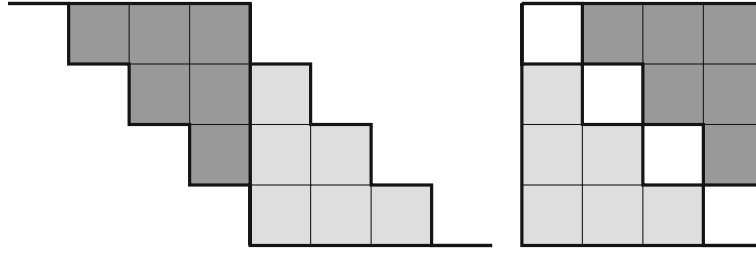


Figure 20: The transformation into a promotion matrix. The highlighted part is cut away and glued on the left.

We now transform this diagram by copying everything to the right of the  $n$ -th column into the triangular empty space on the left, see Figure 20. In this way the labels on the right corners of the  $n$ -th column are duplicated. We obtain an  $n \times n$  grid, where each corner of a cell is labelled with a dominant weight and the labels on the top and bottom border are equal and the labels on the left and right border are equal. This grid is called the *promotion matrix* of  $O$ .

To obtain an adjacency matrix, we fill the cells of this diagram with non-negative integers according to the following rule.

**Definition III.32.** The *filling rule* for oscillating tableaux is

$$\Phi(\lambda, \kappa, \nu, \mu) = \begin{cases} 1 & \text{if } \kappa + \nu - \lambda \text{ contains a negative entry,} \\ 0 & \text{else,} \end{cases} \quad (35)$$

where the cells are labelled as depicted below:

$$\begin{array}{|c|c|} \hline \lambda & \nu \\ \hline \Phi(\lambda, \kappa, \nu, \mu) & \\ \hline \kappa & \mu \\ \hline \end{array} . \quad (36)$$

**Definition III.33.** Denote by  $M_O$  the function that maps an  $r$ -symplectic oscillating tableau of length  $n$  to an  $n \times n$  adjacency matrix using Construction III.31 and the filling rule (35).

Next, we generalize the above construction for  $r$ -fans of Dyck paths and vacillating tableaux.

#### *Chord diagrams for $r$ -fans of Dyck paths*

Given an  $r$ -fan of Dyck paths  $F = (\emptyset = \mu^0, \mu^1, \dots, \mu^n = \emptyset)$ , we construct an adjacency matrix via Construction III.31 using the following filling rule:

**Definition III.34.** The *filling rule* for fans of Dyck paths is

$$\Phi(\lambda, \kappa, \nu, \mu) = \text{number of negative entries in } \kappa + \nu - \lambda, \quad (37)$$

where the cells are labelled as in (36).

**Remark III.35.** Note that for oscillating tableaux at most one negative entry can occur. Thus the filling rule (37) for fans of Dyck paths is a natural generalization of the rule (35).

**Definition III.36.** Denote by  $M_F$  the function that maps an  $r$ -fan of Dyck paths of length  $n$  to an  $n \times n$  adjacency matrix using Construction III.31 and the filling rule (37).

**Example III.37.** Consider the following fan corresponding to the sequence of vectors  $F = (000, 111, 222, 311, 422, 331, 222, 111, 000)$ .

1. We apply promotion a total of  $n = 8$  times, to obtain the full orbit.

```

000 111 222 311 422 331 222 111 000
000 111 200 311 220 111 000 111 000
000 111 222 311 220 111 222 111 000
000 111 200 111 200 311 200 111 000
000 111 220 311 422 311 222 111 000
000 111 220 331 220 311 200 111 000
000 111 222 111 220 111 220 111 000
000 111 000 111 200 311 220 111 000
000 111 222 311 422 331 222 111 000
  
```

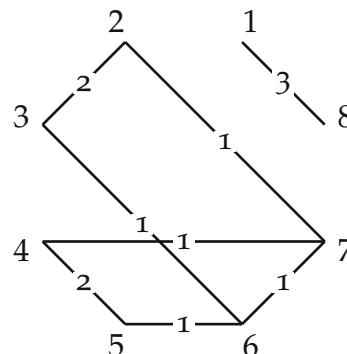
2. We group the results into the promotion matrix and fill the cells of the square grid according to  $\Phi$ . For better readability we omitted zeros.

```

000 111 222 311 422 331 222 111 000
111 000 111 200 311 220 111 000 111
222 111 000 111 222 311 220 111 222
311 200 111 000 111 200 111 200 311
422 311 222 111 000 111 220 311 422
331 220 311 200 111 000 111 220 331
222 111 220 111 220 111 000 111 222
111 000 111 200 311 220 111 000 111
000 111 222 311 422 331 222 111 000
  
```

3. Regard the filling as the adjacency matrix of a graph, the chord diagram.

$$M_F(F) = \begin{pmatrix} 0 & 0 & 0 & 0 & 0 & 0 & 0 & 0 & 3 \\ 0 & 0 & 2 & 0 & 0 & 0 & 1 & 0 & 0 \\ 0 & 2 & 0 & 0 & 0 & 1 & 0 & 0 & 0 \\ 0 & 0 & 0 & 0 & 2 & 0 & 1 & 0 & 0 \\ 0 & 0 & 0 & 2 & 0 & 1 & 0 & 0 & 0 \\ 0 & 0 & 1 & 0 & 1 & 0 & 1 & 0 & 0 \\ 0 & 1 & 0 & 1 & 0 & 1 & 0 & 0 & 0 \\ 3 & 0 & 0 & 0 & 0 & 0 & 0 & 0 & 0 \end{pmatrix}$$



Chord diagrams for vacillating tableaux

Note that  $\mathcal{B}_\square$  is not minuscule and thus Theorem III.27 is not directly applicable. Using Definition III.12 we can embed  $\mathcal{B}_\square$  in  $\mathcal{C}_\square^{\otimes 2}$  which gives a map  $\iota_{V \rightarrow O}$  from vacillating tableaux to oscillating tableaux of twice the length which commutes with the crystal commutor. That is

$$\iota_{V \rightarrow O} \circ \text{pr}_{\mathcal{B}_\square} = \iota_{V \rightarrow O} \circ \sigma_{\mathcal{B}_\square^{\otimes n-1}, \mathcal{B}_\square} = \sigma_{(\mathcal{C}_\square^{\otimes 2})^{\otimes n-1}, \mathcal{C}_\square^{\otimes 2}} \circ \iota_{V \rightarrow O}. \tag{38}$$

This follows directly from the properties of virtualization.

Let  $V$  be a vacillating tableau of length  $n$  and weight zero. Let  $O = (\emptyset = \mu^0, \mu^1, \dots, \mu^{2n} = \emptyset)$  be the corresponding oscillating tableau using  $\iota_{V \rightarrow O}$ . Then we obtain the promotion of  $V$  using the following schema

$$\begin{array}{cccccccccccc}
 \mu^0 & & \mu^1 & & \mu^2 & & \mu^3 & \dots & \mu^{2n-1} & & \mu^{2n} \\
 & & \boxed{\phantom{\mu^1}} & & \boxed{\phantom{\mu^1}} & & \dots & & \boxed{\phantom{\mu^{2n-1}}} & & \boxed{\phantom{\mu^{2n-1}}} \\
 & & \mu^1 & & \dots & & \dots & & \mu^{2n-1} & & \\
 \hat{\mu}^0 & & \boxed{\phantom{\hat{\mu}^0}} & & \boxed{\phantom{\hat{\mu}^0}} & & \dots & & \boxed{\phantom{\hat{\mu}^{2n-3}}} & & \boxed{\phantom{\hat{\mu}^{2n-3}}} \\
 & & \hat{\mu}^1 & & \dots & & \dots & & \hat{\mu}^{2n-2} & & \hat{\mu}^{2n-1} & & \hat{\mu}^{2n}
 \end{array} \tag{39}$$

Following Construction III.31, we apply promotion a total of  $n$  times and use the cut-and-glue procedure to obtain a  $2n \times 2n$  square. We fill the squares using the filling rule for oscillating tableaux as given by (35).

To obtain an  $n \times n$  adjacency matrix, we subdivide the  $2n \times 2n$  matrix into  $2 \times 2$  blocks and take the sum of each block.

**Definition III.38.** Denote by  $M_{V \rightarrow O}$  the function that maps a vacillating tableau  $V$  of weight zero of length  $n$  to an  $n \times n$  adjacency matrix using  $\iota_{V \rightarrow O}$ , Schema (39), Construction III.31, filling rule (35), and block sums.

**Example III.39.** Consider the vacillating tableau of length 9

$$V = (000, 100, 200, 210, 211, 111, 111, 110, 100, 000).$$

We first embed  $V$  into an oscillating tableau using the bijection  $\Psi$  from  $\mathcal{B}_\square$  to  $\mathcal{V}$  given in Definition III.12. Specifically, we use  $\Psi$  to establish a correspondence between the highest weight element in  $\mathcal{B}_\square^{\otimes 9}$  associated to  $V$  and a highest weight element in  $(\mathcal{C}_\square^{\otimes 2})^{\otimes 9}$ , from which we obtain  $\iota_{V \rightarrow O}(V)$  as

$$\begin{aligned}
 \iota_{V \rightarrow O}(V) = & (000, 100, 200, 300, 400, 410, 420, 421, 422, 322, 222, 221, 222, 221, 220, 210, 200, 100, 000, \\
 & 222, 221, 220, 210, 200, 100, 000).
 \end{aligned}$$

1. We apply promotion a total of  $n = 9$  times on the above schema ( $2n = 18$  times on the oscillating tableau  $\iota_{V \rightarrow O}(V)$ ), to obtain the full orbit. Below the first iteration of promotion, we show all 9 applications of promotion.

$$\begin{array}{cccccccccccccccccccc}
 000 & 100 & 200 & 300 & 400 & 410 & 420 & 421 & 422 & 322 & 222 & 221 & 222 & 221 & 220 & 210 & 200 & 100 & 000 \\
 & 100 & 200 & 300 & 310 & 320 & 321 & 322 & 222 & 221 & 220 & 221 & 220 & 221 & 211 & 210 & 110 & 100 & \\
 & 000 & 100 & 200 & 210 & 220 & 221 & 222 & 221 & 220 & 221 & 222 & 221 & 222 & 221 & 220 & 210 & 200 & 100 & 000
 \end{array}$$



```

000 100 200 300 400 410 420 421 422 322 222 221 222 221 220 210 200 100 000
 100 200 300 310 320 321 322 222 221 220 221 220 221 211 210 110 100
 000 100 200 210 220 221 222 221 220 221 222 221 222 221 220 210 200 100 000
  100 110 210 211 221 220 221 222 322 321 322 321 320 310 300 200 100
    000 100 200 210 220 221 222 322 422 421 422 421 420 410 400 300 200 100 000
      100 110 210 211 221 321 421 420 421 420 421 411 410 310 210 110 100
        000 100 200 210 220 320 420 421 422 421 422 421 420 320 220 210 200 100 000
          100 110 210 310 410 411 421 420 421 420 421 321 221 211 210 110 100
            000 100 200 300 400 410 420 421 422 421 422 322 222 221 220 210 200 100 000
              100 200 300 310 320 321 322 321 322 222 221 220 221 211 210 110 100
                000 100 200 210 220 221 222 221 222 221 220 221 222 221 220 210 200 100 000
                  100 110 210 211 221 220 221 222 322 321 320 310 300 200 100
                    000 100 200 210 220 221 222 221 222 322 422 421 420 410 400 300 200 100 000
                      100 110 210 211 221 220 221 321 421 420 421 411 410 310 210 110 100
                        000 100 200 210 220 221 222 221 222 322 422 421 420 320 220 210 200 100 000
                          100 110 210 211 221 321 421 420 421 420 421 321 221 211 210 110 100
                            000 100 200 210 220 320 420 421 422 421 422 322 222 221 220 210 200 100 000
                              100 110 210 310 410 411 421 420 421 321 221 220 221 211 210 110 100
                                000 100 200 300 400 410 420 421 422 322 222 221 222 221 220 210 200 100 000
  
```

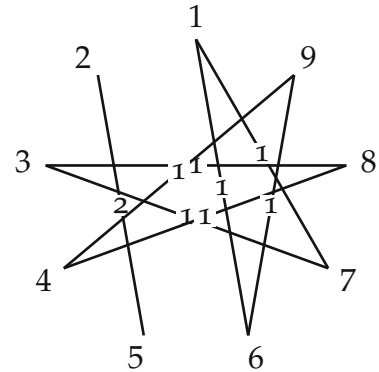
- (2) We group the results into the promotion matrix and fill the cells of the square grid according to  $\Phi$  in (35). For better readability, we subdivided the diagram into  $2 \times 2$  blocks and took the sum of the entries in each block, as well as omitted the zeros.

```

000 200 400 420 422 222 222 220 200 000
      1 1
200 000 200 220 222 220 222 222 220 200
      2
400 200 000 200 220 222 422 422 420 400
      1 1
420 220 200 000 200 220 420 422 422 420
      1 1
422 222 220 200 000 200 400 420 422 422
      2
222 220 222 220 200 000 200 220 222 222
      1 1
222 222 422 420 400 200 000 200 220 222
      1 1
220 222 422 422 420 220 200 000 200 220
      1 1
200 220 420 422 422 222 220 200 000 200
      1 1
000 200 400 420 422 222 222 220 200 000
  
```

- (2) Regard the filling as the adjacency matrix of a graph, the chord diagram.

$$M_{V \rightarrow O}(V) = \begin{pmatrix} 0 & 0 & 0 & 0 & 0 & 1 & 1 & 0 & 0 \\ 0 & 0 & 0 & 0 & 2 & 0 & 0 & 0 & 0 \\ 0 & 0 & 0 & 0 & 0 & 0 & 1 & 1 & 0 \\ 0 & 0 & 0 & 0 & 0 & 0 & 0 & 1 & 1 \\ 0 & 2 & 0 & 0 & 0 & 0 & 0 & 0 & 0 \\ 1 & 0 & 0 & 0 & 0 & 0 & 0 & 0 & 1 \\ 1 & 0 & 1 & 0 & 0 & 0 & 0 & 0 & 0 \\ 0 & 0 & 1 & 1 & 0 & 0 & 0 & 0 & 0 \\ 0 & 0 & 0 & 1 & 0 & 1 & 0 & 0 & 0 \end{pmatrix}$$



Alternatively, we may obtain an adjacency matrix by embedding  $\mathcal{B}_{\square}$  as a connected component of  $\mathcal{B}_{\text{spin}}^{\otimes 2}$  (see Section III.2.3). As discussed in Definition III.21, this embedding gives rise to the map  $\iota_{V \rightarrow F}$  from vacillating tableaux to  $r$ -fans of Dyck paths of twice the length. From the  $r$ -fans of Dyck paths, we apply  $M_F$  to obtain a  $2n \times 2n$

matrix. Subdividing this matrix into  $2 \times 2$  blocks and taking block sums produces an  $n \times n$  adjacency matrix for vacillating tableaux.

**Definition III.40.** Denote by  $M_{V \rightarrow F}$  the function that maps a vacillating tableau  $V$  of weight zero and length  $n$  to an  $n \times n$  adjacency matrix using  $\iota_{V \rightarrow F}$ , Construction III.31, filling rule (37), and block sums.

*Promotion and rotation*

For the various maps  $M_X$  with  $X \in \{O, F, V \rightarrow O, V \rightarrow F\}$  constructed in this section, we obtain the following main result.

**Proposition III.41.** *The map  $M_X$  for  $X \in \{O, F, V \rightarrow O, V \rightarrow F\}$  intertwines promotion and rotation, that is*

$$M_X \circ \text{pr} = \text{rot} \circ M_X.$$

*Proof.* Let  $T$  be either a fan of Dyck paths, an oscillating tableau of weight zero or a vacillating tableau of weight zero of length  $n$  and denote by  $\hat{T}$  its promotion.

For  $0 \leq i, j < n$  let  $\mu^{i,j}$  be the  $(j-i)$ -th entry of  $\text{pr}^i(T)$ , where indexing starts with zero and is understood modulo  $n$ . For  $1 \leq i, j \leq n$  denote by  $m_{i,j}$  the entry in the  $i$ -th row and  $j$ -th column of  $M_X(T)$ . Similarly, denote by  $\hat{\mu}^{i,j}$  the  $(j-i)$ -th entry of  $\text{pr}^i(\hat{T})$  and by  $\hat{m}_{i,j}$  the  $i$ -th row and  $j$ -th column of  $M_X(\hat{T})$ .

In all of our constructions  $m_{i,j}$  depends on the four partitions  $\mu^{i-1,j-1}$ ,  $\mu^{i,j-1}$ ,  $\mu^{i-1,j}$  and  $\mu^{i,j}$  via some function  $m_{i,j} = \tilde{\Phi}(\mu^{i-1,j-1}, \mu^{i,j-1}, \mu^{i-1,j}, \mu^{i,j})$ . Analogously we have  $\hat{m}_{i,j} = \tilde{\Phi}(\hat{\mu}^{i-1,j-1}, \hat{\mu}^{i,j-1}, \hat{\mu}^{i-1,j}, \hat{\mu}^{i,j})$ .

A simple calculation gives

$$\begin{aligned} \hat{m}_{i,j} &= \tilde{\Phi}(\hat{\mu}^{i-1,j-1}, \hat{\mu}^{i,j-1}, \hat{\mu}^{i-1,j}, \hat{\mu}^{i,j}) \\ &= \tilde{\Phi}(\mu^{i,j}, \mu^{i+1,j}, \mu^{i,j+1}, \mu^{i+1,j+1}) = m_{i+1,j+1}, \end{aligned}$$

where indices are understood modulo  $n$ . Thus,  $M_X(\hat{T}) = \text{rot}(M_X(T))$ .  $\square$

Note that the promotion matrix  $M_X(T)$  is sometimes referred to as the *promotion-evacuation diagram* of  $T$  as it also encodes information about the evacuation of  $T$ . Following [30], a generalization of Schützenberger's evacuation operator can be defined on crystals as follows.

**Definition III.42.** Let  $C$  be a crystal and  $u \in C^{\otimes n}$  a highest weight element. Then *evacuation*  $\text{evac}$  on  $u$  is defined as

$$(1_{C^{\otimes n-2}} \otimes \text{pr}) \circ \cdots \circ (1_C \otimes \text{pr}) \circ \text{pr}(u),$$

where  $(1_{C^{\otimes n-m}} \otimes \text{pr})(w_n \otimes \cdots \otimes w_2 \otimes w_1) = w_n \otimes \cdots \otimes w_{m+1} \otimes \text{pr}(w_m \otimes \cdots \otimes w_1)$ .

Given a tableau  $T$  corresponding to a highest weight element  $u$ , we denote by  $\text{evac}(T)$  the tableau associated to the highest weight element  $\text{evac}(u)$ .

**Proposition III.43.** *The map  $M_X$  for  $X \in \{O, F, V \rightarrow O, V \rightarrow F\}$  intertwines evacuation and the anti-transpose, that is*

$$M_X \circ \text{evac} = \text{antr} \circ M_X,$$

where the anti-transpose  $\text{antr}$  of a matrix is its transpose over its anti-diagonal.

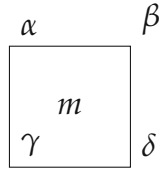


Figure 21: A cell of a growth diagram filled with a non-negative integer  $m$

*Proof.* Let  $T$  be either a fan of Dyck paths, an oscillating tableau of weight zero, or a vacillating tableau of weight zero of length  $n$ . From the definition of  $\text{evac}$  and the construction of  $M_X$ , we have that  $\text{evac}(T)$  is precisely the tableau obtained by reading the right border of  $M_X$  from bottom to top. Note that in order to prove the statement for  $M_{V \rightarrow O}$  it suffices to show it for  $M_O$  as  $\Psi$  intertwines  $\sigma_{\mathcal{B}_{\square}^{\otimes m}, \mathcal{B}_{\square}}$  and  $\sigma_{(\mathcal{C}_{\square}^{\otimes 2})^{\otimes m}, \mathcal{C}_{\square}^{\otimes 2}}$  for all  $m \geq 1$  by Equation (33), where  $\Psi$  is the virtualization map given in Definition III.12. Similarly, in order to prove the statement for  $M_{V \rightarrow F}$  it suffices to prove it for  $M_F$ .

Consider partitions  $\lambda, \kappa, \nu, \mu$  labelling the corner of a cell in  $M_X$  as in (36), where  $X \in \{O, F\}$ . By [41, Lemma 4.1.2], we have  $\mu = \text{dom}_W(\kappa + \nu - \lambda)$  if and only if  $\lambda = \text{dom}_W(\kappa + \nu - \mu)$  as  $\mathcal{B}_{\text{spin}}$  and  $\mathcal{C}_{\square}$  are minuscule. This implies that partitions labelling the corners of every cell in  $M_X \circ \text{evac}$  and  $\text{antr} \circ M_X$  are equal.

To complete the proof we show that filling rules  $\Phi(\lambda, \kappa, \nu, \mu)$  given in (35) and (37) satisfy  $\Phi(\lambda, \kappa, \nu, \mu) = \Phi(\mu, \kappa, \nu, \lambda)$ . As partitions connected by a vertical or horizontal edge in  $M_O$  differ by exactly one box, we have that  $\Phi(\lambda, \kappa, \nu, \mu) = 1$  if and only if  $\lambda = \mu = (\lambda_1, \dots, \lambda_i, 0, \dots, 0)$ ,  $\lambda_i = 1$  for some  $i$ , and  $\kappa = \nu = (\lambda_1, \dots, \lambda_{i-1}, 0, 0, \dots, 0)$ . Thus, the filling rule for oscillating tableaux satisfies  $\Phi(\lambda, \kappa, \nu, \mu) = \Phi(\mu, \kappa, \nu, \lambda)$ . By a similar argument the filling rule for fans of Dyck paths also satisfies the desired symmetry.  $\square$

### III.3.2 Fomin growth diagrams

Generally speaking, a *Fomin growth diagram* is a means to bijectively map sequences of partitions satisfying certain constraints to fillings of a Ferrers shape with non-negative integers [7, 33, 42, 21]. In this setting, we draw the Ferrers shape in French notation (to fix how the growth diagrams are arranged).

To map a filling of a Ferrers shape to a sequence of partitions we iteratively label all corners of cells of the shape with partitions by certain local rules. Given a cell, where already all three partitions on the left and bottom corners are known, the forward rules determine the fourth partition on the top right corner based on the filling of the cell. Conversely, given the three partitions on the top and right corners of a cell, the backwards rules determine the last partition and the filling of the cell. When defining the local rules we label the cells as seen in Figure 21.

For partitions  $\delta$  and  $\alpha$ , we define their union  $\delta \cup \alpha$  to be the partition containing  $\delta_i + \alpha_i$  cells in row  $i$ , where  $\delta_i$  and  $\alpha_i$  denote the number of cells in row  $i$  of  $\delta$  and  $\alpha$  respectively. Recall that we pad partitions with 0's if necessary. We denote  $\delta \cup \delta$  by  $2\delta$ . We define the intersection of two partitions  $\delta \cap \alpha$  to be the partition containing  $\min\{\delta_i, \alpha_i\}$  cells in row  $i$ .

We begin by describing the local rules for a filling of a Ferrers shape with at most one 1 in each row and in each column and 0's everywhere else (omitted for readability). Moreover, we require that any two adjacent partitions in the labelling of our growth diagram (for example,  $\gamma \rightarrow \alpha$  and  $\gamma \rightarrow \delta$  in Figure 21) must either coincide or the one at the head of the arrow is obtained from the other by adding a unit vector. We record the local forward rules and local backward rules for this case of 0/1 filling, which are stated explicitly in [21, p. 4-5].

Given a 0/1 filling of a Ferrers shape and partitions labelling the bottom and left side of the Ferrers shape, we apply the following *local forward rules* to complete the labelling.

- (F1) If  $\gamma = \delta = \alpha$ , and there is no 1 in the cell, then  $\beta = \gamma$ .
- (F2) If  $\gamma = \delta \neq \alpha$ , then  $\beta = \alpha$ .
- (F3) If  $\gamma = \alpha \neq \delta$ , then  $\beta = \delta$ .
- (F4) If  $\gamma, \delta, \alpha$  are pairwise different, then  $\beta = \delta \cup \alpha$ .
- (F5) If  $\gamma \neq \delta = \alpha$ , then  $\beta$  is formed by adding a square to the  $(k + 1)$ -st row of  $\delta = \alpha$ , given that  $\delta = \alpha$  and  $\gamma$  differ in the  $k$ -th row.
- (F6) If  $\gamma = \delta = \alpha$ , and if there is a 1 in the cell, then  $\beta$  is formed by adding a square to the first row of  $\gamma = \delta = \alpha$ .

Given a Ferrers shape and partitions labelling the top and right side, we apply the following *local backward rules* to complete the labelling and recover the filling.

- (B1) If  $\beta = \delta = \alpha$ , then  $\gamma = \beta$ .
- (B2) If  $\beta = \delta \neq \alpha$ , then  $\gamma = \alpha$ .
- (B3) If  $\beta = \alpha \neq \delta$ , then  $\gamma = \delta$ .
- (B4) If  $\beta, \delta, \alpha$  are pairwise different, then  $\gamma = \delta \cap \alpha$ .
- (B5) If  $\beta \neq \delta = \alpha$ , then  $\gamma$  is formed by deleting a square from the  $(k - 1)$ -st row of  $\delta = \alpha$ , given that  $\delta = \alpha$  and  $\beta$  differ in the  $k$ -th row with  $k \geq 2$ .
- (B6) If  $\beta \neq \delta = \alpha$ , and if  $\beta$  and  $\delta = \alpha$  differ in the first row, then  $\gamma = \delta = \alpha$  and the cell is filled with a 1.

**Construction III.44** ([30]). Let  $O = (\emptyset = \mu^0, \mu^1, \dots, \mu^n = \emptyset)$  be an oscillating tableau. The associated triangular growth diagram is the Ferrers shape  $(n - 1, n - 2, \dots, 2, 1, 0)$ . Label the cells according to the following specification:

1. Label the north-east corners of the cells on the main diagonal from the top-left to the bottom-right with the partitions in  $O$ .
2. For each  $i \in \{0, \dots, n - 1\}$  label the corner on the first subdiagonal adjacent to the labels  $\mu^i$  and  $\mu^{i+1}$  with the partition  $\mu^i \cap \mu^{i+1}$ .

3. Use the backwards rules B1-B6 to obtain all other labels and the fillings of the cells.

We denote by  $G_O(O)$  the symmetric  $n \times n$  matrix one obtains from the filling of the growth diagram by putting zeros in the unfilled cells and along the diagonal and completing this to a symmetric matrix.

Starting from a filling of a growth diagram one obtains the oscillating tableau by setting all vectors on corners on the bottom and left border of the diagram to be the empty partition and applying the forwards growth rules F1-F6.

Next, we will extend these local rules to any filling of a Ferrers shape with non-negative integers.

### III.3.3 Fomin growth diagrams: Rule Burge

Given a filling of a Ferrers shape  $(\lambda_1, \dots, \lambda_\ell)$  with non-negative integers, we produce a “blow up” construction of the original shape for the Burge variant which contains south-east chains of 1’s, as done by [21]. We begin by separating entries. If a cell is filled with a positive entry  $m$ , we replace the cell with an  $m \times m$  grid of cells with 1’s along the diagonal (from top-left to bottom-right). If there exist several nonzero entries in one column, we arrange the grids of cells also from top-left to bottom-right, so that the 1’s form a south-east chain in each column. We make the same arrangements for the rows, also establishing a south-east chain in each row. The resulting blow up Ferrers diagram then contains  $c_j$  columns in the original  $j$ -th column, where  $c_j$  is equal to the sum of the entries in column  $j$  or 1 if the  $j$ -th column contains only 0’s, and  $r_i$  rows in the original  $i$ -th row, where  $r_i$  is equal to the sum of the entries in row  $i$  or 1 if the  $i$ -th row contains only 0’s. See Figure 22.

Since the filling of the blow up growth diagram consists of 1’s and 0’s, we now apply the forward local rules. To start, we label all of the corners of the cells on the left side and the bottom side of the blow up growth diagram by  $\emptyset$ . Then we apply the forward local rules to determine the partition labels of the other corners, using the 0/1 filling and partitions defined in previous iterations of the forward local rule. Finally, we “shrink back” the labelled blow up growth diagram to obtain a labelling of the original Ferrers diagram by only considering the partitions labelling positions  $\{(c_1 + \dots + c_j, r_i + \dots + r_\ell) \mid 1 \leq i \leq \ell, 1 \leq j \leq \lambda_{\ell-i+1}\}$ . These positions are precisely the intersections of the bolded black lines in Figure 22. To shrink back, we ignore the labels on intersections involving any blue lines in the blow up growth diagram and assign the partition labelling  $(c_1 + \dots + c_j, r_i + \dots + r_\ell)$  to the position  $(j, \ell - i + 1)$  in the original Ferrers diagram. The resulting labelling has the property that partitions on adjacent corners differ by a vertical strip [21, Theorem 11].

We now describe the direct Burge forward and backwards rules [21, Section 4.4]. Consider a cell filled by a non-negative integer  $m$ , and labelled by the partitions  $\gamma, \delta, \alpha$ , where  $\gamma \subset \delta$  and  $\gamma \subset \alpha$ ,  $\alpha/\gamma$  and  $\delta/\gamma$  are vertical strips. Moreover, denote by  $\mathbb{1}_A$  the truth function

$$\mathbb{1}_A = \begin{cases} 1 & \text{if } A \text{ is true,} \\ 0 & \text{otherwise.} \end{cases}$$

Then  $\beta$  is determined by the following procedure:

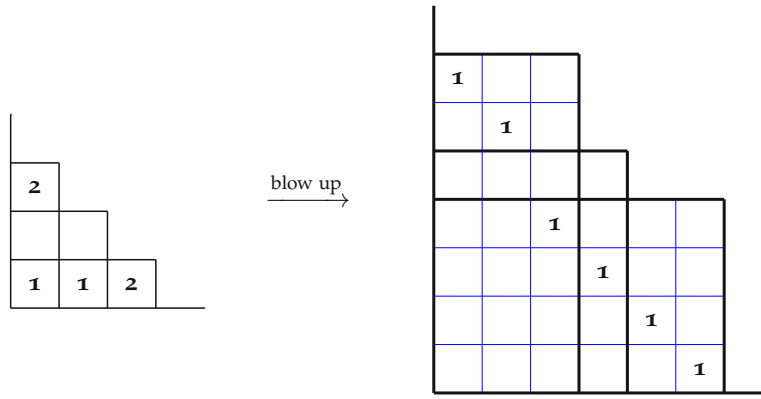


Figure 22: An example of the blow up construction for Burge rules replacing positive integer entries with south-east chains of 1's in each column and row.

**BURGE F0** Set  $\text{CARRY} := m$  and  $i := 1$ .

**BURGE F1** Set  $\beta_i := \max\{\delta_i, \alpha_i\} + \min\{\mathbb{1}_{\gamma_i=\delta_i=\alpha_i}, \text{CARRY}\}$

**BURGE F2** If  $\beta_i = 0$ , then stop and return  $\beta = (\beta_1, \beta_2, \dots, \beta_{i-1})$ . If not, then set  $\text{CARRY} := \text{CARRY} - \min\{\mathbb{1}_{\gamma_i=\delta_i=\alpha_i}, \text{CARRY}\} + \min\{\delta_i, \alpha_i\} - \gamma_i$  and  $i := i + 1$  and go to F1.

Note that this algorithm is reversible. Given  $\beta, \delta, \alpha$  such that  $\beta/\delta$  and  $\beta/\alpha$  are vertical strips, the backwards algorithm is defined by the following rules:

**BURGE B0** Set  $i := \max\{j \mid \beta_j \text{ is positive}\}$  and  $\text{CARRY} := 0$ .

**BURGE B1** Set  $\gamma_i := \min\{\delta_i, \alpha_i\} - \min\{\mathbb{1}_{\gamma_i=\alpha_i=\beta_i}, \text{CARRY}\}$ .

**BURGE B2** Set  $\text{CARRY} := \text{CARRY} - \min\{\mathbb{1}_{\beta_i=\delta_i=\alpha_i}, \text{CARRY}\} + \beta_i - \max\{\delta_i, \alpha_i\}$  and  $i := i - 1$ . If  $i = 0$ , then stop and return  $\gamma = (\gamma_1, \gamma_2, \dots)$  and  $m = \text{CARRY}$ . If not, got to B1.

**Construction III.45.** Let  $F = (\emptyset = \mu^0, \mu^1, \dots, \mu^n = \emptyset)$  be an  $r$ -fan of Dyck paths. The associated triangular growth diagram is the Ferrers shape  $(n - 1, n - 2, \dots, 2, 1, 0)$ . Label the cells according to the following specification:

1. Label the north-east corners of the cells on the main diagonal from the top-left to the bottom-right with the partitions in  $F$ .
2. For each  $i \in \{0, \dots, n - 1\}$  label the corner on the first subdiagonal adjacent to the labels  $\mu^i$  and  $\mu^{i+1}$  with the partition  $\mu^i \cap \mu^{i+1}$ .
3. Use the backwards rules Burge B0, B1 and B2 to obtain all other labels and the fillings of the cells.

We denote by  $G_F(F)$  the symmetric  $n \times n$  matrix one obtains from the filling of the growth diagram by putting zeros in the unfilled cells and along the diagonal and completing this to a symmetric matrix.

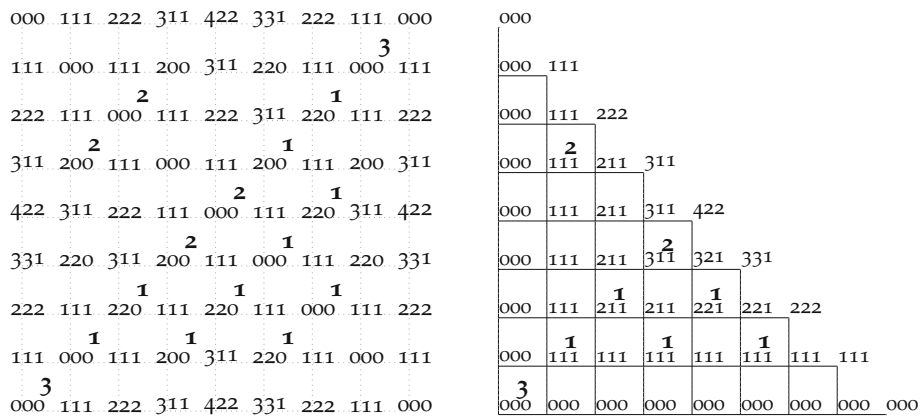


Figure 23: On the left the filled promotion matrix of  $F = (000, 111, 222, 311, 422, 331, 222, 111, 000)$ . On the right the triangular growth diagram for the same fan.

Starting from a filling of a growth diagram one obtains the  $r$ -fan by filling the cells of a growth diagram, setting all vectors on corners on the bottom and left border of the diagram to be the empty partition and applying the forwards growth rules Burge Fo-F2.

An example is given in Figure 23.

### III.3.4 Fomin growth diagrams: Rule RSK

Given a filling of a Ferrers shape  $(\lambda_1, \dots, \lambda_\ell)$  with non-negative integers, we produce a “blow up” construction of the original shape for the RSK variant which contains north-east chains of 1’s, as done by [21]. We begin by separating entries. If a cell is filled with positive entry  $m$ , we replace the cell with an  $m \times m$  grid of cells with 1’s along the off-diagonal (from bottom-left to top-right). If there exist several nonzero entries in one column, we arrange the grids of cells also from bottom-left to top-right, so that the 1’s form a north-east chain in each column. We make the same arrangements for the rows, also establishing a north-east chain in each row. The resulting blow up Ferrers diagram then contains  $c_j$  columns in the original  $j$ -th column, where  $c_j$  is equal to the sum of the entries in column  $j$  or 1 if the  $j$ -th column contains only 0’s, and  $r_i$  rows in the original  $i$ -th row, where  $r_i$  is equal to the sum of the entries in row  $i$  or 1 if the  $i$ -th row contains only 0’s.

Since the filling of the blow up growth diagram consists of 1’s and 0’s, we now apply the forward local rules. To start, we label all of the corners of the cells on the left side and the bottom side of the blow up growth diagram by  $\emptyset$ . Then, we apply the forward local rules to determine the partition labels of the other corners, using the 0/1 filling and partitions defined in previous iterations of the forward local rule. Finally, we “shrink back” the labelled blow up growth diagram to obtain a labelling of the original Ferrers diagram by only partitions labelling positions  $\{(c_1 + \dots + c_j, r_i + \dots + r_\ell) \mid 1 \leq i \leq \ell, 1 \leq j \leq \lambda_{\ell-i+1}\}$ . To shrink back, we assign the partition labelling  $(c_1 + \dots + c_j, r_i + \dots + r_\ell)$  in the blow up growth diagram to the position  $(j, \ell - i + 1)$

in the original Ferrers diagram. The resulting labelling has the property that partitions on adjacent corners differ by a horizontal strip [21, Theorem 7].

The direct RSK forward rules are as follows [21, Section 4.1]: Consider a cell as in Figure 21 filled by a non-negative integer  $m$ , and labelled by the partitions  $\gamma, \delta, \alpha$ , where  $\gamma \subset \delta$  and  $\gamma \subset \alpha$ ,  $\alpha/\gamma$  and  $\delta/\gamma$  are horizontal strips. Then  $\beta$  is determined by the following procedure:

RSK F0 Set CARRY :=  $m$  and  $i := 1$ .

RSK F1 Set  $\beta_i := \max\{\delta_i, \alpha_i\} + \text{CARRY}$

RSK F2 If  $\beta_i = 0$ , then stop and return  $\beta = (\beta_1, \beta_2, \dots, \beta_{i-1})$ . If not, then set CARRY :=  $\min\{\delta_i, \alpha_i\} - \gamma_i$  and  $i := i + 1$  and go to F1.

Note that this algorithm is reversible. Given  $\beta, \delta, \alpha$  such that  $\beta/\delta$  and  $\beta/\alpha$  are horizontal strips, the backwards algorithm is defined by the following rules:

RSK B0 Set  $i := \max\{j \mid \beta_j \text{ is positive}\}$  and CARRY := 0.

RSK B1 Set  $\gamma_i := \min\{\delta_i, \alpha_i\} - \text{CARRY}$ .

RSK B2 Set CARRY :=  $\beta_i - \max\{\delta_i, \alpha_i\}$  and  $i := i - 1$ . If  $i = 0$ , then stop and return  $\gamma = (\gamma_1, \gamma_2, \dots)$  and  $m = \text{CARRY}$ . If not, got to B1.

**Construction III.46.** Let  $V = (\emptyset = \mu^0, \mu^1, \dots, \mu^n = \emptyset)$  be a vacillating tableau of weight zero. The associated triangular growth diagram is the Ferrers shape  $(n - 1, n - 2, \dots, 2, 1, 0)$ . Label the cells according to the following specification:

1. Label the north-east corners of the cells on the main diagonal from the top-left to the bottom-right with the partitions  $2\mu^i$ .
2. For each  $i \in \{0, \dots, n - 1\}$  label the corner on the first subdiagonal adjacent to the labels  $2\mu^i$  and  $2\mu^{i+1}$  with the partition  $2(\mu^i \cap \mu^{i+1})$  when  $\mu^i \neq \mu^{i+1}$  and the partition obtained by removing a cell from the final row of  $2\mu^i$  when  $\mu^i = \mu^{i+1}$ .
3. Use the backwards rules RSK B0, B1 and B2 to obtain all other labels and the fillings of the cells.

We denote by  $G_V(V)$  the symmetric  $n \times n$  matrix one obtains from the filling of the growth diagram by putting zeros in the unfilled cells and along the diagonal and completing this to a symmetric matrix.

Starting from a filling of a growth diagram one obtains the vacillating tableau by setting all vectors on corners on the bottom and left border of the diagram to be the empty partition and applying the forwards growth rules RSK Fo-F2.

The triangular growth diagram of the vacillating tableau from Example III.39 is depicted in Figure 24.



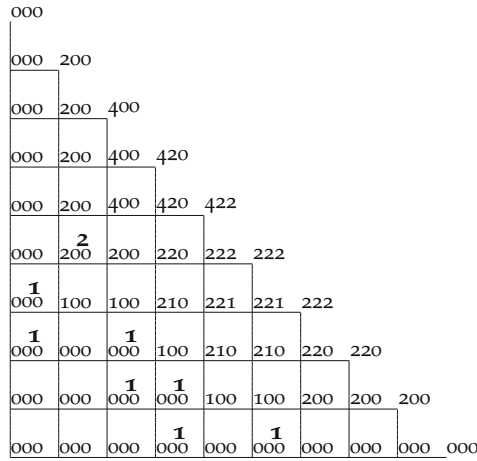


Figure 24: The triangular growth diagram for the vacillating tableau  $V = (000, 100, 200, 210, 211, 111, 111, 110, 100, 000)$ .

### III.4 MAIN RESULTS

In this section, we state and prove our main results for oscillating tableaux, fans of Dyck paths, and vacillating tableaux. In particular, we show in Theorems III.50, III.51 and III.57 that the fillings of the growth diagrams coincide with the fillings of the promotion–evacuation diagrams. This in turn shows that the maps  $M_F$ ,  $M_{V \rightarrow O}$  and  $M_{V \rightarrow F}$  are injective. Having these injective maps to chord diagrams gives a first step towards a diagrammatic basis for the invariant subspaces. In Section III.4.4, we give various new cyclic sieving phenomena associate to the promotion action.

We begin by defining the following notation used later in this section. Let  $M = (a_{i,j})_{i,j=1}^{kn}$  be a  $kn \times kn$  matrix. It will often be convenient to consider  $M$  as the block matrix  $(B_{i,j}^{(k)})_{i,j=1}^n$ , where  $B_{i,j}^{(k)}$  is the  $k \times k$  matrix given by  $(a_{p,q})_{p=k(i-1)+1, q=k(j-1)+1}^{ki, kj}$ . We also follow the convention that for all  $p, q > n$  we have  $B_{p,q}^{(k)} := B_{i,j}^{(k)}$ , where  $p \equiv i \pmod n$  and  $q \equiv j \pmod n$ .

**Definition III.47.** For a  $kn \times kn$  matrix  $M$  with block matrix decomposition given by  $(B_{i,j}^{(k)})_{i,j=1}^n$ , denote by  $\text{blocksum}_k(M)$  the  $n \times n$  matrix  $(b_{i,j})_{i,j=1}^n$ , where  $b_{i,j}$  is equal to the sum of all entries in  $B_{i,j}^{(k)}$ .

Given an  $n \times n$  matrix  $M = (a_{i,j})_{i,j=1}^n$ , we recursively define its skewed partial row sums  $r_{i,j}$  by setting  $r_{i,i} = 0$  for all  $1 \leq i \leq n$  and letting  $r_{i,j+1} = r_{i,j} + a_{i,j}$  for  $1 \leq j \leq n-1$ . Note that as before, we use the convention that  $a_{p,q} = a_{i,j}$  whenever  $p \equiv i \pmod n$  and  $q \equiv j \pmod n$ . Similarly, the skewed partial column sums  $c_{i,j}$  can be defined. Partial inverses to  $\text{blocksum}_k$  are given by  $\text{blowup}_k^{\text{SE}}$  and  $\text{blowup}_k^{\text{NE}}$  which we presently define.

**Definition III.48.** Let  $M = (a_{i,j})_{i,j=1}^n$  be a matrix with non-negative integer entries such that for each row and for each column the sum of the entries is  $k$ . Let  $r_{i,j}$  and  $c_{i,j}$  be its skewed partial row and column sums respectively. Let  $B_{i,j}^{\text{SE}}$  be the  $k \times k$  matrix, where

$B_{i,j}^{SE}$  is the zero-matrix if  $a_{i,j} = 0$  and a zero-one-matrix if  $a_{i,j} \neq 0$  consisting of 1's in positions  $(r_{i,j} + 1, c_{i,j} + 1), \dots, (r_{i,j} + a_{i,j}, c_{i,j} + a_{i,j})$  and zeros elsewhere. We define  $\text{blowup}^{SE}(M)$  to be the block matrix  $(B_{i,j}^{SE})_{i,j=1}^n$ .

Similarly, let  $B_{i,j}^{NE}$  be the  $k \times k$  matrix, where  $B_{i,j}^{NE}$  is the zero-matrix if  $a_{i,j} = 0$  and a zero-one-matrix if  $a_{i,j} \neq 0$  consisting of 1's in positions  $(k - r_{i,j}, k - c_{i,j} - a_{i,j} + 1), \dots, (k - r_{i,j} - (a_{i,j} - 1), k - c_{i,j})$  and zeros elsewhere. We define  $\text{blowup}^{NE}(M)$  to be the block matrix  $(B_{i,j}^{NE})_{i,j=1}^n$ .

**Remark III.49.** Note that  $\text{blowup}^{SE}(M)$  and  $\text{blowup}^{NE}(M)$  are the unique  $kn \times kn$  zero-one-matrices whose blocksum $_k$  equals  $M$  and for all  $1 \leq i \leq n$ , the nonzero entries in the matrices

$$\begin{aligned} & [B_{i,i}, B_{i,i+1}, B_{i,i+2}, \dots, B_{i,i+n-1}] \quad \text{and} \\ & [B_{i,i}, B_{i+1,i}, B_{i+2,i}, \dots, B_{i+n-1,i}] \end{aligned}$$

form a south-east chain or a north-east chain, respectively.

#### III.4.1 Results for oscillating tableaux

The next result was not stated explicitly in [30], but can be deduced from the proof in the paper.

**Theorem III.50.** For an oscillating tableau of weight zero  $O$  the fillings of the growth diagram (Construction III.44) and the fillings of the promotion-evacuation (Construction III.31) diagram coincide, that is

$$G_O(O) = M_O(O).$$

*Proof.* This follows from the proof of [30, Corollary 6.17, Lemma 6.26]. □

#### III.4.2 Results for $r$ -fans of Dyck paths

We state our main results.

**Theorem III.51.** For an  $r$ -fan of Dyck paths  $F$

$$G_F(F) = M_F(F).$$

In other words, the fillings of its growths diagram (Construction III.45) and the fillings of the promotion-evacuation diagram coincide.

In particular we obtain the corollary:

**Corollary III.52.** The map  $M_F$  is injective.

We now state and prove some results which are needed for the proof of Theorem III.51.

**Lemma III.53.** Let  $F$  be an  $r$ -fan of Dyck paths of length  $n$ . Then

$$\iota_{F \rightarrow O} \circ \text{pr}_{\mathcal{B}_{\text{spin}}} (F) = \text{pr}_{\mathcal{C}_{\square}}^r \circ \iota_{F \rightarrow O} (F).$$

*Proof.* Let  $\iota_{F \rightarrow O}(F) = \mu = (\emptyset = \mu^{(0,0)}, \dots, \mu^{(0,rn)} = \emptyset)$ . We first prove that  $\text{pr}_{\mathcal{C}_{\square}^r}(\mu) = \text{pr}_{\mathcal{C}_{\square}^{\otimes r}}(\mu)$ . Let  $\text{pr}_{\mathcal{C}_{\square}^i}(\mu) = (\emptyset = \mu^{(i,0)}, \dots, \mu^{(i,rn)} = \emptyset)$ . From the definition of  $\iota_{F \rightarrow O}$ , we have  $\mu^{(0,k)} = (1^k)$  for all  $0 \leq k \leq r$  where  $(1^0)$  denotes the empty partition  $\emptyset$ . Using the local rules for promotion and induction, we see that the sequence of partitions  $(\mu^{(k,0)}, \dots, \mu^{(k,r-k)})$  is equal to  $((1^0), \dots, (1^{r-k}))$  for all  $0 \leq k \leq r$ . This implies the following equality

$$\begin{aligned} \mu &= ((1^0), (1^1), \dots, (1^r), \mu^{(0,r+1)}, \dots, \mu^{(0,rn)}) \\ &= (\mu^{(r,0)}, \mu^{(r-1,1)}, \dots, \mu^{(0,r)}, \mu^{(0,r+1)}, \dots, \mu^{(0,rn)}). \end{aligned}$$

By a similar argument, the sequence of partitions  $(\mu^{(k,rn-k)}, \dots, \mu^{(k,rn)})$  is equal to  $((1^k), \dots, (1^0))$  for all  $1 \leq k \leq r$  implying

$$\begin{aligned} \text{pr}_{\mathcal{C}_{\square}^r}(\mu) &= (\mu^{(r,0)}, \mu^{(r,1)}, \dots, \mu^{(r,r(n-1)-1)}, (1^r), (1^r - 1), \dots, (1^0)) \\ &= (\mu^{(r,0)}, \mu^{(r,1)}, \dots, \mu^{(r,rn-r-1)}, \mu^{(r,rn-r)}, \mu^{(r-1,rn-r-1)}, \dots, \mu^{(0,r)}). \end{aligned}$$

By Theorem III.27, we obtain the desired equality

$$\begin{aligned} \text{pr}_{\mathcal{C}_{\square}^{\otimes r}}(\mu) &= \text{pr}_{\mathcal{C}_{\square}^{\otimes r}}(\mu^{(r,0)}, \mu^{(r-1,1)}, \dots, \mu^{(0,r)}, \mu^{(0,r+1)}, \dots, \mu^{(0,rn)}) \\ &= (\mu^{(r,0)}, \mu^{(r,1)}, \dots, \mu^{(r,r(n-1))}, \mu^{(r-1,r(n-1)+1)}, \dots, \mu^{(0,rn)}) = \text{pr}_{\mathcal{C}_{\square}^r}(\mu). \end{aligned}$$

Let  $w = w_n \otimes w_{n-1} \otimes \dots \otimes w_1 \in \mathcal{B}_{\text{spin}}^{\otimes n}$  and  $v = v_{rn} \otimes v_{rn-1} \otimes \dots \otimes v_1 \in (\mathcal{C}_{\square}^{\otimes r})^{\otimes n}$  be the highest weight crystal elements associated to  $F$  and  $\mu$ , respectively. In order to show  $\iota_{F \rightarrow O} \circ \text{pr}_{\mathcal{B}_{\text{spin}}}(F) = \text{pr}_{\mathcal{C}_{\square}^{\otimes r}}(\mu)$ , it suffices to show that  $\Psi(\text{pr}_{\mathcal{B}_{\text{spin}}}(w)) = \text{pr}_{\mathcal{C}_{\square}^{\otimes r}}(v)$ , where  $\Psi$  is the crystal isomorphism defined in Definition III.7. Let  $\mathcal{V} \subseteq \mathcal{C}_{\square}^{\otimes r}$  be the virtual crystal defined in Definition III.4. As  $\Psi$  is a crystal isomorphism, we have  $\Psi(\text{pr}_{\mathcal{B}_{\text{spin}}}(w)) = \text{pr}_{\mathcal{V}}(\Psi(w)) = \text{pr}_{\mathcal{V}}(v)$ . As Lusztig's involution for crystals of type  $B_r$  and  $C_r$  interchanges the crystal operators  $f_i$  and  $e_i$ , the virtualization induced by the embedding  $B_r \hookrightarrow C_r$  commutes with Lusztig's involution. In addition virtualization is preserved under tensor products (see for example [4, Theorem 5.8]). Thus, we have  $\text{pr}_{\mathcal{V}}(v) = \text{pr}_{\mathcal{C}_{\square}^{\otimes r}}(v)$ .  $\square$

**Lemma III.54.** *Let  $F$  be an  $r$ -fan of Dyck paths with length  $n$ , and let  $(B_{i,j}^{(r)})_{i,j=1}^n$  be the block matrix decomposition of the  $rn \times rn$  adjacency matrix  $M_O(\iota_{F \rightarrow O}F)$ . Then for all  $1 \leq i \leq n$ , the nonzero entries in the matrices*

$$\begin{aligned} &[B_{i,i+1}^{(r)}, B_{i,i+2}^{(r)}, \dots, B_{i,i+n-1}^{(r)}] \quad \text{and} \\ &[B_{i+1,i}^{(r)}, B_{i+2,i}^{(r)}, \dots, B_{i+n-1,i}^{(r)}] \end{aligned}$$

*form a south-east chain of  $r$  1's.*

*Proof.* By the definition of oscillating tableaux and the local rules for promotion,  $M_O$  is a zero-one matrix. From Lemma III.53, Proposition III.30, and Proposition III.41, it suffices to prove that the nonzero entries in  $[B_{n,n+1}^{(r)}, B_{n,n+2}^{(r)}, \dots, B_{n,2n-1}^{(r)}]$  and  $[B_{2,1}^{(r)}, B_{3,1}^{(r)}, \dots, B_{n,1}^{(r)}]^T$  form a south-east chain. Recall that by construction, the Fomin growth diagram

of  $\iota_{F \rightarrow O}(F)$  is a triangle diagram with the entries of  $\iota_{F \rightarrow O}(F)$  labelling its diagonal. As  $F$  is an  $r$ -fan of Dyck paths, the partition  $(1^r)$  sits at the corners  $(r, r(n-1))$  and  $(r(n-1), r)$  in the Fomin growth diagram of  $\iota_{F \rightarrow O}(F)$ . By Theorem III.50, we have  $M_O(\iota_{F \rightarrow O}(F)) = G_O(\iota_{F \rightarrow O}(F))$ . This implies that the filling of the leftmost  $r$  columns and bottommost  $r$  rows match  $M_O(\iota_{F \rightarrow O}(F))$ . As all the entries of  $M_O(\iota_{F \rightarrow O}(F))$  are either 0 or 1, we have by [21, Theorem 2] that there are exactly  $r$  1's forming a south-east chain in the leftmost  $r$  columns and in the bottommost  $r$  rows.  $\square$

**Remark III.55.** The proof of Lemma III.54 implies that the diagonal block matrices  $B_{i,i}^{(r)}$  of  $M_O(\iota_{F \rightarrow O}F)$  are all zero matrices.

**Proposition III.56.** *Let  $F$  be an  $r$ -fan of Dyck paths of length  $n$ . Then*

$$M_F(F) = \text{blocksum}_r(M_O(\iota_{F \rightarrow O}(F))).$$

Moreover,

$$\text{blowup}_r^{\text{SE}}(M_F(\mathcal{F})) = M_O(\iota_{F \rightarrow O}(\mathcal{F})).$$

*Proof.* By Remark III.55, the diagonal entries of  $M_F(F)$  and  $\text{blocksum}_r(M_O(\iota_{F \rightarrow O}(F)))$  are all zero. Let  $a_{i,j}$  with  $i \neq j$  be the entry in  $M_F(F)$  that is the filling of the cell

labelled by  $\begin{array}{|c|c|} \hline \lambda & \nu \\ \hline \kappa & \mu \\ \hline \end{array}$  in the promotion matrix of  $F$ . To show that the number of 1's appearing in  $B_{i,j}^{(r)}$  of  $M_O(\iota_{F \rightarrow O}(F))$  is also equal to  $a_{i,j}$ , we first compute  $a_{i,j}$  for  $i \neq j$ . By Definition 37,  $a_{i,j}$  is the number of negative entries in  $\kappa + \nu - \lambda$ . Since  $\lambda, \nu$  and  $\kappa, \mu$  are consecutive partitions in an  $r$ -fan of Dyck paths, we know that they differ by a vector of the form  $(\pm 1, \dots, \pm 1)$ . We may write  $\nu - \lambda$  and  $\mu - \kappa$  as

$$\begin{aligned} \nu - \lambda &= \mathbf{e}_{i_1} + \dots + \mathbf{e}_{i_k} - \mathbf{e}_{i_{k+1}} - \dots - \mathbf{e}_{i_r}, \\ \mu - \kappa &= \mathbf{e}_{j_1} + \dots + \mathbf{e}_{j_m} - \mathbf{e}_{j_{m+1}} - \dots - \mathbf{e}_{j_r}, \end{aligned}$$

where

$$\begin{aligned} \{i_1, \dots, i_r\} &= [r] = \{j_1, \dots, j_r\}, \\ i_1 &< \dots < i_k \text{ and } i_{k+1} > \dots > i_r, \\ j_1 &< \dots < j_m \text{ and } j_{m+1} > \dots > j_r. \end{aligned}$$

By the definition of  $\mu$  from the local rules of Lenart [23] (see Section III.2.5), we have

$$\begin{aligned} \mu &= \text{dom}_{\mathfrak{S}_r}(\kappa + \nu - \lambda) \\ &= \text{dom}_{\mathfrak{S}_r}(\kappa + \mathbf{e}_{i_1} + \dots + \mathbf{e}_{i_k} - \mathbf{e}_{i_{k+1}} - \dots - \mathbf{e}_{i_r}). \end{aligned}$$

Recall that  $\text{dom}_{\mathfrak{S}_r}$  applied to a weight sorts the absolute values of the entries of the weight into weakly decreasing order. In particular,  $\text{dom}_{\mathfrak{S}_r}(\kappa + \mathbf{e}_{i_1} + \dots + \mathbf{e}_{i_k} - \mathbf{e}_{i_{k+1}} - \dots - \mathbf{e}_{i_r})$  will change all of the  $-1$  entries of  $\kappa + \mathbf{e}_{i_1} + \dots + \mathbf{e}_{i_k} - \mathbf{e}_{i_{k+1}} - \dots - \mathbf{e}_{i_r}$  to  $+1$  and then sort all entries into weakly decreasing order (note that sorting will not change the number of cells). We thus have two equations for  $\mu$ :

$$\begin{aligned} \mu &= \text{dom}_{\mathfrak{S}_r}(\kappa + \mathbf{e}_{i_1} + \dots + \mathbf{e}_{i_k} - \mathbf{e}_{i_{k+1}} - \dots - \mathbf{e}_{i_r}) \\ &= \kappa + \mathbf{e}_{j_1} + \dots + \mathbf{e}_{j_m} - \mathbf{e}_{j_{m+1}} - \dots - \mathbf{e}_{j_r}. \end{aligned}$$

Therefore,  $\text{dom}_{\mathfrak{S}_r}$  changed  $m - k$  negative entries in  $\kappa + \nu - \lambda$  to  $+1$  in  $\mu$ , showing that  $a_{i,j} = m - k$ .

From the virtualization given in Definition III.7, the partitions labelling the top of the first row of cells in  $B_{i,j}^{(r)}$  are  $\lambda, \lambda^{(1)}, \dots, \lambda^{(r-1)}, \nu$ , where  $\lambda^{(\ell)} = \lambda + \mathbf{e}_{i_1} + \dots \pm \mathbf{e}_{i_\ell}$ . Similarly, the partitions labelling the bottom of the  $r$ -th row of cells in  $B_{i,j}^{(r)}$  are  $\kappa, \kappa^{(1)}, \dots, \kappa^{(r-1)}, \mu$ , where  $\kappa^{(\ell)} = \kappa + \mathbf{e}_{j_1} + \dots \pm \mathbf{e}_{j_\ell}$ . In particular, we have

$$\begin{aligned} \lambda &\subset \lambda^{(1)} \subset \dots \subset \lambda^{(k-1)} \subset \lambda^{(k)} \supset \lambda^{(k+1)} \supset \dots \supset \lambda^{(r-1)} \supset \nu, \\ \kappa &\subset \kappa^{(1)} \subset \dots \subset \kappa^{(m-1)} \subset \kappa^{(m)} \supset \kappa^{(m+1)} \supset \dots \supset \kappa^{(r-1)} \supset \mu. \end{aligned}$$

Let  $\begin{array}{|c|c|} \hline \lambda' & \nu' \\ \hline \kappa' & \mu' \\ \hline \end{array}$  label a cell in the first row of  $B_{i,j}^{(r)}$ , and note that the pairs  $\lambda', \nu'$  and  $\kappa', \mu'$  differ by a unit vector since they are adjacent partitions in an oscillating tableau.

It is impossible for the inclusions  $\begin{array}{|c|c|} \hline \lambda' \subset & \nu' \\ \hline \kappa' \supset & \mu' \\ \hline \end{array}$  since  $\lambda' \subset \nu'$  implies  $\kappa' + \nu' - \lambda' = \kappa' + \mathbf{e}_i$  for some  $i$ , and by definition  $\mu' = \text{dom}_{\mathfrak{S}_r}(\kappa' + \mathbf{e}_i) = \kappa' + \mathbf{e}_i$  which contradicts

$\mu' \subset \kappa'$ . When  $\begin{array}{|c|c|} \hline \lambda' \supset & \nu' \\ \hline \kappa' \subset & \mu' \\ \hline \end{array}$  occurs, we know that  $\kappa' + \nu' - \lambda' = \kappa' - \mathbf{e}_i$  for some  $i$  since  $\nu' \subset \lambda'$ . Since  $\kappa' \subset \mu' = \text{dom}_{\mathfrak{S}_r}(\kappa' - \mathbf{e}_i)$ , it must be that  $\mu' = \kappa' + \mathbf{e}_i$  and therefore  $\kappa' - \mathbf{e}_i$  contained a negative entry. Therefore, when  $\lambda' \supset \nu'$  and  $\kappa' \subset \mu'$  there is a 1

filling the cell. Conversely, when there is a 1 filling a cell labelled  $\begin{array}{|c|c|} \hline \lambda' & \nu' \\ \hline \kappa' & \mu' \\ \hline \end{array}$ , then there is a negative in  $\kappa' + \nu' - \lambda' = \kappa' \pm \mathbf{e}_i$  for some  $i$ , which is only possible when  $\kappa' + \nu' - \lambda' = \kappa' - \mathbf{e}_i$ . As a result,  $\kappa' \subset \mu'$  and  $\lambda' \supset \nu'$ .

By Theorem III.50, each row and each column in  $M_O(\iota_{F \rightarrow O}(F))$  contains exactly one 1. Therefore there is at most one cell in the first row of  $B_{i,j}^{(r)}$  where the containment between the top and bottom pairs of partitions is flipped. By the cases described above, containment between pairs of partitions labelling the bottom of the first row of cells in  $B_{i,j}^{(r)}$  either exactly matches the containment between pairs of partitions labelling the top of the first row or the switch in containment in the bottom occurs immediately to the right of the switch in containment in the top. The same outcome is observed recursively in the remaining rows of cells in  $B_{i,j}^{(r)}$ . Since we already knew the labels of the bottom of the  $r$ -th row to be increasing up to  $\kappa^{(m)}$ , we conclude that the number of 1's appearing in  $B_{i,j}^{(r)}$  is equal to  $m - k$ , which we showed above is equal to  $a_{i,j}$ . Therefore,  $M_F(F) = \text{blocksum}_r(M_O(\iota_{F \rightarrow O}(F)))$ . Further, since the 1's in  $M_O(\iota_{F \rightarrow O}(F))$  form a south-east chain, by Remark III.49 we have  $\text{blowup}_r^{\text{SE}}(M_F(F)) = M_O(\iota_{F \rightarrow O}(F))$ .  $\square$

We can now prove Theorem III.51.

*Proof.* Let  $F = (\mu^0, \dots, \mu^n)$  be an  $r$ -fan of Dyck paths of length  $n$ . We have

$$\begin{aligned} M_F(F) &= \text{blocksum}_r(M_O(\iota_{F \rightarrow O}(F))) && \text{by Proposition III.56} \\ &= \text{blocksum}_r(G_O(\iota_{F \rightarrow O}(F))) && \text{by Theorem III.50.} \end{aligned}$$

It remains to show that  $\text{blocksum}_r(G_O(\iota_{F \rightarrow O}(F))) = G_F(F)$ . The diagonal entries of  $\text{blocksum}_r(G_O(\iota_{F \rightarrow O}(F)))$  and  $G_F(F)$  are all zero by Remark III.55 and by definition of  $G_F$  respectively. As  $G_O$  and  $G_F$  are symmetric matrices, it suffices to show that the lower triangular entries of  $\text{blocksum}_r(G_O(\iota_{F \rightarrow O}(F)))$  and  $G_F(F)$  agree. Let  $G$  denote the triangular growth diagram associated with  $\iota_{F \rightarrow O}(F)$ . By the definition of  $\iota_{F \rightarrow O}$  and Construction III.44, the coordinate  $(kr, (n-k)r)$  is labelled with partition  $\mu^k$  for  $0 \leq k \leq n$ . As  $G$  has a 0/1 filling, the local rules guarantee that the partition  $\nu^k$  labelling the coordinate  $(kr, (n-k-1)r)$  of  $G$  is contained within the partition  $\mu^k \cap \mu^{k+1}$  for  $0 \leq k \leq n-1$ . Moreover,  $|\mu^k/\nu^k| + |\mu^{k+1}/\nu^k|$  is equal to the total number of 1's lying in either a column from  $kr+1$  to  $(k+1)r$  or in a row from  $(n-k-1)r+1$  to  $(n-k)r$ . From Lemma III.54 and the fact that  $G_O$  is symmetric, there exist exactly  $r$  such 1's which implies  $|\mu^k/\nu^k| + |\mu^{k+1}/\nu^k| = r$ . Since  $\mu^k$  and  $\mu^{k+1}$  differ by exactly  $k$  boxes,  $\nu^k = \mu^k \cap \mu^{k+1}$  for all  $0 \leq k \leq n-1$ .

Let  $H$  denote the triangular growth diagram with filling given by the lower triangular entries of  $\text{blocksum}_r(G_O(\iota_{F \rightarrow O}(F)))$  and local rules given by the Burge rules. From Lemma III.54,  $\text{blowup}^{\text{SE}}(\text{blocksum}_r(G_O(\iota_{F \rightarrow O}(F)))) = G_O(\iota_{F \rightarrow O}(F))$ . A result by Krattenthaler [21] implies that the labellings of the hypotenuse of  $H$  are given by  $(\mu^0, \nu^0, \mu^1, \dots, \nu^{n-1}, \mu^n)$ . As the Burge rules are injective and the growth diagram associated to  $F$  under Construction III.45 has hypotenuse labelled by  $(\mu^0, \mu^0 \cap \mu^1, \mu^1, \dots, \mu^{n-1} \cap \mu^n, \mu^n)$ , the lower triangular entries of  $\text{blocksum}_r(G_O(\iota_{F \rightarrow O}(F)))$  and  $G_F(F)$  are equal.  $\square$

### III.4.3 Results for vacillating tableaux

We state our main results.

**Theorem III.57.** *For a vacillating tableau  $V$*

$$G_V(V) = M_{V \rightarrow O}(V) = M_{V \rightarrow F}(V).$$

*In other words, the filling of the growth diagram (see Construction III.46), the filling of the promotion matrix  $M_{V \rightarrow O}(V)$ , and the filling of the promotion matrix  $M_{V \rightarrow F}(V)$  coincide.*

In particular we obtain the corollary:

**Corollary III.58.** *The maps  $M_{V \rightarrow O}$  and  $M_{V \rightarrow F}$  are injective.*

We will first prove the second equality in Theorem III.57. To do so, we need the following lemma.

**Lemma III.59.** *We have the following:*

- (i)  $M_{V \rightarrow O} = \text{blocksum}_2 \circ M_O \circ \iota_{V \rightarrow O}$ .

(ii) Denote by  $E$  the  $r \times r$  identity matrix, then

$$M_{V \rightarrow F} + 2(r-1)E = \text{blocksum}_2 \circ M_F \circ \iota_{V \rightarrow F}.$$

*Proof.* Let  $V$  be a vacillating tableau of length  $n$  and weight zero and let  $X \in \{O, F\}$ . Denote by  $T = (\emptyset = \mu^0, \mu^1, \dots, \mu^{2n} = \emptyset)$  the corresponding oscillating tableau (resp.  $r$ -fan of Dyck path) to  $V$  using  $\iota_{V \rightarrow X}$ .

Recall that  $M_{V \rightarrow X}$  is defined using the Schema (39) to calculate promotion. Let  $\hat{\mu}^1, \dots, \hat{\mu}^{2n-1}$  be the partitions in the middle row in of this schema.

Note that we have  $\mu^2 = \hat{\mu}^{2n-2} = 2\mathbf{e}_1$  and

$$\mu^1 = \hat{\mu}^1 = \hat{\mu}^{2n-1} = \hat{\mu}^{2n-1} = \begin{cases} \mathbf{e}_1 & \text{if } X = O, \\ \mathbf{1} & \text{if } X = F. \end{cases}$$

It is easy to see that the squares

$$\begin{array}{|c|c|} \hline \mu^1 & \mu^2 \\ \hline \emptyset & \hat{\mu}^1 \\ \hline \end{array} \quad \text{and} \quad \begin{array}{|c|c|} \hline \hat{\mu}^{2n-1} & \emptyset \\ \hline \hat{\mu}^{2n-2} & \hat{\mu}^{2n-1} \\ \hline \end{array}$$

satisfy the local rule and

$$\Phi(\mu^1, \emptyset, \mu^2, \hat{\mu}^1) = \Phi(\hat{\mu}^{2n-1}, \hat{\mu}^{2n-2}, \emptyset, \hat{\mu}^{2n-1}) = \begin{cases} 0 & \text{if } X = O, \\ r-1 & \text{if } X = F. \end{cases}$$

Thus we have

$$\text{pr}_X(\iota_{V \rightarrow X}(V)) = (\emptyset, \hat{\mu}_1, \dots, \hat{\mu}_{2n-1}, \emptyset)$$

and obtain  $M_{V \rightarrow X} + \mathbb{1}_{X=F} \cdot 2(r-1)E = \text{blocksum}_2 \circ M_X \circ \iota_{V \rightarrow X}$ .  $\square$

The following relates the growth diagrams for  $\iota_{V \rightarrow O}(V)$  and  $\iota_{V \rightarrow F}(V)$ .

**Lemma III.60.** Denote by  $S$  the  $2r \times 2r$  block diagonal matrix consisting of  $r$  copies of the block  $\begin{bmatrix} 0 & 1 \\ 1 & 0 \end{bmatrix}$  along the diagonal and zeros everywhere else. Then

$$G_F \circ \iota_{V \rightarrow F} = G_O \circ \iota_{V \rightarrow O} + (r-1)S.$$

*Proof.* Let  $V = (\lambda^0, \dots, \lambda^n)$  be a vacillating tableau of weight zero. Denote with  $O = (\mu^0, \dots, \mu^{2n}) = \iota_{V \rightarrow O}(V)$  the corresponding oscillating tableaux and denote with  $F = (\nu^0, \dots, \nu^{2n}) = \iota_{V \rightarrow O}(F)$  the  $r$ -fan of Dyck paths.

Consider the portion of the growth diagram for the oscillating tableau involving only  $(\mu^{2i-2}, \mu^{2i-1}, \mu^{2i})$  and the portion of the growth diagram for the fan of Dyck paths involving only  $(\nu^{2i-2}, \nu^{2i-1}, \nu^{2i})$ . We label the partitions as follows.

$$\begin{array}{|c|c|} \hline \mu^{2i-2} & \\ \hline \alpha & \mu^{2i-1} \\ \hline m & \\ \hline \gamma & \delta & \mu^{2i} \\ \hline \end{array} \quad \begin{array}{|c|c|} \hline \nu^{2i-2} & \\ \hline \hat{\alpha} & \nu^{2i-1} \\ \hline n & \\ \hline \hat{\gamma} & \hat{\delta} & \nu^{2i} \\ \hline \end{array} \quad (40)$$

**claim:** We have  $\mu^{2i-2} = \nu^{2i-2}$ ,  $\mu^{2i} = \nu^{2i}$ ,  $\alpha = \hat{\alpha}$ ,  $\gamma = \hat{\gamma}$ ,  $\delta = \hat{\delta}$ ,  $m = 0$  and  $n = r - 1$ . Moreover all partitions on consecutive corners on the lower left border of the diagrams in (40) differ by at most one cell.

We consider the three cases  $\lambda^{i-1} = \lambda^i$ ,  $\lambda^{i-1} \subset \lambda^i$  and  $\lambda^{i-1} \supset \lambda^i$ .

By Definition III.21, Construction III.44, Definition III.22 and Construction III.45 we have

$$\begin{aligned} \mu^{2i-2} &= \nu^{2i-2} = 2\lambda^{i-1}, & \mu^{2i} &= \nu^{2i} = 2\lambda^i, \\ \alpha &= \mu^{2i-2} \cap \mu^{2i-1}, & \delta &= \mu^{2i-1} \cap \mu^{2i}, \\ \hat{\alpha} &= \nu^{2i-2} \cap \nu^{2i-1}, & \hat{\delta} &= \nu^{2i-1} \cap \nu^{2i}. \end{aligned}$$

**case i** Assume  $\lambda^{i-1} = \lambda^i$ . In this case we have  $\mu^{2i-1} = 2\lambda^i - \mathbf{e}_r$  and  $\nu^{2i-1} = 2\lambda^i + \mathbf{1} - 2\mathbf{e}_r$  and get

$$\begin{aligned} \alpha &= \delta = (2\lambda^i) \cap (2\lambda^i - \mathbf{e}_r) = 2\lambda^i - \mathbf{e}_r, \\ \hat{\alpha} &= \hat{\delta} = (2\lambda^i) \cap (2\lambda^i + \mathbf{1} - 2\mathbf{e}_r) = 2\lambda^i - \mathbf{e}_r. \end{aligned}$$

Using the backwards rules for growth diagrams we obtain

$$\gamma = \hat{\gamma} = 2\lambda^i - \mathbf{e}_r, \quad m = 0 \quad \text{and} \quad n = r - 1.$$

**case ii** Assume  $\lambda^{i-1} \subset \lambda^i$ . In this case we have  $\mu^{2i-1} = \lambda^{i-1} + \lambda^i$  and  $\nu^{2i-1} = 2\lambda^{i-1} + \mathbf{1}$ . Furthermore we obtain

$$\begin{aligned} \alpha &= (2\lambda^{i-1}) \cap (\lambda^{i-1} + \lambda^i) = 2\lambda^{i-1}, \\ \hat{\alpha} &= (2\lambda^{i-1}) \cap (2\lambda^{i-1} + \mathbf{1}) = 2\lambda^{i-1}, \\ \delta &= (\lambda^{i-1} + \lambda^i) \cap (2\lambda^i) = \lambda^{i-1} + \lambda^i, \\ \hat{\delta} &= (2\lambda^{i-1} + \mathbf{1}) \cap (2\lambda^i) = \lambda^{i-1} + \lambda^i. \end{aligned}$$

Using the backwards rules for growth diagrams we obtain

$$\gamma = \hat{\gamma} = 2\lambda^{i-1}, \quad m = 0 \quad \text{and} \quad n = r - 1.$$

**case iii** Assume  $\lambda^{i-1} \supset \lambda^i$ . This case is symmetric to Case II.

This proves the claim.

The rest of the growth diagrams must agree, as the Burge growth rules and Fomin growth rules agree in the case where labels on consecutive corners differ by at most one cell.  $\square$

Note that Lemma III.60 implies

$$\text{blocksum}_2 \circ G_F \circ \iota_{V \rightarrow F} = \text{blocksum}_2 \circ G_O \circ \iota_{V \rightarrow O} + 2(r-1)E. \quad (41)$$

Now we can prove the second identity of Theorem III.57.



*Proof.* We have

$$\begin{aligned}
M_{V \rightarrow O} &= \text{blocksum}_2 \circ M_O \circ \iota_{V \rightarrow O} && \text{by Lemma III.59 (i)} \\
&= \text{blocksum}_2 \circ G_O \circ \iota_{V \rightarrow O} && \text{by Theorem III.50} \\
&= \text{blocksum}_2 \circ G_F \circ \iota_{V \rightarrow F} - 2(r-1)E && \text{by Equation (41)} \\
&= \text{blocksum}_2 \circ M_F \circ \iota_{V \rightarrow F} - 2(r-1)E && \text{by Theorem III.51} \\
&= M_{V \rightarrow F} && \text{by Lemma III.59 (ii).}
\end{aligned}$$

□

It is possible to invert Lemma III.59 (i) as follows.

**Lemma III.61.** *Let  $V$  be a vacillating tableau of weight zero with length  $n$ , and let  $(B_{i,j}^{(2)})_{i,j=1}^n$  be the block matrix decomposition of the  $2n \times 2n$  adjacency matrix  $M_O(\iota_{V \rightarrow O}V)$ . Then for all  $1 \leq i \leq n$ , the nonzero entries in the matrices*

$$\begin{aligned}
&[B_{i,i+1}^{(2)}, B_{i,i+2}^{(2)}, \dots, B_{i,i+n-1}^{(2)}] \quad \text{and} \\
&[B_{i+1,i}^{(2)}, B_{i+2,i}^{(2)}, \dots, B_{i+n-1,i}^{(2)}]
\end{aligned}$$

*form a north-east chain. In particular, we have*

$$\text{blowup}_2^{\text{NE}} \circ M_{V \rightarrow O} = M_O \circ \iota_{V \rightarrow O}.$$

*Proof.* From Propositions III.30 and III.41, it suffices to prove that the nonzero entries in  $[B_{n,n+1}^{(2)}, B_{n,n+2}^{(2)}, \dots, B_{n,2n-1}^{(2)}]$  and  $[B_{2,1}^{(2)}, B_{3,1}^{(2)}, \dots, B_{n,1}^{(2)}]^T$  form a south-east chain. Recall that by construction, the Fomin growth diagram of  $\iota_{V \rightarrow O}(V)$  is a triangle diagram with the entries of  $\iota_{V \rightarrow O}(V)$  labelling its diagonal. As  $V$  is a vacillating tableau of weight zero, the partition  $(2)$  sits at the corners  $(2, 2(n-1))$  and  $(2(n-1), 2)$  in the Fomin growth diagram of  $\iota_{V \rightarrow O}(V)$ . By Theorem III.50, we have  $M_O(\iota_{V \rightarrow O}(V)) = G_O(\iota_{V \rightarrow O}(V))$ . This implies that the filling of the first 2 columns and first 2 rows match  $M_O(\iota_{V \rightarrow O}(V))$ . As all the entries of  $M_O(\iota_{V \rightarrow O}(V))$  are either 0 or 1, we have that all the nonzero entries in the first 2 rows and the first 2 rows form a north-east chain by [21, Theorem 2]. □

We can now prove the first part of Theorem III.57.

*Proof.* Putting together the current results we obtain:

$$\begin{aligned}
\text{blowup}_2^{\text{NE}} \circ M_{V \rightarrow O} &= M_O \circ \iota_{V \rightarrow O} && \text{by Lemma III.61} \\
&= G_O \circ \iota_{V \rightarrow O} && \text{by Theorem III.50.}
\end{aligned}$$

It thus remains to show:  $G_V = \text{blocksum}_2 \circ G_O \circ \iota_{V \rightarrow O}$ . Let  $V$  be a fixed vacillating tableau of weight zero and length  $n$ . Let  $O = \iota_{V \rightarrow O}(V)$ . Let  $M = (m_{i,j})_{1 \leq i,j \leq 2n} = G_O(O)$  and let  $B_{i,j}^{(2)}$  be its block matrix decomposition. Let  $\alpha_{i,j}$  for  $0 \leq j \leq i \leq 2n$  be the partition in the  $i$ -th row and  $j$ -th column in the growth diagram of  $O$ . Above calculation shows that the nonzero entries in the matrices

$$\begin{aligned}
&[B_{i,i+1}^{(2)}, B_{i,i+2}^{(2)}, \dots, B_{i,i+n-1}^{(2)}] \quad \text{and} \\
&[B_{i+1,i}^{(2)}, B_{i+2,i}^{(2)}, \dots, B_{i+n-1,i}^{(2)}]
\end{aligned}$$

form north-east chains.

Thus the squares

$$\begin{array}{cc} \alpha_{2i,2j} & \alpha_{2i,2(j+1)} \\ \hline \alpha_{2(i+1),2j} & \alpha_{2(i+1),2(j+1)} \end{array}$$

with entry  $m_{2i,2j} + m_{2i+1,2j} + m_{2i,2j+1} + m_{2i+1,2j+1}$  satisfy the rules RSK Fo-F2 and RSK Bo-B2. As in proof of Lemma III.60, the entries of the first subdiagonal of  $M$  are zero. Hence  $M$  is uniquely determined by the labels  $\alpha_{2i,2i}$  and  $\alpha_{2i,2i+1}$ . Again by proof of Lemma III.60 we have  $\alpha_{2i,2i} = 2\lambda^i$  and  $\alpha_{2i,2i+1} = (2\lambda^i) \cup (2\lambda^{i+1})$ . As these partitions agree with the labels in Construction III.46, we get  $G_V(V) = \text{blocksum}_2(G_O(O))$ .  $\square$

**Problem III.62.** Find a characterization of the image of the injective maps  $M_F$ ,  $M_{V \rightarrow O}$  and  $M_{V \rightarrow F}$ .

**Remark III.63.** For  $M_O$  the solution to the above problem is known (see [30]). The set of  $r$ -symplectic oscillating tableaux of weight zero are in bijection with the set of  $(r + 1)$ -noncrossing perfect matchings of  $\{1, 2, \dots, n\}$ .

#### III.4.4 Cyclic sieving

The cyclic sieving phenomenon was introduced by Reiner, Stanton and White [31] as a generalization of Stembridge's  $q = -1$  phenomenon.

**Definition III.64.** Let  $X$  be a finite set and  $C$  be a cyclic group generated by  $c$  acting on  $X$ . Let  $\zeta \in C$  be a  $|C|^{th}$  primitive root of unity and  $f(q) \in \mathbb{Z}[q]$  be a polynomial in  $q$ . Then the triple  $(X, C, f)$  exhibits the *cyclic sieving phenomenon* if for all  $d \geq 0$  we have that the size of the fixed point set of  $c^d$  (denoted  $X^{c^d}$ ) satisfies  $|X^{c^d}| = f(\zeta^d)$ .

In this section, we will state cyclic sieving phenomena for the promotion action on oscillating tableaux, fans of Dyck paths, and vacillating tableaux. In Section III.4.4 we review an approach using the energy function. In Sections III.4.4 and III.4.4 we give new cyclic sieving phenomena for fans of Dyck paths and vacillating tableaux, respectively.

#### Cyclic sieving using the energy function

We first introduce the energy function on tensor products of crystals. The energy function is defined on affine crystals, meaning that the crystal  $\mathcal{C}_\square$  needs to be upgraded to a crystal of affine Kac–Moody type  $C_r^{(1)}$  and the crystals  $\mathcal{B}_\square$  and  $\mathcal{B}_{\text{spin}}$  need to be upgraded to crystals of affine Kac–Moody type  $B_r^{(1)}$ . In particular, these affine crystals have additional crystals operators  $f_0$  and  $e_0$ . For further details, see for example [27, 26, 10].

For an affine crystal  $\mathcal{B}$ , the *local energy function*

$$H: \mathcal{B} \otimes \mathcal{B} \rightarrow \mathbb{Z}$$

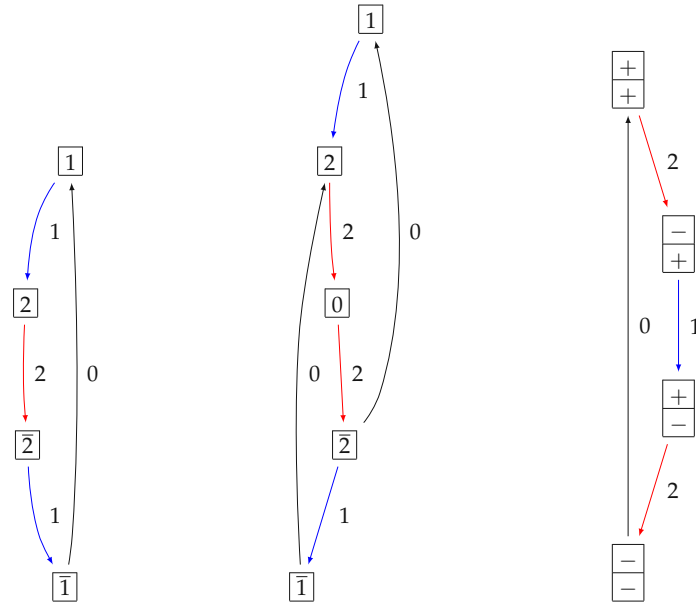


Figure 25: Left: Affine crystal  $\mathcal{C}_{\square}^{\text{af}}$  of type  $C_2^{(1)}$ . Middle: Affine crystal  $\mathcal{B}_{\square}^{\text{af}}$  of type  $B_2^{(1)}$ . Right: Affine crystal  $\mathcal{B}_{\text{spin}}^{\text{af}}$  of type  $B_2^{(1)}$ .

is defined recursively (up to an overall constant) by

$$H(e_i(b_1 \otimes b_2)) = H(b_1 \otimes b_2) + \begin{cases} +1 & \text{if } i = 0 \text{ and } \varepsilon_0(b_1) > \varphi_0(b_2), \\ -1 & \text{if } i = 0 \text{ and } \varepsilon_0(b_1) \leq \varphi_0(b_2), \\ 0 & \text{otherwise.} \end{cases}$$

The crystals we consider here are simple, meaning that there exists a dominant weight  $\lambda$  such that  $\mathcal{B}$  contains a unique element, denoted  $u(\mathcal{B})$ , of weight  $\lambda$  such that every extremal vector of  $\mathcal{B}$  is contained in the Weyl group orbit of  $\lambda$ . We normalize  $H$  such that

$$H(u(\mathcal{B}) \otimes u(\mathcal{B})) = 0.$$

**Example III.65.** The affine crystal  $\mathcal{C}_{\square}^{\text{af}}$  of type  $C_r^{(1)}$  is, for example, constructed in [10, Theorem 5.7]. The case of type  $C_2^{(1)}$  is depicted in Figure 25. Using the ordering  $1 < 2 < \dots < r < \bar{r} < \dots < \bar{2} < \bar{1}$ , we have that  $H(a \otimes b) = 0$  if  $a \leq b$  and  $H(a \otimes b) = 1$  if  $a > b$ .

**Example III.66.** The affine crystal  $\mathcal{B}_{\square}^{\text{af}}$  of type  $B_r^{(1)}$  is, for example, constructed in [10, Theorem 5.1]. The case  $B_2^{(1)}$  is depicted in Figure 25. Using the ordering  $1 < 2 < \dots < r < 0 < \bar{r} < \dots < \bar{2} < \bar{1}$ , we have that  $H(a \otimes b) = 0$  if  $a \leq b$  and  $a \otimes b \neq 0 \otimes 0$ ,  $H(\bar{1} \otimes 1) = 2$ , and  $H(a \otimes b) = 1$  otherwise.

**Example III.67.** The affine crystal  $\mathcal{B}_{\text{spin}}^{\text{af}}$  of type  $B_r^{(1)}$  is constructed in [10, Theorem 5.3]. The case  $B_2^{(1)}$  is depicted in Figure 25. The classical highest weight elements in  $\mathcal{B}_{\text{spin}}^{\text{af}} \otimes \mathcal{B}_{\text{spin}}^{\text{af}}$  are  $(\epsilon_1, \dots, \epsilon_r) \otimes (+, +, \dots, +)$  with  $\epsilon_i = +$  for  $1 \leq i \leq k$  and  $\epsilon_i = -$  for  $k < i \leq r$  for some  $0 \leq k \leq r$ . Denoting by  $m(\epsilon_1, \dots, \epsilon_r)$  the number of  $-$  in the  $\epsilon_i$ , we have

$$H((\epsilon_1, \dots, \epsilon_r) \otimes (+, \dots, +)) = \left\lfloor \frac{m(\epsilon_1, \dots, \epsilon_r) + 1}{2} \right\rfloor.$$

By definition, the local energy is constant on classical components.

The *energy function*

$$E: \mathcal{B}^{\otimes n} \rightarrow \mathbb{Z}$$

is defined as follows for  $b_1 \otimes \cdots \otimes b_n \in \mathcal{B}^{\otimes n}$

$$E(b_1 \otimes \cdots \otimes b_n) = \sum_{i=1}^{n-1} iH(b_i \otimes b_{i+1}).$$

Let us now define a polynomial in  $q$  using the energy function for highest weight elements in  $\mathcal{B}^{\otimes n}$  of weight zero

$$f_{n,r}(q) = q^{c_{n,r}} \sum_{\substack{b \in \mathcal{B}^{\otimes n} \\ \text{wt}(b)=0 \\ e_i(b)=0 \text{ for } 1 \leq i \leq r}} q^{E(b)},$$

where  $r$  is the rank of the type of the underlying root system and  $c_{n,r}$  is a constant depending on the type. Namely,

$$c_{n,r} = \begin{cases} 0 & \text{for } \mathcal{B}_{\square} \text{ all } r \text{ and } \mathcal{B}_{\text{spin}} \text{ for } r \equiv 0, 3 \pmod{4}, \\ q^{\frac{n}{2}} & \text{for } \mathcal{C}_{\square} \text{ all } r \text{ and } \mathcal{B}_{\text{spin}} \text{ for } r \equiv 1, 2 \pmod{4}. \end{cases}$$

The following theorem clarifies statements in [43].

**Theorem III.68.** *Let  $X$  be the set of highest weight elements in  $\mathcal{B}^{\otimes n}$  of weight zero, where the Kirillov–Reshetikhin crystal corresponding to  $\mathcal{B}$  is classically irreducible. Then  $(X, C_n, f_{n,r}(q))$  exhibits the cyclic sieving phenomenon, where  $C_n$  is the cyclic group of order  $n$  on  $n$  tensor factors inherited from the evaluation modules as in [8, Theorem 4.2].*

*Proof.* In [8, Proof of Theorem 4.2], Fontaine and Kamnitzer proved that  $(X, C_n, \tilde{f}_{n,r}(q))$  exhibits the cyclic sieving phenomenon, where  $\tilde{f}_{n,r}(q)$  is a polynomial defined in terms of current algebra actions on Weyl modules of Fourier and Littelmann [9]. These arguments use that the fusion product is independent of the parameters, which was proven by Ardonne and Kedem [1]. When the Kirillov–Reshetikhin crystals are classically irreducible, the cyclic vectors for the evaluation representations are uniquely determined as the tensor product of classically highest weight elements. By [11], this polynomial is equal to the energy function polynomial up to an overall constant, proving the claim.  $\square$

When the crystal  $\mathcal{B}$  is minuscule, it was shown by Fontaine and Kamnitzer [8] that the cyclic action on  $\mathcal{B}^{\otimes n}$  is given by promotion. In particular, for oscillating tableaux and fans of Dyck paths Theorem III.68 gives a cyclic sieving phenomenon with the promotion action since the corresponding crystals are minuscule. The crystals corresponding to vacillating tableaux are not minuscule.

For the vector representation of type  $A$ , highest weight elements in the tensor product of weight zero under RSK are in correspondence with standard tableaux of rectangular shape. The energy function relates to the major index under correspondence. Hence in this case, Theorem III.68 relates to results in [32].

Note that the Kirillov–Reshetikhin crystals corresponding to  $\mathcal{C}_{\square}$ ,  $\mathcal{B}_{\text{spin}}$ , and  $\mathcal{B}_{\square}$  are classically irreducible, and hence Theorem III.68 gives a cyclic sieving phenomenon for oscillating tableaux, fans of Dyck paths, and vacillating tableaux.

### Cyclic sieving for fans of Dyck paths

Recall from Section III.2.3 that highest weight elements of weight zero in  $\mathcal{B}_{\text{spin}}^{\otimes 2n}$  of type  $B_r$  are in bijection with  $r$ -fans of Dyck paths of length  $2n$ . Denote by  $D_n^{(r)}$  the set of all  $r$ -fans of Dyck paths of length  $2n$ . The cardinality of this set is given by  $\prod_{1 \leq i \leq j \leq n-1} \frac{i+j+2r}{i+j}$ , see [6, 20]. Define the  $q$ -analogue of this formula as

$$g_{n,r}(q) = \prod_{1 \leq i \leq j \leq n-1} \frac{[i+j+2r]_q}{[i+j]_q}, \quad (42)$$

where  $[m]_q = 1 + q + q^2 + \dots + q^{m-1}$ .

**Conjecture III.69.** *The triple  $(D_n^{(r)}, C_{2n}, g_{n,r}(q))$  exhibits the cyclic sieving phenomenon, where  $C_{2n}$  is the cyclic group of order  $2n$  that acts on  $D_n^{(r)}$  by applying promotion.*

**Example III.70.** We have

$$q^{-4} f_{4,2}(q) = g_{2,2}(q) = q^4 + q^2 + 1$$

and

$$\begin{aligned} g_{3,2}(q) &= q^{12} + q^{10} + q^9 + 2q^8 + q^7 + 2q^6 + q^5 + 2q^4 + q^3 + q^2 + 1, \\ q^{-6} f_{6,2}(q) &= q^{10} + q^9 + 2q^8 + q^7 + 3q^6 + q^5 + 2q^4 + q^3 + q^2 + 1. \end{aligned}$$

Note that  $g_{3,2}(q) = f_{6,2}(q) \pmod{q^6 - 1}$ .

In general, we conjecture that  $g_{n,r}(q) = f_{2n,r}(q) \pmod{q^{2n} - 1}$  which has been verified for all  $n + r \leq 10$ .

Note that by [20, Theorem 10]

$$g_{n,r}(q) = \prod_{1 \leq i \leq j \leq n-1} \frac{[i+j+2r]_q}{[i+j]_q} = \sum_{\substack{\lambda \\ \lambda_1 \leq r}} s_{2\lambda}(q, q^2, \dots, q^{n-1}).$$

**Remark III.71.** Conjecture III.69 is equivalent to [13, Conjecture 5.2], [15, Conjecture 4.28], and [14, Conjecture 5.9] on plane partitions and root posets.

**Remark III.72.** There is a bijection between  $r$ -fans of Dyck paths of length  $2(n - 2r)$  and  $r$ -triangulations of  $n$ -gons. A cyclic sieving phenomenon in this setting was conjectured by Serrano and Stump [36]. Even though the polynomial in this conjectured cyclic sieving phenomenon is  $g_{n-2r,r}$ , the cyclic group acting is  $C_{2n}$ , which is different from our setting.

### Cyclic sieving for vacillating tableaux

Before giving our cyclic sieving phenomenon result for vacillating tableaux, we review Jagenteufel's major statistic for vacillating tableaux [16]. As vacillating tableaux are in bijection with highest weight elements of  $\mathcal{B}_{\square}^{\otimes n}$ , it suffices to define the major statistic on highest weight elements of  $\mathcal{B}_{\square}^{\otimes n}$ .

Let  $u = u_n \otimes \dots \otimes u_2 \otimes u_1$  be a highest weight element in  $\mathcal{B}_{\square}^{\otimes n}$  of type  $B_r$ . As before let  $<$  denote the ordering  $1 < 2 < \dots < r < 0 < \bar{r} < \dots < \bar{2} < \bar{1}$  on the elements of  $\mathcal{B}_{\square}$ . We say that position  $i$  is a *descent* for  $u$  if

1.  $u_{i+1} > u_i$ , and
2. if the suffix  $u_{i-1} \otimes \cdots \otimes u_2 \otimes u_1$  has an equal number of  $j$ 's and  $\bar{j}$ 's, then  $u_{i+1} \otimes u_i \neq \bar{j} \otimes j$ .

Denote the set of descents of  $u$  by  $\text{Des}(u)$ . Define the *major index* of  $u$ , denoted by  $\text{maj}(u)$ , as the sum of its descents  $\sum_{i \in \text{Des}(u)} i$ . Let  $h_{n,r}(q)$  denote the polynomial in  $q$  given by

$$h_{n,r}(q) = \sum_{u \in V_n^{(r)}} q^{\text{maj}(u)}$$

where  $V_n^{(r)}$  denotes the set of all highest weight elements of weight zero in  $\mathcal{B}_{\square}^{\otimes n}$  of type  $B_r$ .

From [16, Theorem 2.1] and [43, Theorem 6.8], we obtain the following result.

**Theorem III.73.** *The triple  $(V_n^{(r)}, C_n, h_{n,r}(q))$  exhibits the cyclic sieving phenomenon, where the cyclic group on  $n$  elements,  $C_n$ , acts on  $V_n^{(r)}$  by applying promotion.*

Using the descent-preserving bijection in [16], we obtain another interpretation of  $h_{n,r}(q)$  in terms of standard Young tableaux. Adopting the notation and terminology of [37] for standard Young tableaux, we say that  $i$  is a descent for the standard Young tableau  $T$  if  $i + 1$  sits in a lower row than  $i$  in  $T$  in English notation. Given this, we analogously define  $\text{maj}(T)$  to be the sum of the descents of  $T$ . Letting  $\text{SYT}(\lambda)$  denote the set of all standard Young tableaux of shape  $\lambda$ , the polynomial  $h_{n,r}(q)$  can be reinterpreted as follows.

**Theorem III.74.** [16] *Let  $n, r \geq 1$ . Then*

$$h_{n,r}(q) = \sum_{T \in \text{SYT}(\lambda)} q^{\text{maj}(T)},$$

where  $\lambda$  ranges over all partitions of  $n$  with only even parts and length at most  $2r + 1$  when  $n$  is even and  $\lambda$  ranges over all partitions of  $n$  with only odd parts and length exactly  $2r + 1$  when  $n$  is odd.

**Example III.75.** We have

$$\begin{aligned} f_{7,2}(q) &= q^{22} + q^{21} + q^{20} + q^{19} + 2q^{18} + 2q^{17} + 2q^{16} + q^{15} + 2q^{14} + q^{13} + q^{12} \\ h_{7,2}(q) &= q^{18} + q^{17} + 2q^{16} + 2q^{15} + 3q^{14} + 2q^{13} + 2q^{12} + q^{11} + q^{10} \end{aligned}$$

Note that  $f_{7,2}(q) = h_{7,2}(q) \pmod{q^7 - 1}$ .

#### ACKNOWLEDGEMENTS

We wish to thank Sam Hopkins, Joel Kamnitzer, Christian Krattenthaler, Vic Reiner, Martin Rubey, Travis Scrimshaw and Bruce Westbury for discussions. We especially thank Bruce Westbury for his communications regarding Theorem III.68.

## BIBLIOGRAPHY

- [1] E. ARDONNE AND R. KEDEM, *Fusion products of Kirillov-Reshetikhin modules and fermionic multiplicity formulas*, J. Algebra, 308 (2007), pp. 270–294.
- [2] A. AYYER, S. KLEE, AND A. SCHILLING, *Combinatorial Markov chains on linear extensions*, J. Algebraic Combin., 39 (2014), pp. 853–881.
- [3] J. BANDLOW, A. SCHILLING, AND N. M. THIÉRY, *On the uniqueness of promotion operators on tensor products of type A crystals*, J. Algebraic Combin., 31 (2010), pp. 217–251.
- [4] D. BUMP AND A. SCHILLING, *Crystal bases*, World Scientific Publishing Co. Pte. Ltd., Hackensack, NJ, 2017. Representations and combinatorics.
- [5] S. CAUTIS, J. KAMNITZER, AND S. MORRISON, *Webs and quantum skew Howe duality*, Math. Ann., 360 (2014), pp. 351–390.
- [6] M. DE SAINTE-CATHERINE AND G. VIENNOT, *Enumeration of certain Young tableaux with bounded height*, in Combinatoire énumérative (Montreal, Que., 1985/Quebec, Que., 1985), vol. 1234 of Lecture Notes in Math., Springer, Berlin, 1986, pp. 58–67.
- [7] S. V. FOMIN, *The generalized Robinson-Schensted-Knuth correspondence*, Zap. Nauchn. Sem. Leningrad. Otdel. Mat. Inst. Steklov. (LOMI), 155 (1986), pp. 156–175, 195.
- [8] B. FONTAINE AND J. KAMNITZER, *Cyclic sieving, rotation, and geometric representation theory*, Selecta Math. (N.S.), 20 (2014), pp. 609–625.
- [9] G. FOURIER AND P. LITTELMANN, *Weyl modules, Demazure modules, KR-modules, crystals, fusion products and limit constructions*, Adv. Math., 211 (2007), pp. 566–593.
- [10] G. FOURIER, M. OKADO, AND A. SCHILLING, *Kirillov-Reshetikhin crystals for nonexceptional types*, Adv. Math., 222 (2009), pp. 1080–1116.
- [11] G. FOURIER, A. SCHILLING, AND M. SHIMOZONO, *Demazure structure inside Kirillov-Reshetikhin crystals*, J. Algebra, 309 (2007), pp. 386–404.
- [12] A. HENRIQUES AND J. KAMNITZER, *Crystals and coboundary categories*, Duke Math. J., 132 (2006), pp. 191–216.
- [13] S. HOPKINS, *Cyclic sieving for plane partitions and symmetry*, SIGMA Symmetry Integrability Geom. Methods Appl., 16 (2020), pp. Paper No. 130, 40.
- [14] S. HOPKINS, *Order polynomial product formulas and poset dynamics*, ArXiv e-prints, (2020).
- [15] S. HOPKINS, *Minuscule doppelgängers, the coincidental down-degree expectations property, and rowmotion*, Exp. Math., 31 (2022), pp. 946–974.
- [16] J. JAGENTEUFEL, *A Sundaram type bijection for  $SO(2k + 1)$ : vacillating tableaux and pairs consisting of a standard Young tableau and an orthogonal Littlewood-Richardson tableau*, Sémin. Lothar. Combin., 82B (2020), pp. Art. 33, 12.

- [17] M. KASHIWARA, *Crystalizing the  $q$ -analogue of universal enveloping algebras*, *Comm. Math. Phys.*, 133 (1990), pp. 249–260.
- [18] ———, *Similarity of crystal bases*, in *Lie algebras and their representations* (Seoul, 1995), vol. 194 of *Contemp. Math.*, Amer. Math. Soc., Providence, RI, 1996, pp. 177–186.
- [19] M. KHOVANOV AND G. KUPERBERG, *Web bases for  $\mathfrak{sl}(3)$  are not dual canonical*, *Pacific J. Math.*, 188 (1999), pp. 129–153.
- [20] C. KRATTENTHALER, *The major counting of nonintersecting lattice paths and generating functions for tableaux*, *Mem. Amer. Math. Soc.*, 115 (1995), pp. vi+109.
- [21] ———, *Growth diagrams, and increasing and decreasing chains in fillings of Ferrers shapes*, *Adv. in Appl. Math.*, 37 (2006), pp. 404–431.
- [22] G. KUPERBERG, *Spiders for rank 2 Lie algebras*, *Comm. Math. Phys.*, 180 (1996), pp. 109–151.
- [23] C. LENART, *On the combinatorics of crystal graphs. II. The crystal commutator*, *Proc. Amer. Math. Soc.*, 136 (2008), pp. 825–837.
- [24] G. LUSZTIG, *Canonical bases arising from quantized enveloping algebras*, *J. Amer. Math. Soc.*, 3 (1990), pp. 447–498.
- [25] S.-J. OH AND T. SCRIMSHAW, *Identities from representation theory*, *Discrete Math.*, 342 (2019), pp. 2493–2541.
- [26] M. OKADO AND A. SCHILLING, *Existence of Kirillov-Reshetikhin crystals for nonexceptional types*, *Represent. Theory*, 12 (2008), pp. 186–207.
- [27] M. OKADO, A. SCHILLING, AND M. SHIMOZONO, *Virtual crystals and fermionic formulas of type  $D_{n+1}^{(2)}$ ,  $A_{2n}^{(2)}$ , and  $C_n^{(1)}$* , *Represent. Theory*, 7 (2003), pp. 101–163.
- [28] R. PATRIAS, *Promotion on generalized oscillating tableaux and web rotation*, *J. Combin. Theory Ser. A*, 161 (2019), pp. 1–28.
- [29] T. K. PETERSEN, P. PYLYAVSKYY, AND B. RHOADES, *Promotion and cyclic sieving via webs*, *J. Algebraic Combin.*, 30 (2009), pp. 19–41.
- [30] S. PFANNERER, M. RUBEY, AND B. WESTBURY, *Promotion on oscillating and alternating tableaux and rotation of matchings and permutations*, *Algebr. Comb.*, 3 (2020), pp. 107–141.
- [31] V. REINER, D. STANTON, AND D. WHITE, *The cyclic sieving phenomenon*, *Journal of Combinatorial Theory, Series A*, 108 (2004), pp. 17–50.
- [32] B. RHOADES, *Cyclic sieving, promotion, and representation theory*, *J. Combin. Theory Ser. A*, 117 (2010), pp. 38–76.



- [33] T. W. ROBY, V., *Applications and extensions of Fomin's generalization of the Robinson-Schensted correspondence to differential posets*, ProQuest LLC, Ann Arbor, MI, 1991. Thesis (Ph.D.)—Massachusetts Institute of Technology.
- [34] G. RUMER, E. TELLER, AND H. WEYL, *Eine für die Valenztheorie geeignete Basis der binären Vektorinvarianten*, Nachrichten von der Gesellschaft der Wissenschaften zu Göttingen, Mathematisch-Physikalische Klasse, 1932 (1932), pp. 499–504.
- [35] H. M. RUSSELL, *An explicit bijection between semistandard tableaux and non-elliptic  $sl_3$  webs*, J. Algebraic Combin., 38 (2013), pp. 851–862.
- [36] L. SERRANO AND C. STUMP, *Maximal fillings of moon polyominoes, simplicial complexes, and Schubert polynomials*, Electron. J. Combin., 19 (2012), pp. Paper 16, 18.
- [37] R. P. STANLEY, *Enumerative combinatorics. Vol. 2*, vol. 62 of Cambridge Studies in Advanced Mathematics, Cambridge University Press, Cambridge, 1999. With a foreword by Gian-Carlo Rota and appendix 1 by Sergey Fomin.
- [38] ———, *Promotion and evacuation*, Electron. J. Combin., 16 (2009), pp. Research Paper 9, 24.
- [39] J. R. STEMBRIDGE, *A local characterization of simply-laced crystals*, Trans. Amer. Math. Soc., 355 (2003), pp. 4807–4823.
- [40] S. SUNDARAM, *Orthogonal tableaux and an insertion algorithm for  $SO(2n + 1)$* , J. Combin. Theory Ser. A, 53 (1990), pp. 239–256.
- [41] M. A. A. VAN LEEUWEN, *An analogue of jeu de taquin for Littelmann's crystal paths*, Sémin. Lothar. Combin., 41 (1998), pp. Art. B41b, 23 pp.
- [42] ———, *Spin-preserving Knuth correspondences for ribbon tableaux*, Electron. J. Combin., 12 (2005), pp. Research Paper 10, 65.
- [43] B. W. WESTBURY, *Invariant tensors and the cyclic sieving phenomenon*, Electron. J. Combin., 23 (2016), pp. Paper 4.25, 40.
- [44] ———, *Coboundary categories and local rules*, Electron. J. Combin., 25 (2018), pp. Paper No. 4.9, 22.



---

## CURRICULUM VITAE

---

Stephan Pfannerer-Mittas



### PERSONAL INFORMATION



### EDUCATION

- 2024 **PhD in Technical Mathematics**  
Thesis: Rotation invariant diagrammatic basis for invariant spaces  
TU Wien  
Supervisor: Privatdoz. Dr.rer.nat. Martin Rubey
- 2019 **Bachelors degree in Computer Science**  
University of Vienna
- 2018 **Master degree in Technical Mathematics**  
Thesis: Crystals, promotion, evacuation and cactus groups  
TU Wien  
Supervisor: Privatdoz. Dr.rer.nat. Martin Rubey
- 2015 **Bachelor degree in Technical Mathematics**  
TU Wien

### PROFESSIONAL EXPERIENCE

- 2023-2024 **Researcher and Developer**  
ISIS Papyrus Europe AG
- 2022-2023 **Parental leave**
- 2022 **Visiting Scholar**  
Department of Mathematics  
University of California, Davis  
Advisor: Prof. Anne Schilling
- 2018-2022 **Research Assistant**  
Institute for Discrete Mathematics and Geometry  
TU Wien  
FWF Project: P29275  
DOC fellowship by the Austrian Academy of Sciences
- 2015-2017 **Teaching assistant**  
Institute for Discrete Mathematics and Geometry  
TU Wien